Comparing automated vehicles with human drivers

Improving motion comfort with motion planning and suspension control

Zheng, Y.

DOI
10.4233/uuid:d58256b5-2532-462c-b2a0-9c95e1dc6cef

Publication date
2023

Document Version
Final published version

Citation (APA)
Zheng, Y. (2023). *Comparing automated vehicles with human drivers: Improving motion comfort with motion planning and suspension control*. [Dissertation (TU Delft), Delft University of Technology].
https://doi.org/10.4233/uuid:d58256b5-2532-462c-b2a0-9c95e1dc6cef

Important note
To cite this publication, please use the final published version (if applicable).
Please check the document version above.

COMPARING AUTOMATED VEHICLES WITH HUMAN DRIVERS

IMPROVING MOTION COMFORT WITH MOTION PLANNING AND SUSPENSION CONTROL

Yanggu Zheng

IMPROVING MOTION COMFORT WITH MOTION PLANNING AND SUSPENSION CONTROL

COMPARING AUTOMATED VEHICLES WITH HUMAN DRIVERS

IMPROVING MOTION COMFORT WITH MOTION PLANNING AND SUSPENSION CONTROL

COMPARING AUTOMATED VEHICLES WITH HUMAN DRIVERS

Dissertation

for the purpose of obtaining the degree of doctor at Delft University of Technology by the authority of the Rector Magnificus prof.dr.ir. T.H.J.J. van der Hagen chair of the Board for Doctorates to be defended publicly on Monday 30 October 2023 at 10:00 o'clock

by

Yanggu ZHENG

M.Sc. Mechanical Engineering,
Delft University of Technology, Delft, the Netherlands,
born in Beijing, China.

This dissertation has been approved by the promotor.
Composition of the doctoral committee:

Rector Magnificus,	chairperson
Prof. dr. T. Keviczky	Delft University of Technology, promotor
Dr. B. Shyrokau	Delft University of Technology, supervisor
Independent members:	
Prof. dr. ir. J. Hellendoorn	Delft University of Technology
Prof. dr. ir. R. Happee	Delft University of Technology
Prof. dr. A. Sorniotti	University of Surrey, United Kingdoms
Dr. E. Velenis	Cranfield University, United Kingdoms
Prof. dr. ir. J.C.F. de Winter	Delft University of Technology, reserve member

When in doubt, flat out.

Colin Steele McRae

CONTENTS

SUMMARY

This dissertation is dedicated to understanding the potential of improving the motion comfort of automated vehicles and explores multiple options that serve this purpose. Comfort is usually prioritized behind factors such as safety and efficiency but is nevertheless influential to the acceptance of automated vehicles. The goal of enhancing motion comfort overlaps with the need to overcome challenges brought by the motion sickness phenomenon. Motion sickness is found to impact a significant portion of travelers in all types of transport. It tends to develop faster among occupants who are not engaged in the driving task. Its symptoms can cause difficulties for non-driving-related tasks (NDRTs) to be performed effectively by the passengers. Therefore, a part of the research in this dissertation is directed specifically toward mitigating motion sickness in automated vehicles.

The potential improvement in motion comfort is represented by the difference between a performance baseline of human drivers and the level achievable by automated vehicles. The performance is indicated as a combination of motion comfort and time efficiency due to the conflicting nature between them. The measure of comfort is further divided into two branches, one focusing on accelerations in general while the other targets motion sickness specifically by analyzing the frequency composition of the accelerations experienced by the passengers. At first, an attempt to establish the human driver baseline was made by analyzing existing naturalistic driving data at roundabouts. An optimization-based scheme was implemented to overcome measurement noise and erroneous recordings were removed using the technique of principal component analysis. The data suggested a preference for peak accelerations, which is approximately $1.90\,\mathrm{m/s^2}$ in the longitudinal direction and $3.57\,\mathrm{m/s^2}$ in the lateral direction in the most complex type of maneuver. However, no meaningful indication of time efficiency was obtained due to the inconsistent and incomplete coverage of the recordings contained in the readily available dataset. This has directly led to an on-road experiment to collect tailored data for the purpose of understanding human driving comfort. A group of participants was recruited from the public and instructed to drive an instrumented vehicle through a designated route that involves significant speed changes and multiple consecutive turns in quick succession. An average duration of 76.5 s has been observed from the recorded runs while the average acceleration discomfort was found at $211.4\,\mathrm{m^2/s^3}$. The average peak lateral acceleration coincides with the analysis of naturalistic driving data while the average peak longitudinal acceleration is around 48% higher than previous findings due to the extension of the recording coverage.

The upper limit of comfort and time efficiency performance of automated vehicles is determined with an optimization-based motion planning algorithm. A frequency-weighting representation of predicted nauseogenicity has been proposed and incorporated into the algorithm in order to prove the idea of mitigating motion sickness with automated vehicles. Because being free from motion sickness symptoms is deemed as

an interpretation of motion comfort especially meaningful in the context of automated vehicles. The motion planner generates the spatiotemporal trajectory of the vehicle by determining its relative position within the driving lane alongside a speed profile. When compared with optimizing for the alternative objective that targets all planar accelerations equally, a potential reduction of 11.3% in squared motion sickness dose value (MSDV) was achieved when the same amount of travel time was used. The reduction in squared MSDV, when using squared MSDV as the objective, is found to be 32% when compared with the best-performing human driver. Meanwhile, the reduction in general acceleration energy measures 19% with the objective of minimizing acceleration in the motion planner. Additional causes of such differences have been analyzed in order to clarify the conditions of referencing the claimed differences. Whereas the inferior precision of human drivers in controlling vehicle motion is a major contributing factor, the motion planner's assumption of no elevation change and smooth pavement further influenced the reported numbers. One should also bear in mind that human drivers may further tend to reduce physical input efforts and fuel consumption and maintain a safety margin for unexpected traffic interactions. The receding-horizon formulation, reflective of the practically feasible operation of the proposed algorithm, has been further explored. A properly chosen set of preview parameters, including the preview time and planning interval, could lead to an acceptable level of performance loss over the integral planning case (i.e. solving for the entire maneuver) while maintaining a computational complexity close to real-time feasibility.

Further potential lies in recent developments in suspension technology, hence related concepts and their impacts have been analyzed. Specifically, roll-compensated lateral acceleration enabled by active suspension actuators is deemed a possible solution and has been implemented on railroad vehicles for decades. Transferring this concept onto passenger vehicles involves challenges including the demand for capable and affordable actuators on the hardware side but also a suitable control strategy. A nonlinear model predictive control (NMPC) method has been developed for vehicles controlled by human drivers. The reference generation relies on curvature preview to predict the magnitude of lateral acceleration and ensure a phase lead in roll motion over yaw motion. Throughout the highway, rural, and urban driving scenarios, the proposed method outperforms specifically tuned feedforward-PID control, which is representative of the state-of-the-art solution used in the industry. A dedicated warm-start strategy based on hybrid MPC reduced computational time, enabling the NMPC controller to operate in real-time hardware-in-the-loop (HIL) tests. However, the control method does not fully resolve the problem of cooperating with human drivers. The limitations prompt coordination between planar and roll motion in a combined motion planning framework on automated vehicles. Hence, a novel optimization-based planning algorithm coordinating the roll and planar motions has been proposed. A further reduction of up to 30.5% in acceleration comfort could be achieved compared with optimizing only within the horizontal plane, i.e. planning vehicle trajectory and velocity.

Nonetheless, the research work done in this dissertation is of an exploratory nature. The solutions have been studied as proof of concept showing their potential and feasibility. The suggested values in terms of potential performance benefit should be referred to with caution by mentioning the specific scenarios and parameters. Further research

could improve the works in this dissertation by overcoming some of the disadvantages. For example, recent advances in evaluating subjective motion comfort and predicting motion sickness could be utilized to guide the design of motion planning and suspension control algorithms. There is also a strong need for validation in terms of improved motion comfort or reduced motion sickness in real-world experiments. Performing such experiments requires various resources including but not limited to testing grounds, vehicles with self-driving capability, and legislative approvals. The outcome could assist in standardizing the evaluation of motion planners of future AVs regarding their comfort level.

SAMENVATTING

Dit proefschrift is gewijd aan het begrijpen van het potentieel van het verbeteren van het bewegingscomfort van geautomatiseerde voertuigen en onderzoekt meerdere opties die dit doel dienen. Comfort krijgt meestal voorrang op factoren als veiligheid en efficiëntie, maar is desondanks van invloed op de acceptatie van geautomatiseerde voertuigen. Het doel om het bewegingscomfort te verbeteren overlapt met de noodzaak om de uitdagingen van het fenomeen bewegingsziekte te overwinnen. Bewegingsziekte blijkt een aanzienlijk deel van de reizigers in alle soorten vervoer te treffen. Het ontwikkelt zich meestal sneller bij inzittenden die niet betrokken zijn bij de rijtaak. De symptomen kunnen het voor passagiers moeilijk maken om taken uit te voeren die niet met het rijden te maken hebben (NDRT's). Daarom is een deel van het onderzoek in dit proefschrift specifiek gericht op het verminderen van bewegingsziekte in geautomatiseerde voertuigen.

De potentiële verbetering in bewegingscomfort wordt weergegeven door het verschil tussen een basisprestatie van menselijke bestuurders en het niveau dat haalbaar is voor geautomatiseerde voertuigen. De prestatie wordt aangeduid als een combinatie van bewegingscomfort en tijdsefficiëntie, vanwege het conflicterende karakter tussen beide. De meting van comfort is verder onderverdeeld in twee takken, de ene richt zich op versnellingen in het algemeen, terwijl de andere zich specifiek richt op bewegingsziekte door de frequentiesamenstelling van de door de passagiers ervaren versnellingen te analyseren. Eerst werd een poging gedaan om de basislijn van de menselijke bestuurder vast te stellen door bestaande naturalistische rijgegevens op rotondes te analyseren. Er werd een op optimalisatie gebaseerd schema geïmplementeerd om meetruis te ondervangen en foutieve registraties werden verwijderd met behulp van de techniek van principale-componentenanalyse. De gegevens suggereerden een voorkeur voor piekversnellingen van ongeveer 1.90 m/s^2 in de lengterichting en 3.57 m/s^2 in de dwarsrichting bij het meest complexe type manoeuvre. Er werd echter geen zinvolle indicatie van de tijdsefficiëntie verkregen vanwege de inconsistente en onvolledige dekking van de registraties in de direct beschikbare dataset. Dit heeft direct geleid tot een experiment op de weg om gegevens op maat te verzamelen met als doel het menselijk rijcomfort te begrijpen. Een groep deelnemers werd gerekruteerd uit het publiek en kreeg de opdracht om met een met instrumenten uitgerust voertuig door een aangewezen route te rijden waarbij snel opeenvolgende snelheidsveranderingen en meerdere bochten voorkomen. Een gemiddelde duur van 76,5 seconden werd waargenomen bij de opgenomen ritten, terwijl het gemiddelde acceleratieongemak werd gevonden op 211.4 m^2/s^3. De gemiddelde piekversnelling in de dwarsrichting komt overeen met de analyse van gegevens van natuurlijke ritten, terwijl de gemiddelde piekversnelling in de lengterichting ongeveer 48% hoger is dan eerdere bevindingen door de uitbreiding van het registratiebereik.

De bovengrens van comfort en tijdsefficiëntieprestaties van geautomatiseerde voertuigen wordt bepaald met een optimalisatiegebaseerd bewegingsplanningsalgoritme. Een frequentie-gewogen weergave van voorspelde misselijkheid is voorgesteld en opgeno-

men in het algoritme om het idee van het verminderen van bewegingsziekte met geautomatiseerde voertuigen te bewijzen. Omdat het vrij zijn van symptomen van bewegingsziekte wordt beschouwd als een interpretatie van bewegingscomfort die vooral zinvol is in de context van geautomatiseerde voertuigen. De bewegingsplanner genereert het spatiotemporele traject van het voertuig door de relatieve positie binnen de rijbaan te bepalen naast een snelheidsprofiel. In vergelijking met het optimaliseren voor de alternatieve doelstelling die alle vlakke versnellingen gelijkelijk aanpakt, werd een potentiële vermindering van 11,3% in gekwadrateerde dosiswaarde voor bewegingsziekte (MSDV) bereikt wanneer dezelfde hoeveelheid reistijd werd gebruikt. De vermindering in gekwadrateerde MSDV, wanneer gekwadrateerde MSDV als doelstelling wordt gebruikt, blijkt 32% te zijn in vergelijking met de best presterende menselijke bestuurder. Ondertussen is de reductie in algemene versnellingsenergie maatregelen 19 met de doelstelling van het minimaliseren van versnelling in de bewegingsplanner. Aanvullende oorzaken van dergelijke verschillen zijn geanalyseerd om de voorwaarden voor het refereren aan de geclaimde verschillen te verduidelijken. Hoewel de inferieure precisie van menselijke bestuurders bij het besturen van de beweging van het voertuig een belangrijke factor is, heeft de aanname van de bewegingsplanner dat er geen hoogteverschillen zijn en dat het wegdek glad is, de gerapporteerde cijfers verder beïnvloed. Men moet ook in gedachten houden dat menselijke bestuurders verder geneigd kunnen zijn om fysieke inspanningen en brandstofverbruik te verminderen en een veiligheidsmarge aan te houden voor onverwachte verkeersinteracties. De terugwijkende-horizonformulering, die de praktisch haalbare werking van het voorgestelde algoritme weerspiegelt, is verder onderzocht. Een goed gekozen set preview-parameters, waaronder de preview-tijd en het planningsinterval, kan leiden tot een acceptabel niveau van prestatieverlies ten opzichte van het integrale planningsgeval (d.w.z. het oplossen van de gehele manoeuvre), terwijl de rekencomplexiteit dicht bij de realtime haalbaarheid blijft.

Verdere mogelijkheden liggen in recente ontwikkelingen in ophangingstechnologie, vandaar dat gerelateerde concepten en hun effecten zijn geanalyseerd. Meer specifiek wordt rolgecompenseerde laterale versnelling door actieve ophangingsactuatoren beschouwd als een mogelijke oplossing die al tientallen jaren wordt toegepast op spoorwegvoertuigen. De toepassing van dit concept op passagiersvoertuigen brengt uitdagingen met zich mee, waaronder de vraag naar geschikte en betaalbare actuatoren aan de hardwarekant, maar ook een geschikte besturingsstrategie. Er is een niet-lineaire modelvoorspellende controlemethode (NMPC) ontwikkeld voor voertuigen die bestuurd worden door menselijke bestuurders. De referentiegeneratie is gebaseerd op een krommingsvoorspelling om de grootte van de laterale versnelling te voorspellen en een fasevoorsprong in de rolbeweging ten opzichte van de gierbeweging te garanderen. In de rijscenario's op de snelweg, op het platteland en in de stad presteert de voorgestelde methode beter dan de specifiek afgestemde feedforward-PID-regeling, die representatief is voor de state-of-the-art oplossing die in de industrie wordt gebruikt. Een speciale warmstartstrategie op basis van hybride MPC verkort de rekentijd, waardoor de NMPC-regelaar kan werken in real-time hardware-in-the-loop (HIL) tests. De besturingsmethode lost het probleem van samenwerking met menselijke bestuurders echter niet volledig op. De beperkingen vragen om coördinatie tussen vlakke en rolbewegingen in een gecombineerd planningskader voor bewegingen van geautomatiseerde voertuigen.

Daarom is er een nieuw, op optimalisatie gebaseerd planningsalgoritme voorgesteld dat de rollende en vlakke bewegingen coördineert. Een verdere reductie tot 30,5% in acceleratiecomfort kan worden bereikt in vergelijking met het optimaliseren van alleen het horizontale vlak, d.w.z. het plannen van de voertuigbaan en -snelheid.

Desalniettemin is het onderzoekswerk in dit proefschrift van verkennende aard. De oplossingen zijn bestudeerd als proof of concept om hun potentieel en haalbaarheid aan te tonen. Naar de voorgestelde waarden in termen van potentiële prestatievoordelen moet met voorzichtigheid worden verwezen door de specifieke scenario's en parameters te vermelden. Verder onderzoek zou de werken in dit proefschrift kunnen verbeteren door enkele van de nadelen te overwinnen. Recente vooruitgang in het evalueren van subjectief bewegingscomfort en het voorspellen van bewegingsziekte zou bijvoorbeeld gebruikt kunnen worden als leidraad voor het ontwerpen van algoritmen voor bewegingsplanning en ophangingscontrole. Er is ook een sterke behoefte aan validatie in termen van verbeterd bewegingscomfort of minder bewegingsziekte in echte experimenten. Het uitvoeren van dergelijke experimenten vereist verschillende middelen, inclusief maar niet beperkt tot testterreinen, voertuigen die zelf kunnen rijden en wettelijke goedkeuringen. De resultaten zouden kunnen helpen bij het standaardiseren van de evaluatie van het comfortniveau van bewegingsplanners van toekomstige AV's.

1

Introduction

The light which puts out our eyes is darkness to us.
Only that day dawns to which we are awake.

Henry David Thoreau

1

1.1. MOTIVATION

Automated vehicles (AVs), more commonly known to the public as self-driving cars, bear the hope of changing future mobility. Human errors are most frequently found at guilt for causing road accidents, many of which are life-costing. Around 19.1% of the drivers involved in fatal traffic accidents in the US in 2020 were found exceeding speed limits, 11.6% were under alcohol or drug influence, and 7.3% were categorized as operating in a careless manner [1]. In contrast, AVs are believed to operate vigilantly and responsibly without a sense of fatigue. AVs could be equipped with a variety of sensors to simultaneously exploit different sources of information. These additional sensors significantly enhance their perception capability especially in adverse visibility conditions, e.g. in darkness, fog, or heavy precipitation. Meanwhile, AVs are expected to be more capable of controlling vehicle motion and hence improve safety. As demonstrated by the reduction in certain types of road accidents after mandating the anti-lock braking systems (ABS) and electronic stability control (ESC) on passenger vehicles, basic driver assistant functions already have a considerable positive impact [2]–[5]. One can extrapolate with confidence that AVs, when given more control over vehicle motion, would further prevent accidents due to instability. Besides enhancing safety, AVs are expected to bring environmental benefits [6]. They could help reduce the consumption of fossil fuel or alternative energy and utilize the roads more efficiently [7], [8]. These are enabled by the communication and cooperation between AVs in interactive scenarios including merging from ramps [9], forming platoons [10], and crossing intersections without the need for traffic lights. They could also improve society's well-being and productivity, by letting those unable to drive a car still enjoy the convenience of moving unburdened and freeing the hands and eyes of those who used to be at the controls. These attractive advantages have drawn significant and continuously growing research interests and development efforts.

However, the benefit of boosting productivity by deploying AVs is not guaranteed. It faces challenges from a phenomenon called motion sickness. As suggested by its name, motion sickness is a syndrome that occurs when human bodies are subjected to motions. It is commonly observed in various modes of transport as well as in amusement rides. The symptoms of motion sickness can vary from stomach awareness and sweating to nausea and vomiting, depending on the severity. It is difficult for the occupants to efficiently conduct other activities under the influence of motion sickness symptoms [11]. The susceptibility to motion sickness varies between individuals but approximately % of the population is affected by it. The provision of an external view, especially a front-facing one, is found to be highly effective in mitigating motion sickness [12]. Hence, the more susceptible passengers are recommended to take the seats in the front rows. However, most secondary activities tagged as productive require sustained visual attention. This is why bus passengers are generally less likely to be constantly engaged in tasks such as reading or watching videos than those on a train. Meanwhile, drivers are found to suffer from motion sickness less frequently than passengers [13]. This advantage is because of the drivers' active engagement in controlling vehicles and their better ability to predict vehicle motion as a result. In the case of automated vehicles, the benefit of boosted productivity comes primarily from the attention previously paid by the drivers to the driving task. Now that the role has shifted, the used-to-be drivers are no longer

exempted from motion sickness. Therefore, the potential in boosting society's productivity is complicated and constrained by motion sickness. Only the part of the travel time where the vehicle motion is less aggressive, for example, on a motorway absent of congestion, could be utilized in a more productive way. This certainly seems disappointing in contrast to the high expectations from AVs. Nevertheless, a high degree of automation does offer extra opportunities. Researchers have found certain correlations between the occurrence of motion sickness and specific features of vehicle motion. Multiple experimental studies revealed that low-frequency acceleration components play the most important role in causing motion sickness [14]–[16]. Hence a driving style that exhibits less low-frequency accelerations could possibly help prevent or mitigate motion sickness. While it is unrealistic to teach human drivers to consistently follow such a driving style, it is feasible to spread certain driving styles widely alongside the deployment of AVs. The vehicles could behave as programmed by utilizing their advantages in precise perception and actuation.

Aside from motion sickness, the general motion comfort of future passenger vehicles should be improved, too. Further possibilities are brought about by advanced chassis actuation. The suspension system has been widely regarded as responsible for vertical motion comfort. However, recent development has enabled suspension actuators to generate forces actively and thus add energy to the suspension system for active control purposes. This is contrary to the conventional ones where energy can only be dissipated through heat generated by the forced flow of the hydraulic fluid in the shock absorber. These new actuators are known as active suspensions. They are already highly attractive from a vehicle dynamics perspective despite the drawbacks of increased power demand, complexity, and cost. Moreover, the active force generation capability allows manipulating vehicle body attitude to a certain extent. The function of tilting the vehicle body when cornering, first seen on railroad vehicles in the 1970s, could therefore be applied to road vehicles thanks to the active suspension actuators. There remain challenges in coping with the highly dynamic vehicle motion and more importantly, in predicting the inputs of human drivers. AVs could possibly avoid the latter because of the presence of the motion planner. Coordinating the vehicle's tilting motion with the longitudinal, lateral, and yaw motion would be an investigation of unique potential value and contribution to improving the motion comfort of AV passengers.

The main purpose of this dissertation is to explore the concepts derived from the discussions above to enhance the motion comfort of AVs and help realize the societal benefits of boosting productivity. The demonstration of the advantages will be achieved through comparison with baselines represented by what would otherwise be achievable with human-driven vehicles. The latter should be determined with extra caution. An underestimated baseline may likely lead to exaggerated benefits of the proposed methods. The conclusions and recommendations based on these inflated figures are deemed misleading for allocating future efforts and resources. Therefore, the performance baselines in this dissertation are primarily based on separate research works with the objective of finding the actual limits. Through this process, the need for new technical solutions is validated and new insights into human drivers are generated.

1

1.2. RELATED WORKS

1.2.1. MOTION SICKNESS

Transportation is not at all enjoyable to a large portion of the population. Regardless of whether inside a car, a bus, a boat, or an airplane, some passengers would start to develop motion sickness rapidly. Researchers have been working on understanding the underlying mechanism of motion sickness in order to mitigate and prevent its occurrence. The most popular and convincing theory on the cause of motion sickness is sensory conflict. Human beings can sense their ego-motion from various sources, primarily using their eyes and the vestibular system. The former relies on the optic flow, i.e., how the surrounding objects move when imaged in human eyes. It provides a relative sense of motion with respect to certain reference objects. The latter refers to the sensory system existing in vertebrates critical for balancing body movements. It comprises semicircular canals and the otolith organ. The semicircular canals are mainly responsible for sensing spatial orientation, whereas the otolith organ is mainly responsible for sensing translational accelerations. Essentially, the human brain compares these resources of information in order to balance the body. According to the sensory conflict theory [17], a consensus may not be reached in certain circumstances when the two primary sources conflict with each other. This then causes problems for the brain to estimate ego movement and hence motion sickness occurs. It was argued that a mismatch can also occur within the vestibular system itself, given the evidence that a similar nauseous sense could arise when, for example, the head is tilted when subjected to sustained yaw motion.

Several models for predicting the occurrence and severity of motion sickness have been developed based on the sensory conflict theory. A neural mismatch model was proposed in [17], suggesting that motion sickness occurs when the brain is unable to find a pair of motor commands and sensory inputs in its memory that matches the current ones. The mismatch causes motion sickness when its strength exceeds a certain threshold and an update in the stored information happens in the meantime, which allows gradual adaptation to the current inputs and reduction in the severity of motion sickness. While the model can very well explain the occurrence of motion sickness in a variety of situations, it raises the question of whether the symptoms are advantageous reflexes that, for example, increase the chance of survival. It is also only a rule-based model that does not quantitatively predict the severity of motion sickness, nor its evolution in time. The temporal dynamics of motion sickness were modeled in [18], [19] in an attempt to quantify the strength of the sensory conflict, by utilizing an observer that is typically used in control systems to determine states that are not directly measurable (see Fig. 1.1). Despite the similarity in the general trend of subjective discomfort between the actual response of participants and the model output, it was indicated that there were nonlinear dynamic processes that could not be captured by the observer. Furthermore, the imaginary conflict signal had not seen support from any physiological evidence. The observer model was then extended or effectively simplified in [20] where it was asserted that only the conflict between the sensed vertical and expected vertical is a provoking factor of motion sickness.

Meanwhile, skepticism on the sensory conflict theory arises from the hypothesized conflict signal without biological evidence and its shortcomings in distinguishing whether

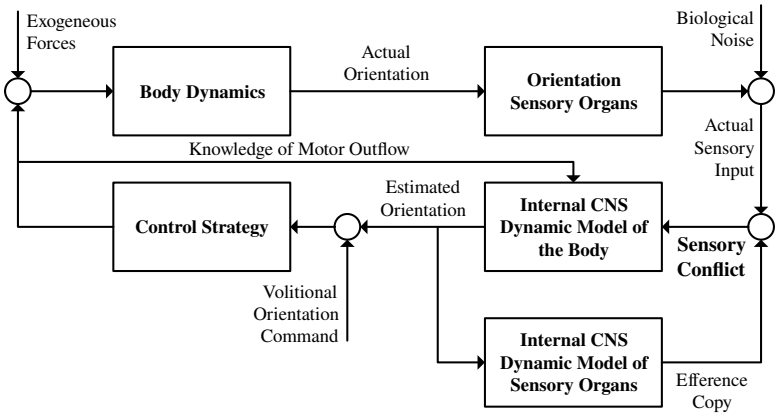

Figure 1.1: The observer model of motion sickness according to the sensory conflict theory, adopted from [18].

certain situations would or would not be nauseogenic [21]. This is aligned with the acknowledgment that observer-based models could well mimic the trajectory of motion sickness in multiple situations but not universally and reliably predict its occurrence. An alternative theory to motion sickness was proposed in [22], based on the observations of postural instability as a company to motion sickness symptoms. It is asserted that rather than failing to estimate the body posture, failing to stabilize it is what causes motion sickness. According to this theory, increasing physical restraint should help reduce motion sickness. This prediction is dismissed by experiments in [23] that no significant difference was found. The postural instability theory also cannot explain the occurrence of visually induced motion sickness, e.g., when using virtual reality equipment. Some believe that postural instability is still a second-order effect of a centralized control mechanism, similar to other motion sickness symptoms albeit preceding them in time [24], [25]. Therefore, understanding, modeling, and predicting motion sickness remains an open research area.

There were other attempts aimed at directly linking body motion to the occurrence and intensity of motion sickness by skipping the discussions over the underlying mechanism. Early studies focused on seasickness, mainly caused by translational motion in the vertical direction combined with pitch and roll rotations. The concept of motion sickness dose value (MSDV) was proposed for vertical oscillations, indicating that the incidence of vomiting is strongly correlated to a value equivalent to the root-mean-square acceleration times the square-root of the duration [26]. The knowledge generated from these studies was partly incorporated into the standards for evaluating human body vibrations and comfort [27]. However, the motion regimes in road transportation are fundamentally different. Passengers are more often subjected to lateral and longitudinal accelerations combined with yaw rotations. A series of studies were conducted focusing on the occurrence of motion sickness in public road transport [14]–[16], where a strong correlation between motion sickness and low-frequency lateral accelerations was observed. Several further experiments were conducted in a more controlled setup to determine the exact frequency range that is the most influential. The horizontal translational oscilla-

tions at around 0.2 Hz are reported as the most nauseogenic according to experiments on human subjects [28]. Further research suggests that between 0.0315 and 0.2 Hz, the lateral oscillation is comparably provoking [29]. The relative importance between longitudinal and lateral motion in provoking sickness is not validated but it was recommended that the same weighting could be used [29]. The comfort threshold for fore-aft, lateral, and vertical vibrations was studied albeit for a higher frequency range than what is interesting for motion sickness research [30]. Meanwhile, no significant variance in the subjects' frequency sensitivity from 0.15 to 0.5 Hz has been observed in terms of group-average motion sickness index but the individual differences were strong[31]. Nevertheless, the findings in these studies agree that low-frequency acceleration is the major contributing factor to motion sickness. This might provide an opportunity for AVs to exploit for better comfort.

1.2.2. MOTION PLANNING

In the context of automated vehicles, motion planning often refers to the intermediate decision layer between the perception of the environment and motion control [32]. Based on the understanding of the surrounding environment, a motion planner determines how an automated vehicle should behave on the road and generates the exact path and velocity for the vehicle, which then serves as the reference for chassis and powertrain controllers to follow, although the structure could vary as in some approaches control command comes directly from a motion planner [33]. In a broader scope, the plan of the route to reach the destination could be considered high-level motion planning, too [34]. In this dissertation, the primary focus is still on the more commonly used hierarchy of perception-decision-action while the alternative approaches will be discussed only briefly. Motion planning algorithms are responsible for multiple aspects of the performance of an automated vehicle. Safe navigation and interaction with other road users are evidently the most important next to other aspects including saving energy and improving traffic capacity, as well as the specific interest of this dissertation, enhancing motion comfort.

Motion planning for comfort inherited some features from the studies on ensuring the smooth motion of wheeled or car-like robots [35]–[37]. In these studies, smoothness is a quality beneficial for minimizing the risk of mechanical damage to the robot itself or to the payload it carries. Many considered a fixed-speed motion that translates the requirement into ensuring continuity of curvature in the path or trajectory. A trajectory with continuous curvature ensures continuous lateral accelerations and bounded jerk in theory. This can be achieved with the use of Clothoid segments [38], [39], also known as the Euler spiral. There were complaints about the difficulty of computing the parameters and hence some approximate methods were developed. Nevertheless, its use case is mostly limited to smoothing the transition between line segments. A higher smoothness level could be achieved by constructing the trajectory with parametric curves such as Bezier curves [40], [41] or splines [42], [43]. By discretizing the state or action space, the techniques of lattice planning and motion primitives have been utilized [44]–[46]. In lattice planning, a grid of nodes is pre-defined in the discrete state space. Possible trajectory segments to transition from one node to another are calculated. When planning with motion primitives, on the other hand, discrete actions are to be chosen in order to

find the next node. In either approach, the resulting motion plan is limited to choosing from precalculated trajectory segments.

Some studies focused on planning vehicle velocity alone. This could be considered a generalized category of motion planning in 1-dimensional space. Velocity planning sometimes concerns energy-saving benefits. For example, the powertrain characteristics could be incorporated when deciding the acceleration magnitude in order to operate in the most efficient range [47], [48]. Vehicle speed could also be planned such that the vehicle arrives at a signalized intersection at the moment when it has the right to pass [49], [50]. A less aggressive acceleration could be chosen accordingly and the amount of dissipated kinetic energy is minimized. Similarly, the acceleration process on the motorway ramps could be planned for a safe and comfortable merging [48], [51]. This already partly overlaps with the need for improving comfort as less change in speed will be incurred. Smooth transitions between different target velocities could be achieved by using parametric curves [41], [52]. Optimization-based approaches have been explored where the aim was to minimize maneuver time without violating constraints on jerks [53].

Nevertheless, the aforementioned approaches do not find the 'most comfortable possible' motion plan. Reaching this goal depends fundamentally on the interpretation of comfort. In the Cambridge Academic Content Dictionary, comfort is defined as the pleasant and satisfying feeling of being physically or mentally free from pain and suffering [54]. In our view, the pain and suffering would most likely originate from motion sickness in the context of automated vehicles and their users. The mitigation of motion sickness relies on the quantitative prediction of its occurrence and severity. Such knowledge is continuously accumulated and discussed in 1.2.1. For motion planning algorithms, it is the most convenient to use planar accelerations to indicate discomfort. It partly covers the interest in low-frequency accelerations as the high-frequency components are less significant due to the filtering effect of vehicle dynamics. It is possible to optimize comfort by using the total acceleration in the objective function of an optimization problem [55]. Incorporating frequency sensitivity for predicting motion sickness is challenging for a numerical optimization framework [56]. There are mainly two approaches to performing such computation. One approach is decomposing the signal with Fast Fourier Transform (FFT) [57]. The components are weighted according to recommendations and summed to obtain the total power. This approach gives a high level of freedom in applying arbitrary weights. The computational complexity of this approach is tremendous, as FFT is performed for each evaluation of the objective function. This approach also causes problems for gradient-based optimization algorithms prone to converge to a local minimum. The other approach is to employ a band-pass filter. The actual acceleration is fed through a band-pass filter and the output of the filter is effectively the weighted acceleration. This approach is less demanding on computation because the weighting is merely an additional part of the dynamics described by the prediction model. However, the weighting on different frequency components is less flexible and with lower accuracy. This is constrained by the order of a band-pass filter being an integer. The asymptotic slope of the weighting curve has to be a multiple of -20dB/decade and cannot change abruptly at the cut-off frequencies. Besides, the order of the filter directly impacts the complexity of computation. Meanwhile, this drawback may not be as significant because of the uncertainty in the recommended weight-

ing pattern. A one-to-one matching of the weighting curve might not be necessary as the recommendations mostly agree on a frequency range of interest but not on the exact severity of predicted motion sickness.

1.2.3. ACTIVE SUSPENSION AND CONTROL

The suspension system is critical to the comfort and handling quality of a road vehicle. Its main function is to support the vehicle body while isolating and absorbing the disturbances from the road. Apart from the vertical oscillations, suspensions are further responsible for minimizing the pitch and roll rotations of the vehicle body when longitudinal or lateral accelerations are present or asymmetric loads are placed on the wheels. The supportive and stabilizing function of the suspension system is enabled by the relative motion between the wheel and the vehicle body, and the forces generated in this process. The primary source of such forces is the elastic component, most commonly in the form of a spring, and the damping component, i.e., a damper or shock absorber. The former plays a supportive role by keeping the vehicle body around an equilibrium while the latter dissipates the energy stored in the former, suppressing the residual oscillations. In the majority of past and current passenger vehicles, the spring and damper have a fixed set of characteristics that is designed by the manufacturer. The spring and damper characteristics are chosen to achieve a finely balanced compromise between comfort and handling, an indicator of safety characterized by stable road-wheel contact (often referred to as road holding). As constrained by the dynamics of the wheel-body system, improving comfort-related performance indicators causes deteriorating handling performance. In other words, more stable body motion is achieved at the cost of less stable wheel motion.

Active suspensions were developed to push the boundary of this trade-off. Depending on their actuation capability, active suspensions are typically classified into adaptive, semi-active, and fully active suspensions. Adaptive suspensions feature multiple user-selected damping modes so that the dynamic characteristics of the suspension can adapt to user preferences. Semi-active suspensions often include electronically controlled dampers that have continuously adjustable damping or achieve a similar effect with fast switching between a softer and a stiffer mode [58], [59]. The fundamental difference between the fully active suspension and the rest is its capability to add energy to the suspension system. This is most commonly enabled by an additional pump in the hydraulic circuit [60] but could also be achieved with electromagnetic actuation [61]. Active force generation in the suspension system promotes simultaneous improvement in both comfort and handling [62]. More interestingly, the fully active suspension allows active control of the vehicle body's attitude. This is beneficial to the comfort in other motion regimes than what suspensions are primarily designed for. The concept of tilting the vehicle body during a turn was proposed in the 1960s for railway applications [63] to accommodate the demand for operating faster trains on the existing routes (see Fig. 1.3). The banking angle effectively projects gravity in the opposite direction of the centrifugal force experienced by the passengers. It hence reduces the passengers' perceived disturbance on their body postures and the incidence of motion sickness (see Fig. 1.2). However, the implementation of this concept was complicated by the coupling effects discussed in 1.2.1, that a combined rotational motion regime may strongly provoke

Figure 1.2: Balancing centrifugal force with gravity by leaning the body of a single-track vehicle inwards.

motion sickness. Therefore, extra caution should be taken when implementing the curve tilting concept where the yaw rotation is coupled with the roll. It has been recommended that yaw rotation should trail the roll, meaning that the desired roll angle should be approached prior to the entry of a turn. While this requirement could be met on railroad vehicles given the fixed track and the long and gentle turns, the transfer to the automotive domain is faced with challenges. Essentially, the control of such functionality of the active suspensions relies on the prediction of vehicle motion, especially the yaw rotation and lateral acceleration. The desired tilt angle needs time to be reached as the roll rate should be bounded for rotation-related comfort. The steering input cannot be used as a predictor with a sufficient leading margin. Existing applications rely on the camera view for such prediction [64]. By previewing road curvature and measuring vehicle speed, lateral acceleration could be roughly estimated. Nevertheless, the tilting behavior is conservative to avoid surprising the driver. In automated vehicles, this function could be facilitated by the additional sensing and processing capability. Vehicle motion becomes more predictable thanks to the advances in motion planning and chassis control, hence the roll motion could be better coordinated and the actuation capability from the active suspensions could be better utilized.

1.3. OVERVIEW OF CHAPTERS

This dissertation comprises six chapters in total. The following text aims to help the readers navigate through the contents by explaining the focus of each chapter and the connections in between. Chapter 1 has explained the motivation leading to the research works in this dissertation next to the technical background and related works described above. The four chapters that follow provide detailed explanations of the research work conducted and discussions about how the results should be interpreted. Essentially, the dissertation tries to answer how and how much future automated vehicles could improve motion comfort over the existing ones controlled by human drivers. For this purpose, the first step was to quantify the performance of human drivers, which will be the topic of Chapter 2. Then, the potential improvement over human drivers using motion planning algorithms is investigated in Chapter 3. The use of active suspensions is intro-

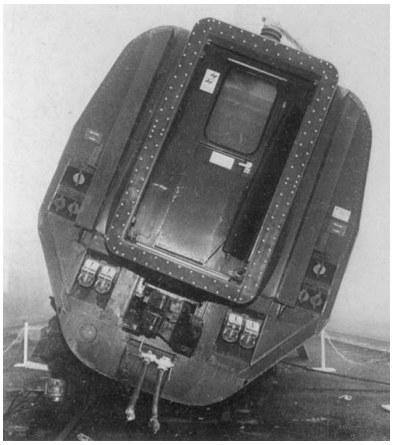

Figure 1.3: The Advanced Passenger Train prototype vehicle undergoing the test for maximum tilting angle, from [65]

duced first in Chapter 4, with an attempt to determine the limitations of the preview-based curve tilting function in a human-driven vehicle. In Chapter 5, the motion planning framework proposed in Chapter 3 is modified to incorporate the possibility of curve tilting, demonstrating the extra benefit of equipping automated vehicles with active suspensions. Chapter 6 contains conclusions based on the findings from Chapters 2-5 and recommendations for future works in a similar direction. A more informative summary of the contents of Chapters 2-5 can be found below.

1.3.1. CHAPTER 2

Two approaches to evaluating and quantifying the performance of human drivers in terms of comfort and time efficiency are introduced. The first approach is based on a naturalistic driving dataset published online. The data was collected for purposes other than measuring the driving performance of human drivers. Using optimization-based processing methods, the noise and discontinuity problem in the raw data was resolved. However, only insights into the peak acceleration level of human drivers were obtained. This was due to the lack of control over the start and end of the recordings, which lead to inconsistent distances among the trajectories. Hence, it is not fair to compare the duration of the recorded runs. In order to overcome these drawbacks, a dedicated experiment was designed and conducted in the Netherlands. The accelerations were measured with an onboard inertial measurement unit (IMU) and the test runs were timed according to GPS positions. The size of the participant group, namely 16, was limited by time and budget. Nevertheless, valuable knowledge has been obtained from the driving data recorded from their driving. The data is highly useful in understanding the limitations of human driving capability and in demonstrating the potential improvement achievable with automated vehicles.

1.3.2. CHAPTER 3

An optimization-based motion planning framework is proposed and evaluated. The fundamental goal is to calculate a trajectory for the vehicle to follow that provides optimal motion comfort by fully utilizing the permissible driving space. Two measures of comfort are explored here: one is the general acceleration comfort and the other is the frequency-weighted acceleration comfort closely related to motion sickness. Time efficiency is another component of the objectives. Including this factor prevents the choice of unnecessarily low speeds that are undesirable by both the passengers onboard and other road users. The weight placed on time efficiency effectively regulates the aggressiveness of the planned motion. The performance of the motion planners is compared to the human driving data obtained and analyzed in Chapter 2. It is evident that automated vehicles could improve motion comfort over human drivers by an attractive margin. The potential is greater in mitigating motion sickness than in minimizing accelerations in general.

1.3.3. CHAPTER 4

The use of nonlinear model predictive control (NMPC) techniques is explored in order to improve the control quality of the curve tilting functionality in a human-driven vehicle. Similar to previous studies, the function relies on the preview of road curvature to ensure that the roll motion has a phase lead over the yaw motion. While NMPC is a powerful tool to improve control performance, it suffers from a significant computational burden when deployed as a real-time control system. Therefore, a warm-start strategy is developed in order to facilitate online optimization. This is achieved by pre-computing an explicit sub-optimal control law that serves as an informed initial guess of the solution to the optimal control problem. The control quality and real-time capability of the proposed method were verified in a hardware-in-the-loop simulation setup using different driving scenarios. The proposed method could return a control input before the next sampling step by performing a limited number of iterations in online optimization. The control quality is better than the state-of-the-art industrial solution of proportional–integral–derivative (PID) control with feedforward and scenario-specific tuning. Nevertheless, the application is still hampered by the difficulty in predicting vehicle motion. More potential is expected from the combination of automated driving and active suspensions.

1.3.4. CHAPTER 5

The recommended direction of incorporating curve tilting into the motion planning problem is investigated. The possibility of reducing lateral acceleration with active attitude control is explored using the motion planning framework proposed in Chapter 3. In this study, the roll angle of the vehicle body is further included as a part of the decision variables. Hence the planar motion and the roll rotation are coordinated, which prompts better utilization of the active suspensions' capability. Further reduction of overall acceleration discomfort was achieved over the case without active suspensions. Furthermore, the accurate execution of the planned planar motion was found to simplify the control of active suspensions. The disturbances in terms of centrifugal accelerations can be compensated for thanks to the knowledge of future vehicle motion. This partly offsets the

need for a complex control algorithm such as what was described in Chapter 4.

1.4. CONTRIBUTIONS

The research works described in this dissertation have contributed to several steps forward in various directions in the field of motion comfort in automated vehicles. These include:

- Analysis of a naturalistic driving dataset that reveals the preferences of human drivers in maximum longitudinal and lateral accelerations. The distribution of peak magnitudes helps determine a generally acceptable level of aggressiveness of automated vehicles.
- Experimental collection of human driving data on public roads that quantifies the performance of human drivers in motion comfort and time efficiency. The data, published in an open-access dataset, provide especially valuable insights into the distribution of acceleration power in the frequency domain that is interesting for motion sickness-related studies. It also reveals additional considerations from human drivers that lead to the different features in the motion profiles.
- Formulation of a frequency-weighting approach in a spatiotemporal motion planning framework that enables a targeted minimization of accelerations in the most sickness-inducing frequency range. The effectiveness of the formulation is demonstrated by comparison with a non-weighted variant. A receding-horizon variant further revealed the additional computational complexity involved, showing that a lower update frequency is feasible for real-time implementation.
- Design of an NMPC controller that realizes the curve tilting concept with active suspensions. The method outperforms the state-of-the-art approach in terms of tracking quality. The dedicated warm-start strategy reduces online computational demand and enables real-time implementation on prototype hardware with scarce computational resources.
- Formulation of a novel 3-dimensional motion planning algorithm that computes a coordinated plan of planar and roll motion of automated vehicles. The algorithm suggests a considerable advantage over only optimizing the planar motion.

BIBLIOGRAPHY

[1] N. C. for Statistics and Analysis, "Traffic safety facts 2020: A compilation of motor vehicle crash data", National Highway Traffic Safety Administration, Washington, DC, Tech. Rep. DOT HS 813 375, Oct. 2022.

[2] L. Evans and P. H. Gerrish, "Antilock brakes and risk of front and rear impact in two-vehicle crashes", *Accident Analysis & Prevention*, vol. 28, no. 3, pp. 315–323, 1996.

[3] A. Lie, C. Tingvall, M. Krafft, and A. Kullgren, "The effectiveness of esp (electronic stability program) in reducing real life accidents", *Traffic Injury Prevention*, vol. 5, no. 1, pp. 37–41, 2004.

[4] C. J. Kahane and J. N. Dang, "The long-term effect of abs in passenger cars and ltvs", National Highway Traffic Safety Administration, Washington, DC, Tech. Rep. DOT HS 811 182, Aug. 2009.

[5] A. Lyckegaard, T. Hels, and I. M. Bernhoft, "Effectiveness of electronic stability control on single-vehicle accidents", *Traffic Injury Prevention*, vol. 16, no. 4, pp. 380–386, 2015.

[6] M. Taiebat, A. L. Brown, H. R. Safford, S. Qu, and M. Xu, "A review on energy, environmental, and sustainability implications of connected and automated vehicles", *Environmental science & technology*, vol. 52, no. 20, pp. 11 449–11 465, 2018.

[7] A. Talebpour and H. S. Mahmassani, "Influence of connected and autonomous vehicles on traffic flow stability and throughput", *Transportation research part C: emerging technologies*, vol. 71, pp. 143–163, 2016.

[8] D. Milakis, M. Snelder, B. Van Arem, B. Van Wee, and G. H. de Almeida Correia, "Development and transport implications of automated vehicles in the netherlands: Scenarios for 2030 and 2050", *European Journal of Transport and Infrastructure Research*, vol. 17, no. 1, 2017.

[9] Z. Gao, Z. Wu, W. Hao, K. Long, Y.-J. Byon, and K. Long, "Optimal trajectory planning of connected and automated vehicles at on-ramp merging area", *IEEE Trans. Intell. Transp. Syst.*, vol. 23, no. 8, pp. 12 675–12 687, 2022.

[10] M. Wang, S. van Maarseveen, R. Happee, O. Tool, and B. van Arem, "Benefits and risks of truck platooning on freeway operations near entrance ramp", *Transp. Research Record*, vol. 2673, no. 8, pp. 588–602, 2019.

[11] J. Smyth, S. Birrell, A. Mouzakitis, and P. Jennings, "Motion sickness and human performance–exploring the impact of driving simulator user trials", in *Int. Conf. Applied Human Factors and Ergonomics*, Springer, 2018, pp. 445–457.

[12] T. Irmak, D. M. Pool, and R. Happee, "Objective and subjective responses to motion sickness: The group and the individual", *Experimental Brain Research*, vol. 239, no. 2, pp. 515–531, 2021.

[13] T. Wada, "Motion sickness in automated vehicles", in *Advanced Vehicle Control AVEC'16*, Crc Press, 2016, pp. 169–174.

[14] M. Turner and M. J. Griffin, "Motion sickness in public road transport: The relative importance of motion, vision and individual differences", *British J. Psychology*, vol. 90, no. 4, pp. 519–530, 1999.

[15] M. Turner, "Motion sickness in public road transport: Passenger behaviour and susceptibility", *Ergonomics*, vol. 42, no. 3, pp. 444–461, 1999.

[16] M. Turner and M. J. Griffin, "Motion sickness in public road transport: The effect of driver, route and vehicle", *Ergonomics*, vol. 42, no. 12, pp. 1646–1664, 1999.

[17] J. T. Reason, "Motion sickness adaptation: A neural mismatch model", *J. Royal Society of Medicine*, vol. 71, no. 11, pp. 819–829, 1978.

[18] C. M. Oman, "Sensory conflict in motion sickness: An observer theory approach", 1989.

[19] C. M. Oman, "Motion sickness: A synthesis and evaluation of the sensory conflict theory", *Canadian J. Physiology and Pharmacology*, vol. 68, no. 2, pp. 294–303, 1990.

[20] J. Bos and W. Bles, "Modelling motion sickness and subjective vertical mismatch detailed for vertical motions", *Brain Res. Bulletin*, vol. 47, no. 5, pp. 537–542, 1998.

[21] T. A. Stoffregen and G. E. Riccio, "An ecological critique of the sensory conflict theory of motion sickness", *Ecological Psychology*, vol. 3, no. 3, pp. 159–194, 1991.

[22] G. E. Riccio and T. A. Stoffregen, "An ecological theory of motion sickness and postural instability", *Ecological Psychology*, vol. 3, no. 3, pp. 195–240, 1991.

[23] L. Warwick-Evans, N. Symons, T. Fitch, and L. Burrows, "Evaluating sensory conflict and postural instability. theories of motion sickness", *Brain research bulletin*, vol. 47, no. 5, pp. 465–469, 1998.

[24] R. S. Kennedy and K. M. Stanney, "Postural instability induced by virtual reality exposure: Development of a certification protocol", *International Journal of Human-Computer Interaction*, vol. 8, no. 1, pp. 25–47, 1996.

[25] J. E. Bos, "Nuancing the relationship between motion sickness and postural stability", *Displays*, vol. 32, no. 4, pp. 189–193, 2011.

[26] A. Lawther and M. J. Griffin, "Prediction of the incidence of motion sickness from the magnitude, frequency, and duration of vertical oscillation", *J. Acoustical Society of America*, vol. 82, no. 3, pp. 957–966, 1987.

[27] "Mechanical vibration and shock — evaluation of human exposure to whole-body vibration — part 1: General requirements", International Organization for Standardization, Geneva, CH, Standard, May 1997.

[28] J. F. Golding, A. Mueller, and M. A. Gresty, "A motion sickness maximum around the 0.2 hz frequency range of horizontal translational oscillation", *Aviation, Space, and Environ. Medicine*, vol. 72, no. 3, pp. 188–192, 2001.

[29] B. E. Donohew and M. J. Griffin, "Motion sickness: Effect of the frequency of lateral oscillation", *Aviation, Space, and Environ. Medicine*, vol. 75, no. 8, pp. 649–656, 2004.

[30] M. Morioka and M. J. Griffin, "Magnitude-dependence of equivalent comfort contours for fore-and-aft, lateral and vertical whole-body vibration", *J. Sound and Vibration*, vol. 298, no. 3, pp. 755–772, 2006.

[31] T. Irmak, K. N. de Winkel, D. M. Pool, H. H. Bülthoff, and R. Happee, "Individual motion perception parameters and motion sickness frequency sensitivity in fore-aft motion", *Experimental Brain Res.*, vol. 239, no. 6, pp. 1727–1745, 2021.

[32] L. Claussmann, M. Revilloud, D. Gruyer, and S. Glaser, "A review of motion planning for highway autonomous driving", *IEEE Transactions on Intelligent Transportation Systems*, vol. 21, no. 5, pp. 1826–1848, 2019.

[33] L. Ferranti, B. Brito, E. Pool, *et al.*, "Safevru: A research platform for the interaction of self-driving vehicles with vulnerable road users", in *2019 IEEE Intelligent Vehicles Symposium (IV)*, IEEE, 2019, pp. 1660–1666.

[34] Z. Li, I. V. Kolmanovsky, E. M. Atkins, J. Lu, D. P. Filev, and Y. Bai, "Road disturbance estimation and cloud-aided comfort-based route planning", *IEEE transactions on cybernetics*, vol. 47, no. 11, pp. 3879–3891, 2016.

[35] J.-P. Laumond *et al.*, *Robot motion planning and control*. Springer, 1998, vol. 229.

[36] X.-N. Bui, J.-D. Boissonnat, P. Soueres, and J.-P. Laumond, "Shortest path synthesis for dubins non-holonomic robot", in *Proceedings of the 1994 IEEE International Conference on Robotics and Automation*, IEEE, 1994, pp. 2–7.

[37] A. Scheuer and T. Fraichard, "Continuous-curvature path planning for car-like vehicles", in *Proceedings of the 1997 IEEE/RSJ International Conference on Intelligent Robot and Systems. Innovative Robotics for Real-World Applications. IROS'97*, IEEE, vol. 2, 1997, pp. 997–1003.

[38] J. A. Silva and V. Grassi, "Clothoid-based global path planning for autonomous vehicles in urban scenarios", in *Proc. IEEE Int. Conf. Robot. and Automat. (ICRA)*, IEEE, 2018, pp. 4312–4318.

[39] S. Zhang, Y. Chen, S. Chen, and N. Zheng, "Hybrid A*-based curvature continuous path planning in complex dynamic environments", in *Proc. IEEE Intell. Transp. Syst. Conf. (ITSC)*, IEEE, 2019, pp. 1468–1474.

[40] X. Qian, I. Navarro, A. de La Fortelle, and F. Moutarde, "Motion planning for urban autonomous driving using bézier curves and mpc", in *Proc. IEEE 19th Int. Conf. Intell. Transp. Syst. (ITSC)*, Ieee, 2016, pp. 826–833.

[41] R. Lattarulo, L. González, and J. Perez, "Real-time trajectory planning method based on n-order curve optimization", in *Proc. 24th Int. Conf. Syst. Theory, Control and Computing (ICSTCC)*, IEEE, 2020, pp. 751–756.

[42] F. Hegedüs, T. Bécsi, S. Aradi, Z. Szalay, and P. Gáspár, "Real-time optimal motion planning for automated road vehicles", *IFAC-PapersOnLine*, vol. 53, no. 2, pp. 15 647–15 652, 2020.

[43] H. Cao and M. Zoldy, "Implementing B-spline path planning method based on roundabout geometry elements", *IEEE Access*, vol. 10, pp. 81 434–81 446, 2022.

[44] C. L. Bottasso, D. Leonello, and B. Savini, "Path planning for autonomous vehicles by trajectory smoothing using motion primitives", *IEEE Trans. Control Syst. Technol.*, vol. 16, no. 6, pp. 1152–1168, 2008.

[45] M. McNaughton, C. Urmson, J. M. Dolan, and J.-W. Lee, "Motion planning for autonomous driving with a conformal spatiotemporal lattice", in *Proc. IEEE Int. Conf. Robot. and Automat. (ICRA)*, IEEE, 2011, pp. 4889–4895.

[46] M. Mischinger, M. Rudigier, P. Wimmer, and A. Kerschbaumer, "Towards comfort-optimal trajectory planning and control", *Veh. Syst. Dynamics*, vol. 57, no. 8, pp. 1108–1125, 2019.

[47] B. Zhang, W. Cao, and T. Shen, "Two-stage on-board optimization of merging velocity planning with energy management for hevs", *Control Theory and Technology*, vol. 17, no. 4, pp. 335–345, 2019.

[48] S. Xu and H. Peng, "Design and comparison of fuel-saving speed planning algorithms for automated vehicles", *IEEE Access*, vol. 6, pp. 9070–9080, 2018.

[49] G. Mahler and A. Vahidi, "An optimal velocity-planning scheme for vehicle energy efficiency through probabilistic prediction of traffic-signal timing", *IEEE Transactions on Intelligent Transportation Systems*, vol. 15, no. 6, pp. 2516–2523, 2014.

[50] E. R. Müller, B. Wahlberg, and R. C. Carlson, "Optimal motion planning for automated vehicles with scheduled arrivals at intersections", in *2018 European Control Conference (ECC)*, IEEE, 2018, pp. 1672–1678.

[51] I. A. Ntousakis, I. K. Nikolos, and M. Papageorgiou, "Optimal vehicle trajectory planning in the context of cooperative merging on highways", *Transportation research part C: emerging technologies*, vol. 71, pp. 464–488, 2016.

[52] D. González, V. Milanés, J. Pérez, and F. Nashashibi, "Speed profile generation based on quintic bézier curves for enhanced passenger comfort", in *Proc. IEEE 19th Int. Conf. Intell. Transp. Syst. (ITSC)*, IEEE, 2016, pp. 814–819.

[53] A. Artuñedo, J. Villagra, and J. Godoy, "Jerk-limited time-optimal speed planning for arbitrary paths", *IEEE Transactions on Intelligent Transportation Systems*, vol. 23, no. 7, pp. 8194–8208, 2021.

[54] C. U. Press, *Cambridge Academic Content Dictionary* (Cambridge Academic Content Dictionary). Cambridge University Press, 2008, ISBN: 9780521871433. [Online]. Available: https://books.google.nl/books?id=gaYUAAAACAAJ.

[55] H. Shin, D. Kim, and S.-E. Yoon, "Kinodynamic comfort trajectory planning for car-like robots", in *Proc. IEEE/RSJ Int. Conf. Intell. Robots and Syst. (IROS)*, IEEE, 2018, pp. 6532–6539.

[56] Z. Htike, G. Papaioannou, E. Siampis, E. Velenis, and S. Longo, "Fundamentals of motion planning for mitigating motion sickness in automated vehicles", *IEEE Trans. Veh. Technol.*, vol. 71, no. 3, pp. 2375–2384, 2021.

[57] D. Li and J. Hu, "Mitigating motion sickness in automated vehicles with frequency-shaping approach to motion planning", *IEEE Robot. and Automat. Lett.*, vol. 6, no. 4, pp. 7714–7720, 2021.

[58] Y. Liu, T. Waters, and M. Brennan, "A comparison of semi-active damping control strategies for vibration isolation of harmonic disturbances", *Journal of sound and vibration*, vol. 280, no. 1-2, pp. 21–39, 2005.

[59] C. Poussot-Vassal, C. Spelta, O. Sename, S. M. Savaresi, and L. Dugard, "Survey and performance evaluation on some automotive semi-active suspension control methods: A comparative study on a single-corner model", *Annual Reviews in Control*, vol. 36, no. 1, pp. 148–160, 2012.

[60] S. Cytrynski, U. Neerpasch, R. Bellmann, and B. Danner, "The active suspension of the new mercedes-benz gle", *ATZ worldwide*, vol. 120, no. 12, pp. 42–45, 2018.

[61] B. L. Gysen, J. J. Paulides, J. L. Janssen, and E. A. Lomonova, "Active electromagnetic suspension system for improved vehicle dynamics", *IEEE transactions on vehicular technology*, vol. 59, no. 3, pp. 1156–1163, 2009.

[62] H. E. Tseng and D. Hrovat, "State of the art survey: Active and semi-active suspension control", *Vehicle system dynamics*, vol. 53, no. 7, pp. 1034–1062, 2015.

[63] H. Harris, E. Schmid, and R. Smith, "Introduction: Theory of tilting train behaviour", *Proceedings of the Institution of Mechanical Engineers, Part F: Journal of Rail and Rapid Transit*, vol. 212, no. 1, pp. 1–5, 1998.

[64] M. Bär, *Vorausschauende Fahrwerkregelung zur Reduktion der auf die Insassen wirkenden Querbeschleunigung*. Forschungsges. Kraftfahrwesen (fka), 2014.

[65] D. Boocock and B. King, "The development of the prototype advanced passenger train", *Proceedings of the Institution of Mechanical Engineers*, vol. 196, no. 1, pp. 35–46, 1982.

2

Comfort Performance of Human Drivers

Great minds discuss ideas;
average minds discuss events;
small minds discuss people.

Eleanor Roosevelt

Parts of this chapter have been published in IEEE International Conference on Intelligent Transportation Systems [1] and in review at IEEE Transactions on Intelligent Transportation Systems.

2.1. INTRODUCTION

Automated driving must demonstrate its superiority over human drivers in order to be accepted by, and ultimately attractive for the general public. Meanwhile, explainable behaviors similar to human drivers are helpful in this process, too. For either purpose, an in-depth understanding of human drivers is a necessary first step. Multiple studies explored promoting human-like driving by training a motion planner with trajectories recorded from human drivers [2]–[4]. They mainly emphasize resemblance to human actions but lack an in-depth understanding of the reasoning behind such actions. Moreover, the comfort aspects of human drivers are not extensively covered by existing literature. Specifically, there is no consensus on the choices of comfort indicator and scenario despite several valuable attempts [5], [6].

Comfort is an abstract and subjective concept that is difficult to quantify. Here, it is interpreted as a state with minimal discomfort caused by vehicle motion. It was recommended in standards to use the root-mean-square (RMS) value of the accelerations as a measure of vibrational discomfort. While it can be useful for sustained exposure of human bodies to mechanical vibrations, the focus does not match the motion comfort discussed in this dissertation. In most use cases of passenger vehicles, mechanical vibrations mainly arise from the powertrain and the road. The electrified powertrain has made substantial improvement over that relying on combustion engines in this regard. The road excitations are primarily filtered out by the suspension design and control, while the pavement quality of roads is usually high in the areas where the deployment of automated vehicles is deemed suitable. These aspects of motion comfort are not what human drivers or automated driving are primarily responsible for. Instead, the planar motions are more relevant as the most significant disturbance comes from the inertial accelerations. The planar accelerations are the results of driving inputs to the vehicle including steering wheel angle, pedal positions, and possibly the gear shifts. The RMS value may still be used on longitudinal and lateral accelerations as a measure of average comfort level for long journeys. However, averaging over time is affected by the diluting effect that driving slowly may appear to be more comfortable according to the RMS accelerations. Hence, the RMS could be misleading when used as the sole indicator of motion comfort, especially when evaluating transitional vehicle motions. In such situations, the duration is more sensitive to the choice of speed, contrary to longer trips where fixed-speed driving could be the majority.

The discussion above indicates the necessity of including time as a factor when evaluating motion comfort. Improving comfort can come at the cost of extending travel time. While turning, a gentle motion is reflected by a smaller lateral acceleration achieved by adopting a lower speed. Less aggressive acceleration and braking mean the vehicle takes a longer period of time to reach the goal speed, traveling a longer distance at a lower speed in between. These additions to the total trip time would cause frustration to the passengers. It is possible to factor in and eventually minimize such frustration by evaluating motion comfort with a two-fold indicator, with time being the additional dimension. It reflects the goal of improving motion comfort without consuming extra time, or from another perspective, saving time without sacrificing comfort. It further describes a choice of balance between comfort and time, which can be influenced by the urgency of the trip or individual preferences.

This chapter introduces two separate approaches to establishing a quantitative understanding of the comfort-related driving performance of human drivers. In the first approach, the ACFR naturalistic driving dataset [7] was analyzed. The dataset was collected at 5 public roundabouts with a total of over 23,000 recorded trajectories of passing vehicles. The traffic vehicles were tracked primarily using LiDAR, which is installed on top of the data collection vehicle parked close to the intersection. The position of recorded vehicles was estimated using the center of its bounding box. There were multiple naturalistic driving datasets available when this study was conducted with various scopes. The ACFR dataset focuses on the scenario of roundabouts, which is especially relevant and interesting for comfort-related research. On one hand, a roundabout usually involves quick consecutive changes in vehicle orientation combined with significant changes in speed. These features make it a preferable scenario that is sufficiently challenging to expose the differences among human drivers themselves as well as between human drivers and motion planners of automated vehicles. On the other hand, the scenario is compact in both space and time. This is beneficial for the purpose of comparison as the impact of uncontrolled factors is limited.

In the second approach, an experiment was designed and conducted in order to collect the driving data that better suited the research goal. The experiment was motivated by the certain limitations of analyzing existing naturalistic driving datasets. Despite being in a smaller quantity, the data collected through a dedicated experiment allows more control over the conditions. Typically, two types of experiment setups are available for this purpose. The first option is to use a driving simulator. Moving-base driving simulators can be highly beneficial, especially when investigating safety-critical scenarios [8], [9] because it minimizes the risk of causing physical harm to the participants and test equipment. In a virtual environment, it is possible to fully control factors such as traffic, weather, and lighting that are otherwise uncontrollable in the real world. This improves the consistency of recording between repetitions. A positive correlation has been found between better performance on a driving simulator and a higher pass rate on the driving test [10]. However, this does not imply a matching between the magnitudes of the vehicle motion in the virtual and real world. Motion cueing is the main limiting factor causing the mismatch. The perceived vehicle motion is downscaled significantly despite the efforts in improving the motion cueing algorithms [11]. In addition, the visualization of the virtual world could be of insufficient fidelity. Even with realistic graphics, the loss of depth perception could still cause the driver to perceive the surroundings differently and hence behave differently. Nevertheless, it is not guaranteed that a higher-fidelity simulator leads to more valid experiment results reflective of real-world driving performance. There are further issues with learning and adapting to a driving simulator before the participants could feel comfortable and confident in driving in the virtual world. The importance of adaptation has been shown with experimental studies [12], [13]. The majority of participants recruited from the general public would have little to no experience with a driving simulator. There is a risk that the results are not representative of the drivers' actual performance due to a lack of adaptation and influences from the simulator setup being used. Therefore, an on-road experiment using an instrumented vehicle was proposed. It is easier for any participant with basic driving experience to adapt to and perform properly. The measurement quality of accelerations can be improved sig-

nificantly over data collected in a remote fashion. These advantages outweigh the concern of an uncontrolled environment, especially in terms of traffic interaction, as well as the significantly higher demand on time and effort arising from sensor installation and testing, data processing, and vehicle maintenance.

2.2. PROCESSING OF NATURALISTIC DRIVING DATASET

2.2.1. OPTIMIZATION-BASED TRAJECTORY RECONSTRUCTION

The volume of data contained in the ACFR dataset is highly beneficial from a statistics viewpoint. However, the data is provided in a raw condition that requires further processing. As mentioned before, the position of passing vehicles was measured with the LiDAR sensor mounted on the roof of a parked vehicle, calculated as the center of the bounding box generated from the point cloud. This method is highly dependent on the robustness of the algorithm responsible for generating bounding boxes, hence the position data is sensitive to factors such as the orientation of the measured vehicle. This becomes an evident problem when the position data is differentiated in time in order to obtain velocity and acceleration that are of major interest when analyzing motion comfort. An optimization-based trajectory reconstruction method was proposed for handling the noise and error in the raw measurement data. The motion profiles are reconstructed based on the point-mass kinematics (2.1) to ensure feasibility and continuity. The motion of the vehicle is described by x, y, velocity v, and heading angle ψ. The motion is controlled by the longitudinal acceleration $\dot{v}$ and angular acceleration $\ddot{\psi}_i$. The equations of motion are integrated with an Euler step of t_s, the sampling time of the original data. The motion profile obtained from an input sequence is evaluated with a cost function in the form of (2.2) that penalizes the spatial deviation from the measured positions added to the input effort involved.

$$\begin{aligned} x_{i+1} &= x_i + v_i \cos\psi_i \cdot t_s \\ y_{i+1} &= y_i + v_i \sin\psi_i \cdot t_s \\ v_{i+1} &= v_i + \dot{v}_i \cdot t_s \\ \dot{\psi}_{i+1} &= \dot{\psi}_i + \ddot{\psi}_i \cdot t_s \\ \psi_{i+1} &= \psi_i + \dot{\psi}_i \cdot t_s \end{aligned} \tag{2.1}$$

$$\begin{aligned} J_1 &= \sum_{i=1}^{N} \left({\varepsilon_i}^T Q \varepsilon_i + {u_i}^T R u_i \right) \\ \varepsilon_i &= \begin{bmatrix} x_i \\ y_i \end{bmatrix}_{\text{rec}} - \begin{bmatrix} x_i \\ y_i \end{bmatrix}_{\text{est}}, u_i = \begin{bmatrix} \dot{v}_i \\ \ddot{\psi}_i \end{bmatrix} \end{aligned} \tag{2.2}$$

By minimizing this cost function, an optimal reconstruction of the recorded trajectory could be achieved. The total processing time of the entire dataset is approximately 3 days on a desktop PC (Intel Xeon W-2145 CPU). A 7th-order polynomial fitting method was implemented as an alternative approach, in order to demonstrate the benefits of incorporating basic kinematics and penalizing the input effort. Each trajectory is described with the x- and y-coordinates versus time and the two sequences are fitted into

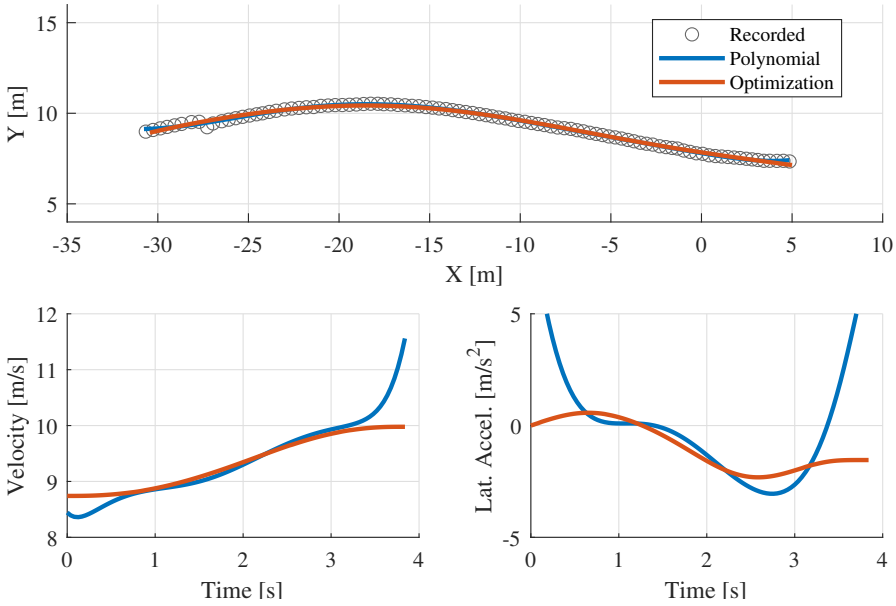

Figure 2.1: An example of the reconstructed trajectory by the optimization-based method in comparison to polynomial fitting.

two corresponding polynomials. The comparison between the two methods is given in Fig. 2.1, performed on a random recording in the dataset. It is evident that the original data is of poor quality. A strong discontinuity can be found on the left-hand side of the recorded trajectory. Both methods are able to reconstruct a smooth spatial path. However, the velocity and acceleration profiles from the polynomial method are less feasible because it solely minimizes the fitting error. The optimization-based method reflects a more reasonable driving behavior in contrast.

2.2.2. ERROR DETECTION AND REMOVAL

The ACFR dataset contains an unknown amount of erroneous recordings that are not representative of driving a passenger vehicle, for example, those of a bicycle, motorcycle, bus, or truck. To exclude these samples, the DBSCAN (density-based spatial clustering of applications with noise) algorithm is adopted. Essentially, the algorithm clusters the samples according to a distance metric (e.g., the Euclidean distance). In each iteration, a new cluster starts with a random sample that does not yet belong to any existing cluster. The cluster grows by repetitively including the nearby samples whose distance to existing samples in the cluster is below a certain threshold. The reconstructed trajectories are first interpolated into an equal number of steps so that the dimensions match. The trajectories recorded at the same location and having identical entry-exit combinations are grouped together and DBSCAN is performed separately on each group. The samples belonging to the largest cluster are considered the most representative and the rest

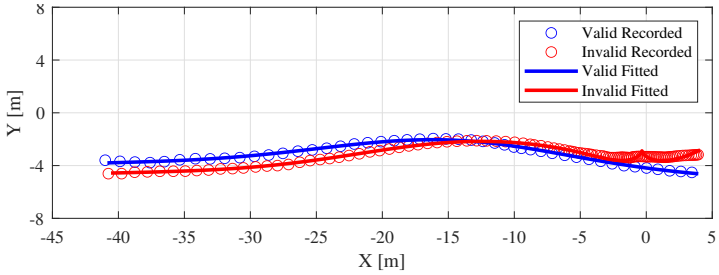

Figure 2.2: Comparison between an acceptable sample and a sample deemed invalid by DBSCAN.

are discarded. The standard implementation of DBSCAN in MATLAB is used, where the critical parameter is the distance metric. Ideally, the parameter is tuned to distinguish between erroneous samples and the samples that are only different so that the diversity in the accepted samples is still preserved. This parameter is adapted to different types of maneuvers, considering that a longer maneuver would naturally have a larger variance between drivers. Although it is infeasible to manually check all the samples, a random example of rejected recording is present in Fig. 2.2 in comparison to an accepted one. The rejected recording indeed exhibits a different behavior as the object had a significantly lower speed towards the end and departed from the drive lane after the roundabout. This could be, e.g., a cyclist mistakenly classified as a motor vehicle, diverting to the sidewalk. Fig. 2.3 shows the variance of the data before and after removing the outliers. The points on the 2-D plane represent the coefficient of the first and second principal components (PC1 and PC2, respectively) determined by the principal component analysis (PCA). The high-ranking principal components are the projected directions in which the samples have a larger variance. Thus PCA highlights the data variation in a compact manner and also simplifies the visualization. The results suggest a better concentration of data after the outliers are removed. The processed and validated recordings are collected in a dataset that is open-access via IEEE DataPort[1].

2.3. DESIGN OF DRIVING EXPERIMENT

As to be presented later in this Chapter (See Section 2.5), several shortcomings have been identified from the approach of relying on existing naturalistic driving datasets, especially one for a different purpose and with remote measurement methods. They hence motivated the conduction of a dedicated experimental study intended for gathering driving data specifically relevant to the evaluation of driving comfort and motion sickness. This Section explains the experimental design in detail.

2.3.1. PROCEDURES

Volunteers were recruited publicly to participate in the experiment. The participants were required to drive an instrumented vehicle through a part of the public road as the test route. They were specifically asked to drive smoothly and fast while staying within

[1] https://ieee-dataport.org/open-access/reconstructed-roundabout-driving-dataset

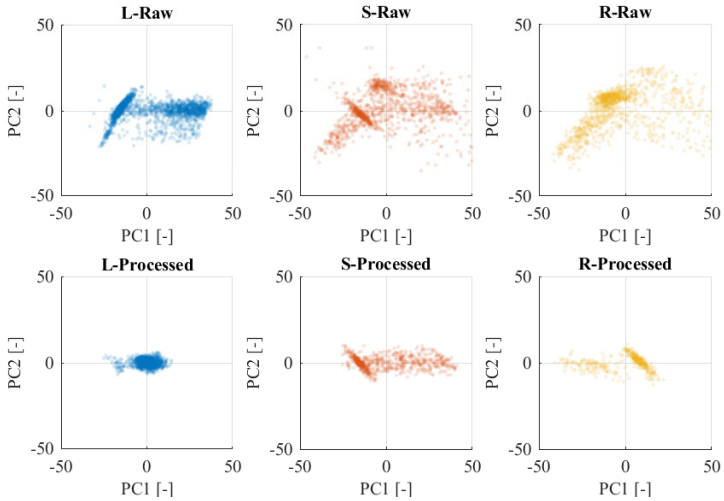

Figure 2.3: A compact visualization of data variance with PCA before (upper row) and after (lower row) removing the outliers.

the range of aggressiveness they are confident with. They were briefed about the experiment and non-sensitive personal data including gender, age range, driving frequency and experience, and familiarity with the route were collected. This is to verify if there is a statistical bias in the group. After getting seated in the vehicle, the participants were given sufficient time to familiarize themselves with the driver interface before they started driving. While driving to the starting point of the test route, they were given the opportunity to get accustomed to the vehicle's handling, e.g. the steering and pedal feel and the vehicle's response. During the actual test, the participants drove the vehicle through a pre-defined route while the position and acceleration data were being recorded. It is obvious that interacting with other road users has a negative impact on the measured driving performance characterized by the duration of the drive and the total accelerations. Therefore, the experiment was only conducted outside rush hours. All tests were in one of the following time slots: 9:45-12:00, 13:15-15:30, or 18:15-20:30. Furthermore, each participant needed to drive the route twice in order to increase the chance of capturing a run without being influenced by other vehicles in the traffic.

2.3.2. TEST ROUTE

A challenging scenario is needed to sufficiently expose the variance in driving performance. Ideally, the test route requires the vehicle to change its speed across a wide range and negotiate a fair amount of turns. In addition, the distance and duration should be reasonably short and with a minimal trivial portion where most drivers would behave very similarly by driving almost straight and sticking to the speed limit. For these reasons, a test route located to the west of Woerden, the Netherlands has been chosen. As depicted in Fig. 2.4, the start of the route is on the exit ramp of Motorway A12 on the side of eastbound traffic. At the end of the ramp is a double-lane roundabout (further

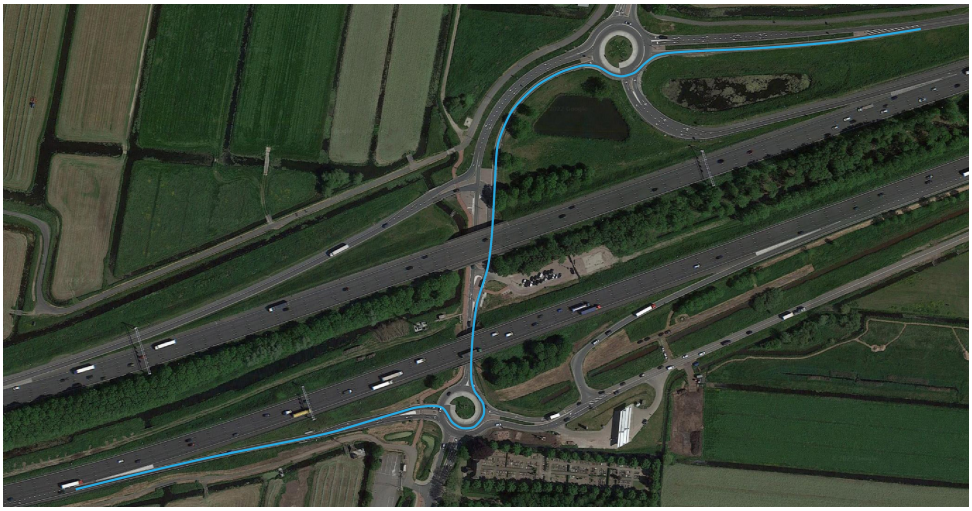

Figure 2.4: Illustration of the test route on the satellite image.

referred to as RB1) where the vehicle needs to turn to the left by taking the 3rd exit. Following up is an intermediate sector where the vehicle follows the road and passes 3 turns in a right-left-right order (further referred to as RLR). The vehicle then enters the second roundabout (further referred to as RB2) where it takes the exit towards distributor road N420 further to the east. After departing the roundabout, the vehicle is allowed to accelerate until the speed limit is reached. Through the test route, there are two occasions where the test vehicle may need to yield to other road users, namely when the vehicle enters RB1 and RB2. For the rest of the route, the test vehicle travels on a priority lane where it would not be impeded by other road users according to traffic rules.

2.3.3. PARTICIPANTS

The majority of participants were recruited from the neighboring area using flyers distributed to residential addresses and companies. This potentially promotes a more inclusive group than recruiting only on campus. Besides, the test route is an important part of the daily commute of the local population. Most participants were familiar with the route prior to the experiment and therefore did not require much learning and practice in order to perform to the best of their capability. A total of 16 participants registered for the experiment. According to the collected non-sensitive personal data, only 2 participants reported that they were not familiar with the test route and 3 reported that they drive a car less frequently than once a week. Meanwhile, 12 participants have been in possession of a driving license for over 10 years and three reported over 4 years. In terms of age, 5 participants were under 30 at the time of the experiment, 2 were above 60, and the rest were between 31 and 59. The largest bias was present in terms of gender with only 4 female participants in the group. Given these figures, the group can be considered representative of an averagely skillful and experienced human driver.

Figure 2.5: Instrumented vehicle used in the experiment

2.3.4. VEHICLE AND DATA ACQUISITION

The experiments were conducted on a Hyundai Kona (Fig. 2.5) that features an automatic transmission (AT) and a hybrid powertrain. The AT was chosen on purpose in order to reduce the participants' workload during the experiment. It eliminates the need to consider gear changing and to learn the clutch pedal characteristics. The hybrid powertrain was a compromised option as no combustion engine-powered vehicle with AT was available. To minimize the impact of driving with a less familiar powertrain, the regenerative braking is set to the minimum so that releasing the throttle pedal does not cause a strong deceleration.

The Racelogic VBOX VBSS100 GPS speed sensor and the XSENS MTi-100 inertial measurement unit (IMU) were used for data acquisition. The 100-Hz speed sensor had two roof-mounted GPS antennas secured with vacuum cups and tension straps. The antennas were aligned on a horizontal plane and with the centerline of the vehicle. According to [14], a passenger car typically has its center of gravity located behind the front axle by 35-50% of the wheelbase, and at 35-40% of the overall vehicle height. Therefore, the IMU was mounted on the bottom of the central glove box, which is the closest horizontal surface to the center of gravity according to the aforementioned figures. The IMU was calibrated when the vehicle was parked on a horizontal surface to ensure proper alignment.

With the GPS sensor, the recording of each test run was triggered automatically when the vehicle crossed a predefined gate defined with GPS coordinates. This ensured the reliable timing of the test run. However, the IMU sensor could not share this trigger signal and therefore had to be operated manually based on some landmark features. In practice, a misalignment of less than 0.2 s is observed when comparing the recorded data,

which was compensated for when processing the data. The surrounding environment of the test route posed further challenges to the GPS sensor. Because the experiment was conducted on open public roads, the GPS signal was occasionally blocked by other vehicles of a larger size (e.g., semi-trailer trucks) as well as static objects such as trees and lamp posts. Moreover, the test route included an underpass across the motorway A4 where the connection to satellites was lost for approximately 15 s. The vehicle trajectory for this period of time could only be estimated with IMU measurements.

2.3.5. DATA PROCESSING

The motion of the vehicle was reconstructed using both sources of information, i.e., from GPS and IMU. As mentioned above, there were certain practical challenges in estimating the actual vehicle trajectory. An optimization-based processing method was developed in order to overcome these challenges. In principle, our method finds a motion profile by minimizing a cost function that includes the error between the measured and estimated positions and accelerations:

$$J(X_{\text{est}}) = w_1 J_{\text{GPS}} + w_2 J_{\text{IMU}} \tag{2.3}$$

Where,

$$\begin{aligned} J_{\text{GPS}} &= \sum_{k=1}^{N} \left(\left(x_{\text{GPS},k} - x_k\right)^2 + \left(y_{\text{GPS},k} - y_k\right)^2 \right) \\ J_{\text{IMU}} &= \sum_{k=1}^{N} \left(\left(a_{x,\text{IMU},k} - a_{x,k}\right)^2 + \left(a_{y,\text{IMU},k} - a_{y,k}\right)^2 \right) \end{aligned} \tag{2.4}$$

The decision variable X_{est} in the optimization problem includes heading angles and velocities along with the initial position:

$$X_{est} = \left[x_0, y_0, \psi_1 \cdots \psi_N, v_1 \cdots v_N\right] \tag{2.5}$$

The positions and accelerations can be calculated based on the decision variables as follows:

$$\begin{aligned} x_{k+1} &= x_k + v_k T_s \cos\psi_k \\ y_{k+1} &= y_k + v_k T_s \sin\psi_k \\ a_{x,k} &= (v_{k+1} - v_k) f_s \\ a_{y,k} &= v_k \left(\psi_{k+1} - \psi_k\right) f_s \end{aligned} \tag{2.6}$$

As mentioned in Subsection 2.3.4, the obstruction of the GPS signal causes the positional measurements to be less reliable. Hence the IMU measurement should be trusted more by placing a larger weight on the acceleration error. For the most part of the maneuver, a weight distribution of $w_1 = 1, w_2 = 5$ is used, which accounts for the relative scale between position and acceleration errors. For the period where the connection is lost, however, zero weight is given to the position error while the acceleration error is penalized alone with $w_2 = 10$. This does not mean that the estimated accelerations during this section of the route will match the IMU measurements exactly. The solution to the optimization problem still needs to balance the two error types for the other parts of the test run.

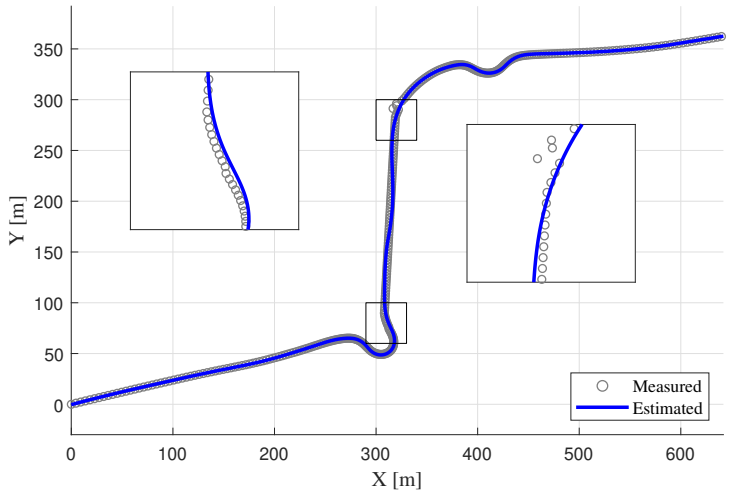

Figure 2.6: An example of the motion reconstruction method: estimated path vs. GPS measurement.

The following example is used to demonstrate the effectiveness of our proposed method for reconstructing vehicle motion during the test runs. The measured and estimated trajectories are compared in Fig. 2.6 and the accelerations and velocities in Fig. 2.7. Using our optimization-based method, the estimated trajectory exhibits a stable curvature when the measurement is of poor quality or unavailable. The estimated accelerations follow the measurements closely in general. The mismatch in longitudinal acceleration is more significant, possibly because of the elevation changes along the test route. The exit ramp where the initial braking phase happened shows a downward slope so that gravity is projected along the vehicle's longitudinal axis. Combining with positional measurement helped mitigate such effects.

2.4. RESULTS

2.4.1. FROM NATURALISTIC DRIVING DATASET

The analysis of the naturalistic driving dataset reveals some insights into how human drivers navigate the roundabouts. Fig. 2.8 is a collection of reconstructed trajectories overlaid on the satellite image of the roundabout. The color variation reflects the change in the velocity of the vehicle. The satellite image shows that the horizontal road at this specific location has a wide median. The geometry is optimized to allow the traffic along that direction to pass easily. The effect is evident from the higher average velocity adopted by the corresponding traffic. The vehicles turning in other directions, on the other hand, have to reduce speed to incorporate the larger curvature. The right-turning vehicles approach the minimal distance to the center island in the third quadrant (i.e. the lower-left quarter) and the minimal velocity is obtained in approximately the same location. Driving in this manner reduces the maximum curvature of the path and thus reduces the lateral disturbance on the occupants. The distribution of maximum abso-

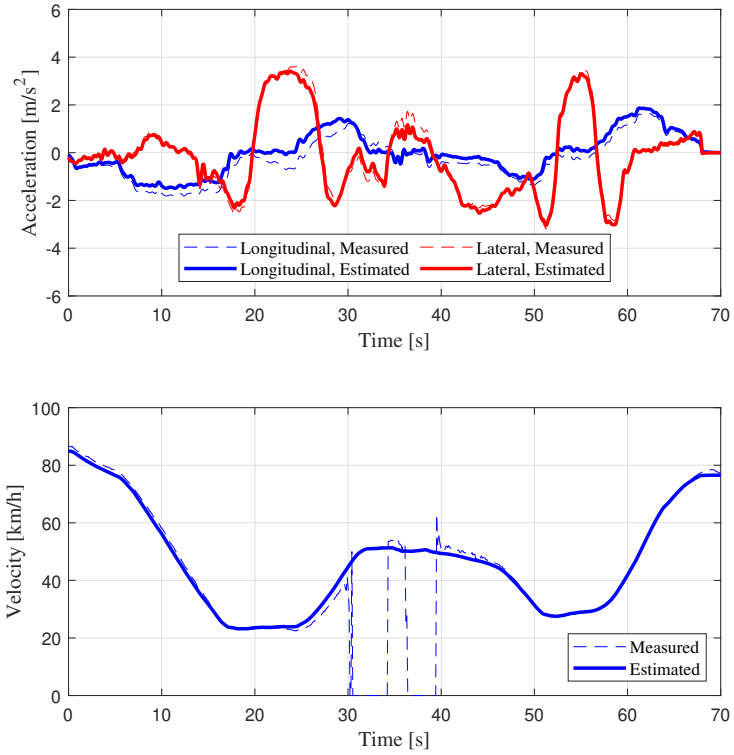

Figure 2.7: An example of the motion reconstruction method: estimated accelerations vs. IMU measurement (top) and estimated velocity vs. GPS measurement (bottom).

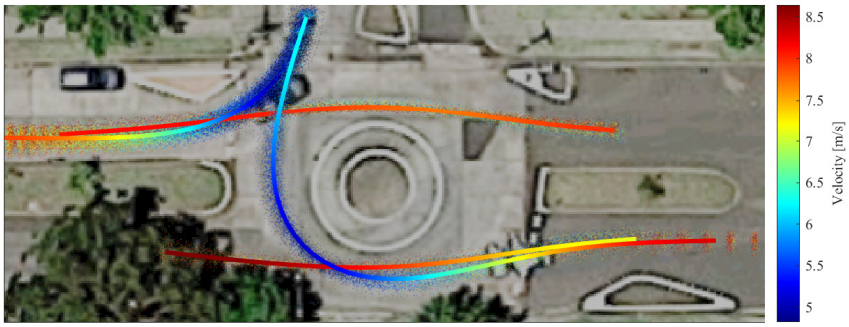

Figure 2.8: Naturalistic driving trajectories of human drivers at a roundabout. The velocity is reflected in the color map on the right. The bold lines represent the average trajectories from the same type of maneuver.

Table 2.1: Statistics of the fitted Gamma distributions.

Travel Direction	Acceleration [m/s^2]	Mode	Mean	SD
Left	Longitudinal	1.25	1.35	0.37
	Lateral	2.82	2.93	0.57
Straight	Longitudinal	0.54	0.82	0.48
	Lateral	1.42	1.55	0.44
Right	Longitudinal	1.15	1.28	0.39
	Lateral	3.62	3.80	0.82

lute longitudinal and lateral accelerations are given in Fig. 2.9. Both variables at each recording location were fitted into a Gamma distribution. The statistics of the fitted distribution are given in Table 2.1. The figures may not be fully representative due to the incompleteness of the recordings. The traffic vehicles are only detected shortly before the entry. It is likely that the velocity has been adjusted before the recording starts. The same applies to the speed-up phase after leaving the roundabout. This is evident from the fact that the highest recorded velocity is in the range of 8.5 m/s or 31 km/h, much lower than the speed limit for urban roads.

2.4.2. FROM ON-ROAD EXPERIMENT

A total of 31 test runs have been recorded during the experiment while in one other case, the participant did not follow the correct test route. Among these, 14 are considered usable. The decision is primarily based on the fact that the minimum speed of the vehicle is over 18 km/h. It suggests that the test vehicle was not required to yield when entering either of the two roundabouts. The total acceleration energy calculated with the reconstructed motion profiles is on average 12.2% lower than that from the IMU signals. This amount of reduction accounts for factors including road elevation change, rotation of the vehicle body (roll and pitch), and noise. Without knowing the ground truth, one cannot rule out the possibility that the resulting motion profiles contain underestimated accelerations at some parts. However, this risk is accepted because it then

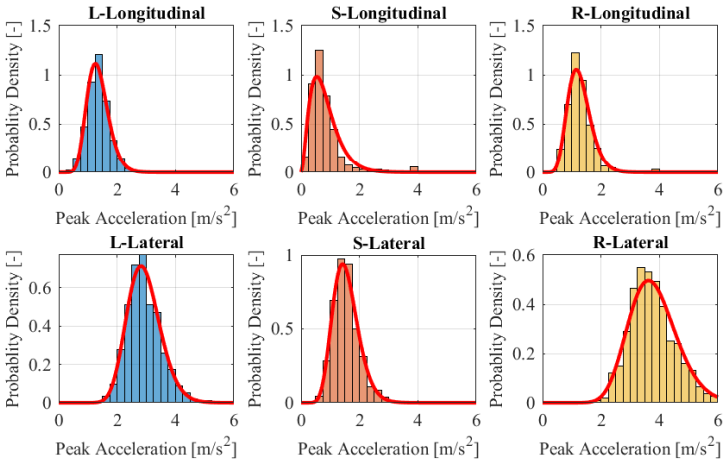

Figure 2.9: Distribution of peak longitudinal and lateral accelerations obtained by human drivers at a roundabout. The sample counts on the histograms are normalized to the form of a probability distribution function and the fitted Gamma distribution is described by the red line.

indicates a higher performance level of human drivers. Comparing with such a baseline performance avoids claiming an exaggerated advantage of automated vehicles.

The collection of all motion profiles from the participants, characterized by their velocity and planar accelerations, are shown in Fig. 2.10. The signals are plotted against the normalized distance, i.e. the relative position within the test run. In terms of initial velocity when crossing the starting line, the values vary roughly between 79 and 91 km/h because the participants were not given strict instructions to maintain a specific speed. The participants adopted a speed of around 22 km/h upon entering the first roundabout, with a gradually increasing magnitude in longitudinal acceleration. In the intermediate sector, the participants mostly maintained a constant speed of around 40 km/h before decelerating for the second roundabout, where they could choose a slightly higher speed thanks to a larger curvature radius. The acceleration after leaving the roundabout peaks at a magnitude of under 2 m/s^2 before falling due to the power constraint of the vehicle and the potential idea of avoiding excessive jerk upon reaching the speed limit. Similar to what was observed in the naturalistic driving dataset, the peak longitudinal acceleration is lower than that of the lateral acceleration (1.90 and 3.57 m/s^2 on average, respectively). Compared to the distribution of peak accelerations observed from the ACFR dataset, the lateral accelerations match well with a difference of merely 6% less than the right-hand turn at the roundabouts. The peak longitudinal accelerations recorded from the on-road experiment are around 48% higher than what the dataset showed. Such difference could be attributed to the higher complexity of the test route chosen for the experiment. The involvement of significant speed changes (e.g. on the exit ramp from the motorway) possibly prompted more aggressive ac-/deceleration.

The longer test runs recorded from the experiment further enabled the analysis of the frequency composition of the acceleration signals. This was not possible with the ACFR dataset where most recordings had a duration shorter than 10 seconds. The power

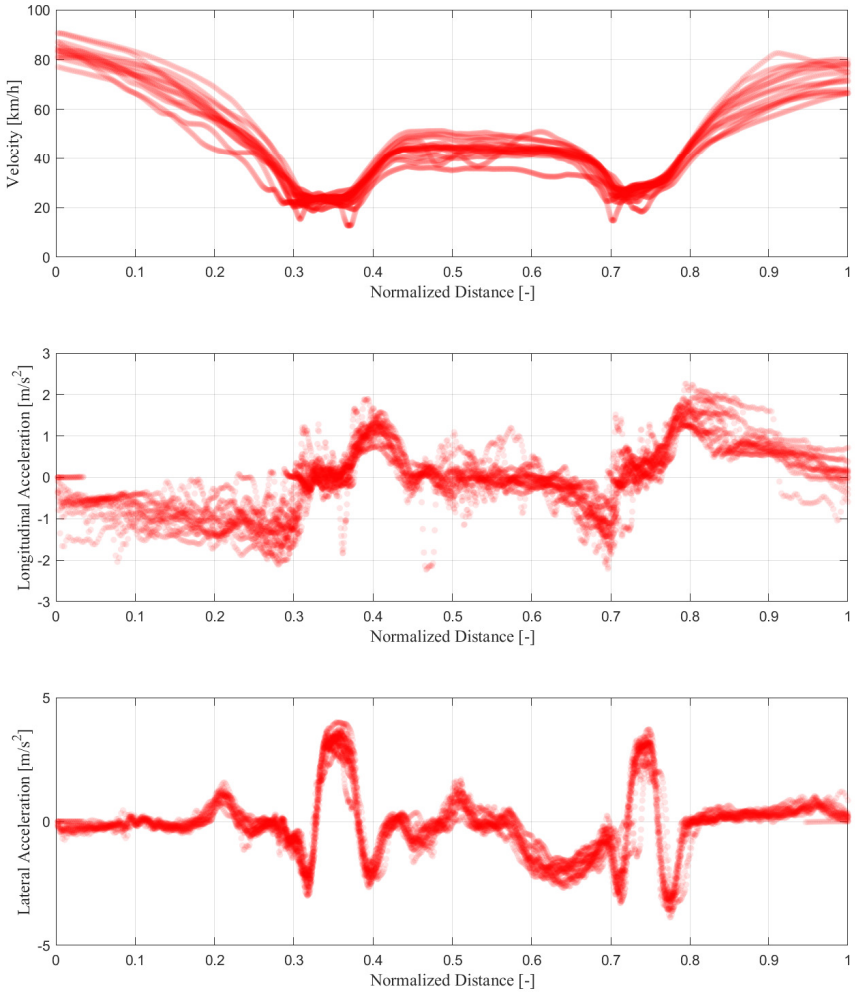

Figure 2.10: The velocity and acceleration profiles of all valid test runs. The horizontal axis is the normalized distance, representing the vehicle's progress into the test route.

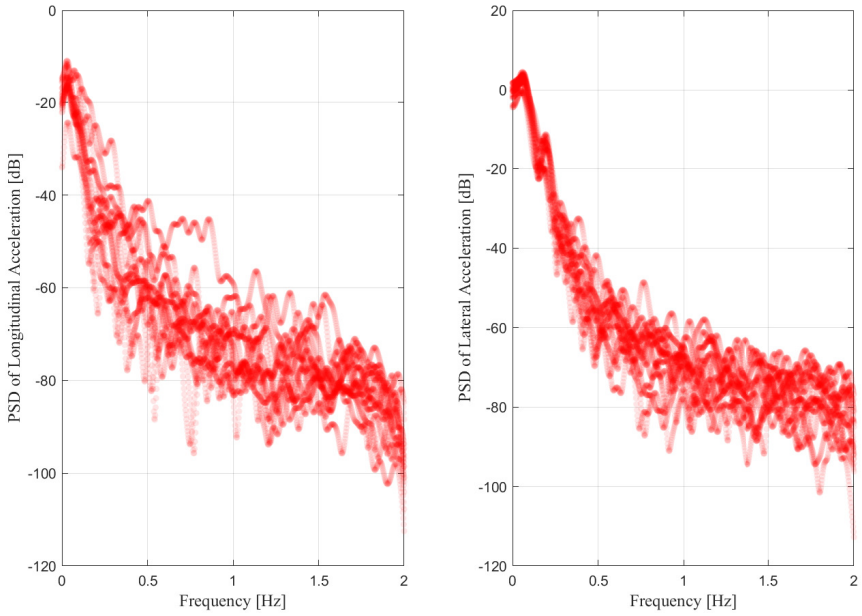

Figure 2.11: The PSD of the longitudinal and lateral acceleration signals recorded from the test runs.

spectral density of the accelerations is shown in Fig. 2.11. In both longitudinal and lateral acceleration, the majority of power is distributed below 0.5 Hz. In this frequency range, the magnitude and variance in the PSD of lateral acceleration between the participants are significantly lower than that in the longitudinal direction. This is already evident from Fig. 2.10 where the longitudinal acceleration signals are scattered across a wide range. Presumably, this is due to more freedom in selecting vehicle speed than in choosing its spatial trajectory. The latter is constrained by the shape of the road. It is also likely that the control of longitudinal motion is more difficult than that of lateral motion. The longitudinal response of the vehicle is less predictable due to the low-level controllers in the powertrain and transmissions, as well as the need for switching between two pedals. Contrary to the steering wheel that provides direct haptic feedback in the form of wheel torque, the control of pedals relies on the perceived vehicle acceleration. The prolonged loop involves more delays and low-level dynamics that potentially harm the control quality of the vehicle's longitudinal motion.

2.5. CONCLUDING REMARKS

This chapter has been dedicated to understanding the driving preferences and performance of human drivers in balancing comfort and time efficiency. The goal was approached with two different methods. Initially, insights into how human drivers negotiate a roundabout were obtained through processing and analyzing the ACFR naturalistic driving dataset. The scenario was chosen for its maneuvering complexity and compactness. The original data was processed with significant efforts, including the use of an

optimization-based motion reconstruction method, in order to overcome the noise and errors. The processed dataset containing smoothed velocity and acceleration information has been made openly accessible via IEEE DataPort[2]. The data suggests that most frequently, the peak acceleration falls between 0.54 and 1.25 m/s^2 and the lateral acceleration between 1.42 and 3.62 m/s^2, depending on the type of maneuver being performed. The longitudinal acceleration appears to be significantly lower than the lateral acceleration. This is partly attributed to the absence of the major acceleration and deceleration phases in the recordings. Lower peak lateral accelerations are observed from vehicles driving straight at the roundabout as the geometry was optimized to improve traffic flow capacity in this direction. Nevertheless, the roundabouts alone are not fully representative of the daily use of a passenger vehicle and the incomplete recordings in the dataset prevent us from fairly evaluating the time efficiency of human drivers. Thus some doubts remain about the observed distribution of the longitudinal acceleration.

In an attempt to partly address the disadvantages of relying on existing naturalistic driving data, a subsequent experiment-based study was conducted. The driving data of publicly recruited participants have been collected while they drove an instrumented vehicle through the predefined route. An optimization-based processing method similar to that in the first approach was used to handle sensor noise and bias and thus obtain a more accurate estimate of the actual vehicle motion. The data gathered through the time span of 10 days revealed more about the performance and preferences of human drivers. The peak acceleration observed from this more complex scenario closely matches the naturalistic driving data in the lateral direction while suggesting a significantly higher value in longitudinal motion. The difference is primarily caused by the inclusion of the part of driving where major speed changes occur. Moreover, the experimental data enabled the part of the analysis on time efficiency which was not possible in the previous attempt. The participants consumed an average of 76.5 s of travel time through the 920-meter route in traffic-free conditions while incurring a total acceleration energy of 211.4. Overall, it appears that human drivers control the lateral dynamics better than the longitudinal dynamics, evident from the distribution of lateral accelerations being more concentrated in both time and frequency domains. Also observed in the frequency-domain analysis is that the acceleration power is primarily distributed in the low-frequency area. It could partly support the arguments in [15] on using only a high-pass filter to evaluate motion sickness because the higher frequency components are filtered by vehicle dynamics. Nevertheless, such filtering effects do not accurately match the recommended frequency weighting in [16].

Due to the limited resources, the number of participants is relatively small and the gender composition is male-dominant. Combined with the lack of control over the traffic situation, only 14 recorded runs were considered useful for our purpose. The small sample size may limit the findings from being considered statistically significant and convincing. Hence, it is recommended not to consider the group average as a performance baseline representative of human drivers. Instead, the best-performing drivers could be used in order not to underestimate human drivers and exaggerate the potential of automated vehicles. Contrary to common expectations, however, the female participants in the experiment are not distributed towards the more gentle side. It might be

[2] https://ieee-dataport.org/open-access/reconstructed-roundabout-driving-dataset

explained by the fact that male participants refrained from driving more aggressively because the vehicle was not their own property. The male drivers' aggression might also be misinterpreted as the conclusion was more often drawn from a higher rate of traffic violations, which does not necessarily means a higher acceleration magnitude in all situations. It is nevertheless recommended to conduct such an experiment with a larger participant group with extra attention on a balanced meta-data distribution. Besides, the limitations of GPS measurement of vehicle trajectory are exposed due to the occlusion by tall objects around the test route, including trees, lamp posts, and heavy vehicles, even when the test route is chosen on purpose to avoid an underpass. Alternative or complementary position measurement techniques are needed. For example, one could use cameras to estimate the vehicle's relative position within the lane using intrinsic parameters. Regarding the choice of a test vehicle, some participants appeared to have no experience with an automatic transmission. The phenomenon roots in the limited popularity of automatic transmissions in Europe. This might partly offset the benefit of having a simpler learning process with one fewer pedal to adapt to. The hybrid powertrain could have further complicated the speed control task for the participants due to the switching of power sources between the combustion engine and the electric motor. It is uncertain if a fully electric vehicle would be more suitable. In order to observe more naturalistic driving behavior, the participants might have to drive their own vehicles. However, this would make it more difficult to find participants due to the increased demand and risk allocated to the participants. It also involves repeated installation and testing of the experimental setup, requiring significantly more time and physical effort. Alternatively, one may seek access to driving data collected by insurance companies that offer usage-based insurance options [17]. The drivers undertaking such insurance are required to upload data from an additional accelerometer and GPS sensor in order to prove their safe driving. Despite the challenges, upscaling the data acquisition with onboard measurement is valuable for a deeper understanding of human drivers with more certainty. A larger dataset could serve more convincingly as a performance baseline for motion planners to compare with. The raw and processed data gathered through the experiment have been uploaded onto an open-access data platform[3]. Sharing the research data from this study would benefit researchers in a relevant field and allow more potential value to be extracted.

[3] https://data.4tu.nl/datasets/1ba011fc-7621-444d-ba7e-e3443aeddd98

BIBLIOGRAPHY

[1] Y. Zheng, B. Shyrokau, and T. Keviczky, "Comfort and time efficiency: A roundabout case study", in *Proc. IEEE Int. Intell. Transp. Syst. Conf. (ITSC)*, IEEE, 2021, pp. 3877–3883.

[2] T. Gu and J. M. Dolan, "Toward human-like motion planning in urban environments", in *2014 IEEE Intelligent Vehicles Symposium Proceedings*, IEEE, 2014, pp. 350–355.

[3] M. Menner, K. Berntorp, M. N. Zeilinger, and S. Di Cairano, "Inverse learning for human-adaptive motion planning", in *2019 IEEE 58th Conference on Decision and Control (CDC)*, IEEE, 2019, pp. 809–815.

[4] L. Chen, L. Platinsky, S. Speichert, *et al.*, "What data do we need for training an av motion planner?", in *2021 IEEE International Conference on Robotics and Automation (ICRA)*, IEEE, 2021, pp. 1066–1072.

[5] H. Bellem, T. Schönenberg, J. F. Krems, and M. Schrauf, "Objective metrics of comfort: Developing a driving style for highly automated vehicles", *Transportation research part F: traffic psychology and behaviour*, vol. 41, pp. 45–54, 2016.

[6] K. N. de Winkel, T. Irmak, R. Happee, and B. Shyrokau, "Standards for passenger comfort in automated vehicles: Acceleration and jerk", *Applied Ergonomics*, vol. 106, p. 103 881, 2023.

[7] A. Zyner, S. Worrall, and E. M. Nebot, "ACFR five roundabouts dataset: Naturalistic driving at unsignalized intersections", *IEEE Intell. Transp. Syst. Magazine*, vol. 11, no. 4, pp. 8–18, 2019.

[8] X. Li, A. Rakotonirainy, and X. Yan, "How do drivers avoid collisions? a driving simulator-based study", *J. Safety Research*, vol. 70, pp. 89–96, 2019.

[9] L. Quante, M. Zhang, K. Preuk, and C. Schießl, "Human performance in critical scenarios as a benchmark for highly automated vehicles", *Automotive Innovation*, vol. 4, no. 3, pp. 274–283, 2021.

[10] J. C. de Winter, S. De Groot, M. Mulder, P. Wieringa, J. Dankelman, and J. Mulder, "Relationships between driving simulator performance and driving test results", *Ergonomics*, vol. 52, no. 2, pp. 137–153, 2009.

[11] Y. R. Khusro, Y. Zheng, M. Grottoli, and B. Shyrokau, "Mpc-based motion-cueing algorithm for a 6-dof driving simulator with actuator constraints", *Vehicles*, vol. 2, no. 4, pp. 625–647, 2020.

[12] S. Sahami and T. Sayed, "How drivers adapt to drive in driving simulator, and what is the impact of practice scenario on the research?", *Transp. Research Part F: Traffic Psychology and Behaviour*, vol. 16, pp. 41–52, 2013.

[13] A. Ronen and N. Yair, "The adaptation period to a driving simulator", *Transp. Research Part F: Traffic Psychology and Behaviour*, vol. 18, pp. 94–106, 2013.

[14] G. J. Heydinger, R. A. Bixel, W. R. Garrott, M. Pyne, J. G. Howe, and D. A. Guenther, "Measured vehicle inertial parameters-nhtsa's data through november 1998", *SAE Trans.*, pp. 2462–2485, 1999.

[15] D. Li and J. Hu, "Mitigating motion sickness in automated vehicles with frequency-shaping approach to motion planning", *IEEE Robot. and Automat. Lett.*, vol. 6, no. 4, pp. 7714–7720, 2021.

[16] B. E. Donohew and M. J. Griffin, "Motion sickness: Effect of the frequency of lateral oscillation", *Aviation, Space, and Environ. Medicine*, vol. 75, no. 8, pp. 649–656, 2004.

[17] P. Handel, I. Skog, J. Wahlstrom, *et al.*, "Insurance telematics: Opportunities and challenges with the smartphone solution", *IEEE Intelligent Transportation Systems Magazine*, vol. 6, no. 4, pp. 57–70, 2014.

3

COMFORT-ORIENTED MOTION PLANNING

To achieve great things, two things are needed; a plan, and not quite enough time.

Leonard Bernstein

Parts of this chapter have been accepted to IEEE Transactions on Intelligent Vehicles and in review at IEEE Transactions on Intelligent Transportation Systems.

3.1. INTRODUCTION

It has been argued in Section 1.1 the importance of improving motion comfort and mitigating motion sickness with automated driving. The motion planning algorithm plays a critical role in the vehicle's comfort level. Given the perception inputs on available driving space and other road users, a motion planer essentially generates the desired path and velocity profile that low-level tracking controllers should then follow. Early studies aim at improving general motion comfort in a qualitative manner by ensuring the continuity of the motion. There are works on constructing the motion with curve components that feature continuous curvature. This guarantees a bounded jerk if the vehicle travels at a constant speed and is often achieved with variations of clothoid [1], [2]. Some studies exploit the smoothness of parametric curves, e.g., splines and Bezier curves, to plan a path or velocity profile [3]–[6]. These approaches ensure that the higher-order time derivatives of the motion profile are bounded. The parametric curves can also be incorporated into an optimization-based framework where the placement of control points is optimized. In addition, state lattices and motion primitives have been used by some authors to improve smoothness under a sampling- or optimization-based planning framework [7]–[9]. Most studies mentioned above do not explicitly consider motion sickness or accelerations in general and therefore have limited applicability in the dynamic driving scenarios that automated vehicles encounter. Although there has been an attempt to analyze the frequency components in the resulting acceleration patterns arising from the use of different transition curves [10].

Some studies exploit optimization techniques to reduce acceleration. A comfort-oriented planner was proposed for car-like mobile robots, where the motion is planned by minimizing a cost function concerning travel time, accelerations, and clearance from an obstacle [11]. This study also mentioned the trade-off between time and comfort in motion planning. The trade-off problem in real traffic is investigated for a roundabout scenario where naturalistic driving data is analyzed [12]. Furthermore, an optimal planning framework has been proposed, which considers the possibility of reducing lateral accelerations with active roll motion [13]. Some recent works paid more attention to mitigating motion sickness by considering the frequency sensitivity discussed above. Explicit minimization of MSDV in addition to travel time has been explored in [14], where the vehicle motion is formulated in curvilinear coordinates and details were provided on the distribution of acceleration energy in the frequency domain and on the trade-off between comfort and travel time [14]. An alternative approach to the problem was proposed using a time-domain planning algorithm by including a second-order high-pass filter in the objective function [15]. The weighting is done in the frequency domain after performing the Fourier transform of the acceleration signals.

This chapter focuses on the description and validation of an optimization-based motion planning algorithm proposed for mitigating motion sickness. It targets the frequency range of interest in a different approach than in the existing studies. Detailed explanations of calculating frequency-weighted accelerations using a band-pass filter are provided. The effectiveness of frequency weighting is demonstrated by comparing it to using an alternative objective, where all accelerations are penalized equally. A receding-horizon formulation of the algorithm is further proposed, which resembles real-world deployment more closely. The real-time capability of the receding-horizon planner has

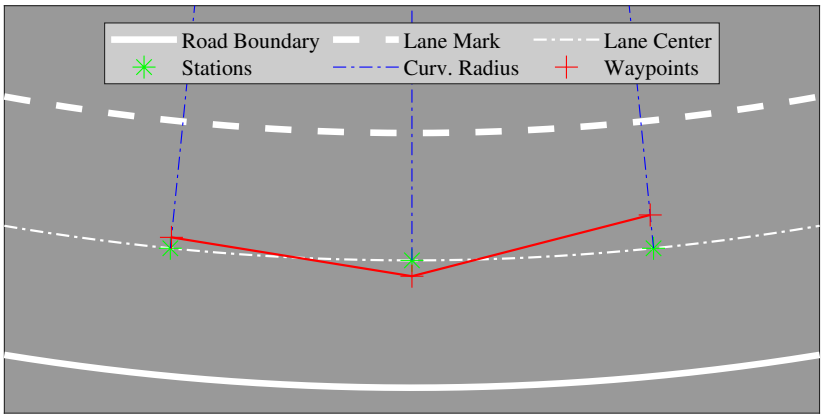

Figure 3.1: A visual explanation of the definition of stations and waypoints on a demonstrative road section with right-hand traffic.

been examined for different combinations of parameters. The motion planner variants are then compared with the human driving data gathered in the experiment described in Chapter 2.

3.2. OPTIMIZATION PROBLEM

This section introduces the underlying components that construct an optimization problem reflecting the goal of mitigating motion sickness in automated vehicles. The vehicle motion is defined within the lane space using the lateral position relative to the lane center, in addition to vehicle velocity. The relative lateral position and velocity are the decision variables that enable the evaluation of the objective function that should be minimized. The optimization problem is formulated for an integral approach and a receding-horizon approach. The former represents the theoretical upper limit of performance while the latter reflects a level that is achievable in practice.

3.2.1. MOTION DEFINITION

The proposed motion planner assumes that the vehicle drives on well-paved roads with clear lane marks so that the information about the available driving space along the road is clearly defined by the perception systems. The vehicle trajectory is constructed through a series of waypoints. Along the center of the lane where the vehicle is driving, a string of stations is distributed with a nominal interval d_{nom}. To locate a waypoint with regards to its corresponding station, we first define a local lateral axis at the station perpendicular to the normal driving direction (see Fig.). Then the location of the waypoint P_k is determined by its lateral position y_k. The station is placed at $y_k = 0$, i.e., at the lane

center. With a positive y_k, the vehicle deviates to the left-hand side of the lane. Connecting the waypoints results in a spatial trajectory while assigning a velocity to each waypoint further defines the trajectory in time. This allows for calculating the accelerations of the vehicle when the steps below are followed. First, the Euclidean distance between waypoint k and $k+1$ is given by:

$$d_k = \sqrt{(X_{k+1} - X_k)^2 + (Y_{k+1} - Y_k)^2} \tag{3.1}$$

Assuming that the vehicle has constant longitudinal acceleration when traveling this distance, we could determine the longitudinal acceleration given the velocity at waypoint k and $k+1$ with:

$$a_{x,k} = \frac{v_{k+1}^2 - v_k^2}{2d_k} \tag{3.2}$$

Further assuming that the vehicle heading at waypoint k, denoted by $\vec{h}_k$, points from waypoint k to waypoint $k+1$:

$$\vec{h}_k = \begin{pmatrix} X_{k+1} \\ Y_{k+1} \end{pmatrix} - \begin{pmatrix} X_k \\ Y_k \end{pmatrix} \tag{3.3}$$

The change of heading can be calculated as the angle between $\vec{h}_k$ and $\vec{h}_{k+1}$:

$$\psi_k = \frac{\vec{h}_k \cdot \vec{h}_{k+1}}{\left|\vec{h}_k\right| \left|\vec{h}_{k+1}\right|} \tag{3.4}$$

The curvature of the vehicle path in this section is given by:

$$\kappa_k = \frac{\Delta\psi_k}{d_k} \tag{3.5}$$

The lateral acceleration is then approximated using the average speed:

$$a_{y,k} = \left(\frac{1}{2}v_{k+1} + \frac{1}{2}v_k\right)^2 \kappa_k \tag{3.6}$$

Here, the accelerations are calculated purely from the waypoint locations and velocities without considering vehicle dynamics. In this formulation, we only constrain the lateral position of the waypoints according to the lane width and the velocities according to speed limits. Because the main goal of this study is to explore how to effectively incorporate the frequency sensitivity in motion sickness into an optimization-based motion planning scheme, and to demonstrate how time efficiency and motion comfort can be balanced. Therefore, we try to design here a general motion plan in the form of a spatiotemporal trajectory that receives minimal influence from the choice of prediction model and constraints. The accurate tracking of the desired trajectory is expected to be handled by the low-level tracking controllers that incorporate individual differences in vehicle dynamics. In addition, including a vehicle dynamics model in the optimization problem increases the computational complexity. If the computation time from the current formulation is sufficiently short and the resulting motion plan would show signs of infeasibility, it is possible to add a low-level loop consisting of a vehicle dynamics model and a tracking controller, resembling the approach proposed in [16].

3.2.2. OBJECTIVES

The primary objective of the proposed method is to minimize the incidence of motion sickness indicated by frequency-weighted accelerations. Nevertheless, the motion planner should also take into account the factor of time efficiency in the optimization. This prevents the planner from driving unnecessarily slow and hence ensures a driving behavior that is acceptable to the passengers and other road users. We define the objective of the optimization as a weighted sum of motion sickness and time efficiency:

$$J_{\text{MS}} = D_{\text{MS}} + W\,T \tag{3.7}$$

Where D_{MS} is a criterion related to motion sickness, T is a measure of time efficiency, and W is the weighting factor on time efficiency. A larger W means a shorter travel time is preferred over a less sickening ride. A viable range of W should be determined beforehand through simulation while the user could be given the freedom to adjust it during the trip according to personal preferences. The time efficiency is described by the total duration of the planned motion. Under the assumption of constant longitudinal acceleration between two adjacent waypoints, travel time at a given step can be found as:

$$\Delta t_k = \frac{2d_k}{v_{k+1} + v_k} \tag{3.8}$$

The total duration is simply the sum of the travel time of all the steps:

$$T = \sum_k \Delta t_k \tag{3.9}$$

Quantitative evaluation of motion sickness, on the other hand, is less straightforward. We adopt the following form as is used in [11], [12]:

$$D_{\text{MS, Motion}} = \sum_{k=1}^{N} \left(a_{xf,k}^2 + a_{yf,k}^2\right) \Delta t_k \tag{3.10}$$

Where, a_{xw} and a_{yw} are the frequency-weighted longitudinal and lateral accelerations, respectively. The total energy of the frequency-weighted accelerations is used to quantify the comfort level related to motion sickness. This is effectively the square of MSDV for longitudinal and lateral motion proposed in [17]:

$$\text{MSDV} = \left(\int_0^T \left(a_{xw}^2 + a_{yw}^2\right) dt\right)^{1/2} \tag{3.11}$$

The benefit of using squared MSDV instead is that the penalization on discomfort is amplified by itself. This choice may not directly impact the resulting trade-off given that W is varied through a wide range. Rather, it influences the way that W regulates the balance between time and comfort. With the squared MSDV, W has to be increased more sharply to further promote aggressive driving behavior. This could be more friendly to the users when they are given the option of W especially when they are inexperienced.

In order to apply frequency-weighting on accelerations, we implement two separate band-pass filters, incorporating the different frequency sensitivities in the longitudinal

and lateral directions. Each band-pass filter can be expressed as a transfer function constructed from a low-pass filter and a high-pass filter:

$$H(s) = \frac{a_{\text{fil}}(s)}{a_{\text{act}}(s)} = \frac{1}{\tau_1 s + 1} \frac{s}{\tau_2 s + 1} \tag{3.12}$$

Where τ_1 and τ_2 are the time constants corresponding to the desired cut-off frequencies of the band-pass filter. The transfer function has an equivalent continuous-time state-space formulation of:

$$\begin{aligned} \dot{x} &= Ax + Ba_{\text{act}} \\ a_{\text{fil}} &= Cx \end{aligned} \tag{3.13}$$

The state-space matrices are calculated as:

$$\begin{aligned} A &= \begin{pmatrix} -{\tau_1}^{-1} - {\tau_1}^{-1} & 1 \\ -{\tau_1}^{-1}{\tau_2}^{-1} & 0 \end{pmatrix} \\ B &= \begin{pmatrix} {\tau_1}^{-1}{\tau_2}^{-1} \\ 0 \end{pmatrix} \\ C &= \begin{pmatrix} 1 & 0 \end{pmatrix} \end{aligned} \tag{3.14}$$

Given a time step of Δt and assuming zero-order hold for the input, the state-space model can be discretized as:

$$\begin{aligned} x_{k+1} &= A_d x_k + B_d a_{\text{act},k} \\ a_{\text{fil},k} &= C_d x_k \end{aligned} \tag{3.15}$$

Where,

$$\begin{aligned} A_d &= e^{A\Delta t} \\ B_d &= A^{-1}(A_d - I)B \\ C_d &= C \end{aligned} \tag{3.16}$$

Given the current filter states and assuming the actual acceleration to be constant through a time period Δt, it is possible to calculate the filtered acceleration at the end of the period using the method described above. This is useful to find the frequency-weighted acceleration when the vehicle travels between two consecutive waypoints. Because the step travel time, Δt_k varies per waypoint, the matrix exponential $e^{A\Delta t_k}$ is different for every time step. Diagonalization is a commonly used technique in calculating matrix exponentials. Instead of diagonalizing $A\Delta t_k$ for every given Δt_k, we first diagonalize matrix A:

$$\Omega = P^{-1}AP \tag{3.17}$$

The matrix exponential is then equivalent to:

$$e^{A\Delta t} = Pe^{\Omega\Delta t}P^{-1} \tag{3.18}$$

The matrix exponential of diagonal matrix $\Omega\Delta t$ is simply:

$$e^{\Omega\Delta t} = \begin{pmatrix} e^{\omega_{11}\Delta t} & 0 \\ 0 & e^{\omega_{22}\Delta t} \end{pmatrix} \tag{3.19}$$

Because matrix P is invariant of Δt, it can be pre-computed without the need to repeat the computation in every evaluation step. Using these steps, we reduce the complexity of computation from a matrix exponential to the exponential of two real numbers on top of basic matrix multiplications with a size of 2-by-2. This allows us to efficiently determine the value of $D_{\text{MS,Motion}}$ given a time-stamped acceleration sequence. However, the output of a band-pass filter accumulated through the travel time is not equal to the squared MSDV because the filter has its temporal dynamics. Both the internal states of the filter and the output require extra time to dissipate and converge to zero after the input is removed. This process needs to be taken into account as the output in this period contains a part of the information describing the nauseogenicity of the acceleration input. Neglecting it would allow the optimal solution to exploit the filter dynamics by commanding unreasonably high acceleration towards the end of the planning horizon. Hence, we calculate the output of the filter given zero input for a period of 30 seconds at a sampling time of 0.2s and include this amount in the evaluation of the planned motion:

$$D_{\text{MS, Tail}} = \sum_{k=N+1}^{N+N_{\text{Tail}}} \left(a_{xf,k}^2 + a_{yf,k}^2\right) \Delta t_k \tag{3.20}$$

The choice of 30 seconds is based on the choice of τ_1 for lateral accelerations. The total cost term reflecting motion sickness is:

$$D_{\text{MS}} = D_{\text{MS, Motion}} + D_{\text{MS, Tail}} \tag{3.21}$$

To demonstrate the effectiveness of the proposed formulation in targeting a specific frequency range in accelerations, we add an alternative objective where the frequency dependency is neglected. This variant is further referred to as minimal-acceleration planning or MA in short. It minimizes a cost function of similar form to (3.7) although the term D_{MS} is replaced with D_{MA}, a measure of general acceleration comfort:

$$D_{\text{MA, Motion}} = \sum_{k=1}^{N} \left(a_{x,k}^2 + a_{y,k}^2\right) \Delta t_k \tag{3.22}$$

The rest of its implementation is identical to the proposed sickness-mitigating planning method (further referred to as MS).

3.2.3. INTEGRAL APPROACH

The integral approach here refers to planning for the entire driving scenario by solving a single large-scale optimization problem in the following form:

$$\begin{aligned} \text{min:} \quad & J(\mathbf{X}) \\ \text{where:} \quad & \mathbf{X} = \left[y_1 \dots y_N, v_1 \dots v_N\right] \\ \text{s.t.:} \quad & y_{\min} \le y_1 \dots y_N \le y_{\max} \\ & v_{\min} \le v_1 \dots v_N \le v_{\max} \end{aligned} \tag{3.23}$$

where N is the total number of stations for the scenario. The choice of J depends on the purpose of the planner. It contains either D_{MS} for mitigating motion sickness or D_{MA} for minimizing overall acceleration. The process of evaluating J using the decision variables

X given a road profile has been shown above. In the case of the integral approach, the motion planner is given all the information about the maneuvering scenario and produces an optimal motion plan in one go. This approach requires detailed and highly accurate information and could be difficult to realize in practice. In case of unpredictable events from other road users, the motion plan may have to be abandoned in order to respond. It nevertheless provides a benchmark that represents the ideal performance that a motion planner could achieve. It can be used to evaluate other planning methods that aim to improve computational efficiency.

3.2.4. RECEDING-HORIZON APPROACH

In the receding-horizon approach, the planner solves an optimization problem repeatedly over a receding horizon, concerning motion predictions for only a limited distance ahead:

$$\begin{aligned} \text{min:} \quad & J(\mathbf{X}_{\text{RH}}) \\ \text{where:} \quad & \mathbf{X}_{\text{RH}} = \left[y_1 \dots y_{Np}, v_1 \dots v_{Np} \right] \\ \text{s.t.:} \quad & y_{\min} \leq y_1 \dots y_{Np} \leq y_{\max} \\ & v_{\min} \leq v_1 \dots v_{Np} \leq v_{\max} \end{aligned} \tag{3.24}$$

where N_p represents the number of stations distributed within the preview distance D_p. It concerns a shorter distance ahead that is visible to the vehicle instead of being given the full knowledge of the driving scenario. The rest of the formulation is identical to the integral approach. This approach is more applicable in the real world as it receives up-to-date information about a limited distance ahead. After reaching the first waypoint planned previously, new information is processed to update the motion plan. In this way, the vehicle could also respond to unforeseeable changes in the traffic situation. The optimization problem to be solved at each step has significantly lower complexity and is easier to solve on automotive-level hardware, potentially enabling real-time operation. Although the limited preview range may impact the optimality of the planned motion when compared to the integral approach that gives the theoretically optimal solution.

The preview distance is expected to be the most influential factor and needs to be chosen with care. However, a fixed preview distance cannot achieve a good balance between having good resolution and keeping a low complexity when the vehicle speed is allowed to vary in a wide range. A long preview distance is needed to ensure safety when driving on motorways while a shorter preview distance is enough for driving in built-up areas. In order to account for varying velocities, we propose a speed-dependent preview distance for the receding-horizon planner. Instead of a fixed value, we instead calculate the preview distance using the vehicle's velocity multiplied by a chosen preview time T_p, i.e., $D_{p,k} = v_k T_p$. The distance is divided equally into N_p intervals to find reference stations. The N_p defined in (3.24) is further referred to as the planning horizon. Consequently, the nominal sampling time T_s is T_p/N_p. Because in reality, the travel time between two consecutive waypoints depends on the velocity in that segment. We investigate the performance corresponding to different combinations of T_p and N_p as listed in Table 3.1. We choose $T_p = 3\,\text{s}$ as the minimum for safety concerns. It is realistic to consider a case where the vehicle has to reduce its speed from 100 km/h to a full stop. With a preview time of 3 s, the vehicle has approximately 83 m to complete the deceleration process, leading to an average longitudinal deceleration of approximately $4.7\,\text{m/s}^2$.

T_p [s]	N_p [-]	T_s [s]
3	30	0.1
3	15	0.2
3	6	0.5
4	40	0.1
4	20	0.2
4	8	0.5
5	50	0.1
5	25	0.2
5	10	0.5

Table 3.1: Preview parameters of the receding-horizon planner

Sustained deceleration with such a level of aggressiveness will not be considered as comfortable and a preview time shorter than this may even be a threat to safety. On the other hand, we chose the longest preview time of 5 s. This is based on the observed computation time when combining T_p =5 s and T_s =0.1 s. The simulation then becomes extremely time-consuming.

3.3. SIMULATION RESULTS

3.3.1. INTEGRAL PLANNING

The comparison between MS and MA planners using the integral approach can be found in Fig. 3.2. Both motion profiles have a travel time of approximately 69 s. This value is chosen according to the fastest human driver run that we have recorded. The MS planner initiates the first deceleration later and with a higher peak magnitude than the MA planner. The entry velocity to the first right-hand turn is significantly lower (at around 12 s), leading to a lower lateral acceleration through the first roundabout. At the intermediate part of the road, the MS planner commands a swifter acceleration to the speed limit, exhibiting higher peak lateral acceleration through the turns. Then upon entering the second roundabout, the MS planner again adopts a lower speed for the turning part and then accelerates more aggressively to reach the speed limit of 80 km/h. In general, the MS planner is more aggressive in changing vehicle speed while taking sharper corners more gently. This is partly an effect of applying separate filters to the longitudinal and lateral accelerations.

3.3.2. VARYING PARAMETERS IN RECEDING-HORIZON PLANNING

When using the receding-horizon planner, the preview time T_p and planning horizon N_p (or the resulting nominal sampling time T_s) greatly influence the planning performance. One may naturally expect that a longer T_p and larger N_p would be beneficial. This is mostly true in the case of MA planning as Fig. 3.3 suggests. The loss of acceleration comfort is limited when using a smaller N_p or longer T_s up to 0.5 s. The major difference is caused by preview time as highlighted in Fig. 3.4. All three motion profiles are with $T_s = 0.2s$ and have a duration of 69 s. It is obvious from the first braking maneuver that a longer preview time leads to more gentle deceleration. At the first right-hand turn, a

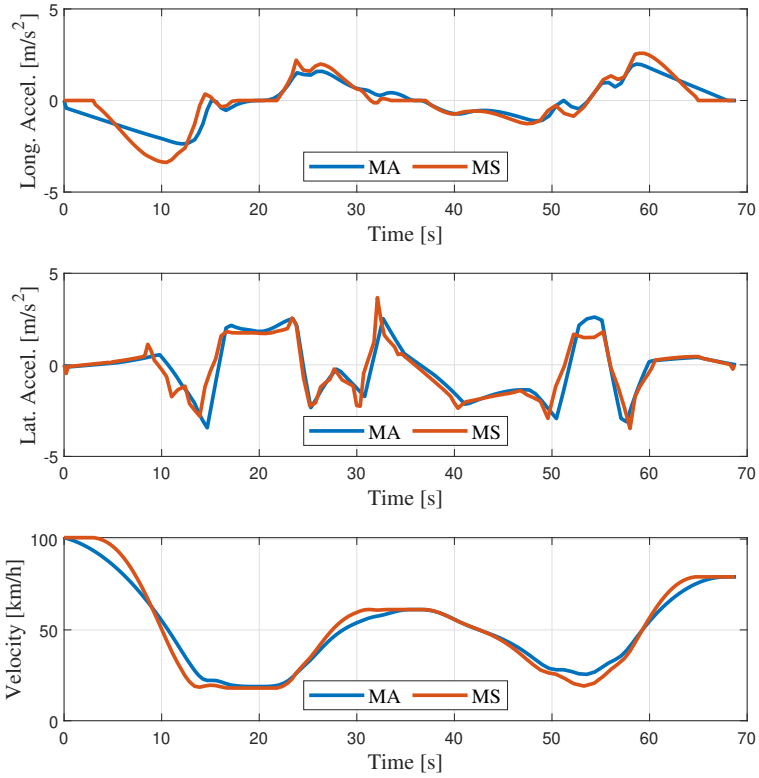

Figure 3.2: Comparison of motion profiles between planner variations aimed at motion sickness mitigation and acceleration minimization.

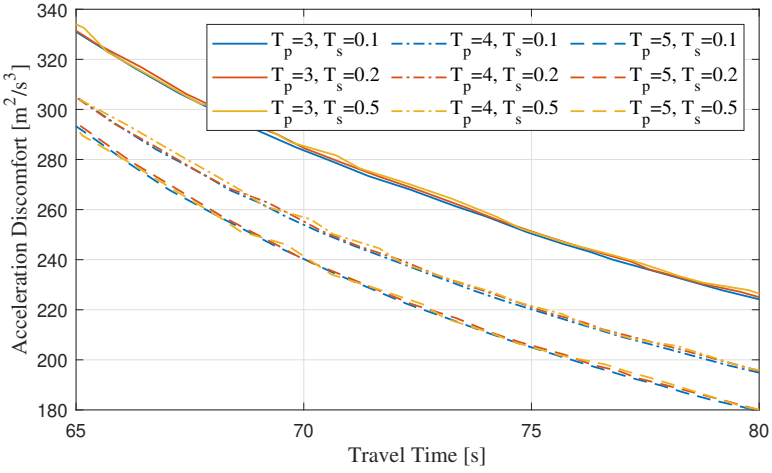

Figure 3.3: Comparison of acceleration comfort and time efficiency performance of receding-horizon planner variations using different preview times and sampling times.

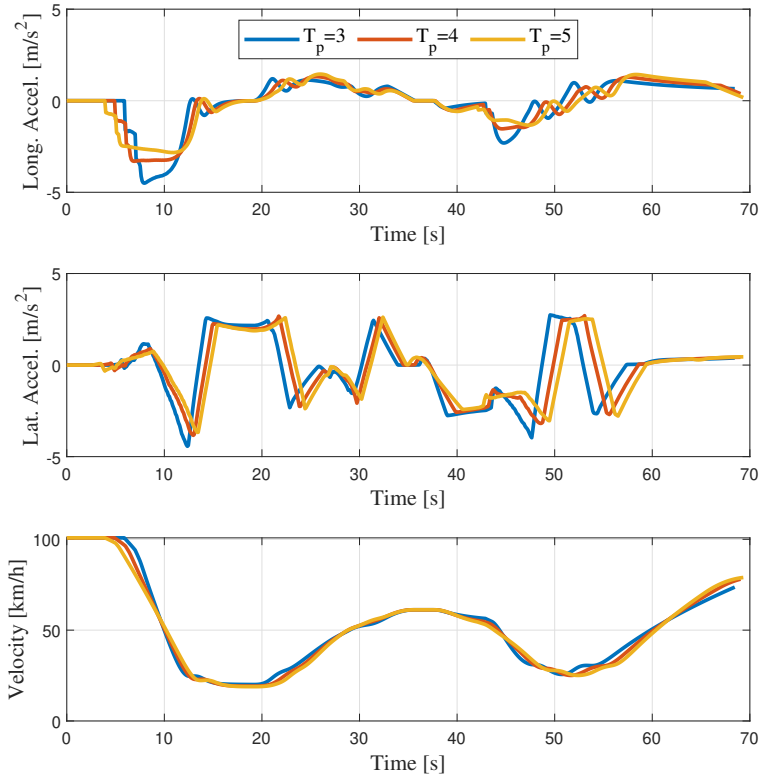

Figure 3.4: Comparison of motion profiles of the receding-horizon motion planner aimed at acceleration minimization using different preview times.

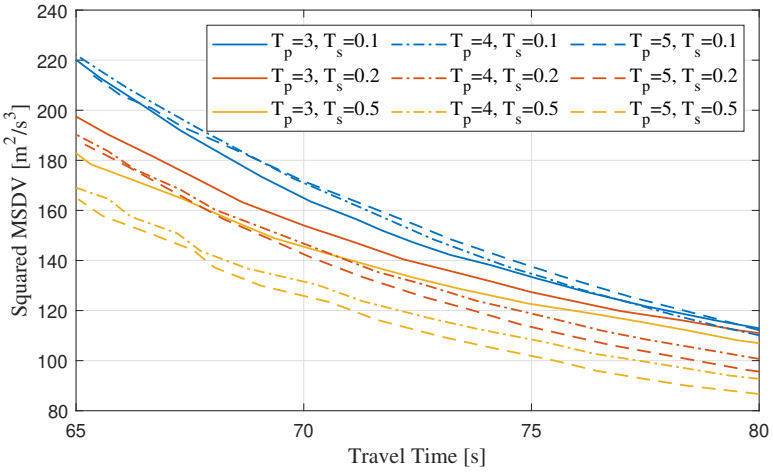

Figure 3.5: Comparison of nauseogenicity and time efficiency performance of receding-horizon planner variations using different preview times and sampling times.

shorter preview time leads to more aggressive turning due to the less desirable positioning of the vehicle (i.e., not as far to the left). At around 30 s, the planner with a shorter preview time is more reluctant in speeding up between consecutive turns because the benefit of taking the turns slowly outweighs the time-saving effect when they are calculated for a shorter distance ahead. Similar observations can be made at the second roundabout. The MS planner behaves somewhat differently than expected when varying T_p and T_s. The former has a similar effect on the planned motion as is observed with the MA planner, that a longer T_p leads to better overall performance. The latter, however, causes a more significant difference that is acting in the opposite direction. Contrary to what is commonly expected, a longer T_s has led to better overall performance when combined with a longer T_p (Fig. 3.5). This might be a consequence of using a discrete-time band-pass filter. When the step time between two waypoints Δt_k is shorter, the planner is given the opportunity to command a very high initial acceleration without getting penalized due to the slow dynamics of the filter. Then because only the first step in this plan is actually applied and the rest is discarded, the resulting motion features more abrupt jumps in acceleration. This statement is supported by Fig. 3.6 where all three motion profiles are with $T_p = 5s$ and have a duration of 75 s.

3.3.3. EFFICACY OF FREQUENCY WEIGHTING

It has been demonstrated by previous examples that incorporating frequency sensitivity in the optimization scheme leads to obvious changes in the shape of the accelerations. To quantify whether the features are reflected by quantitative measures, we collect and compare the value of D_{MS}. In the MS planners, the value is directly available by solving the optimization problem. In the MA planners, however, we need to obtain this by passing the time-stamped acceleration sequence through the band-pass filter. The long-tail effect is also taken into account here. Using the integral approach, the

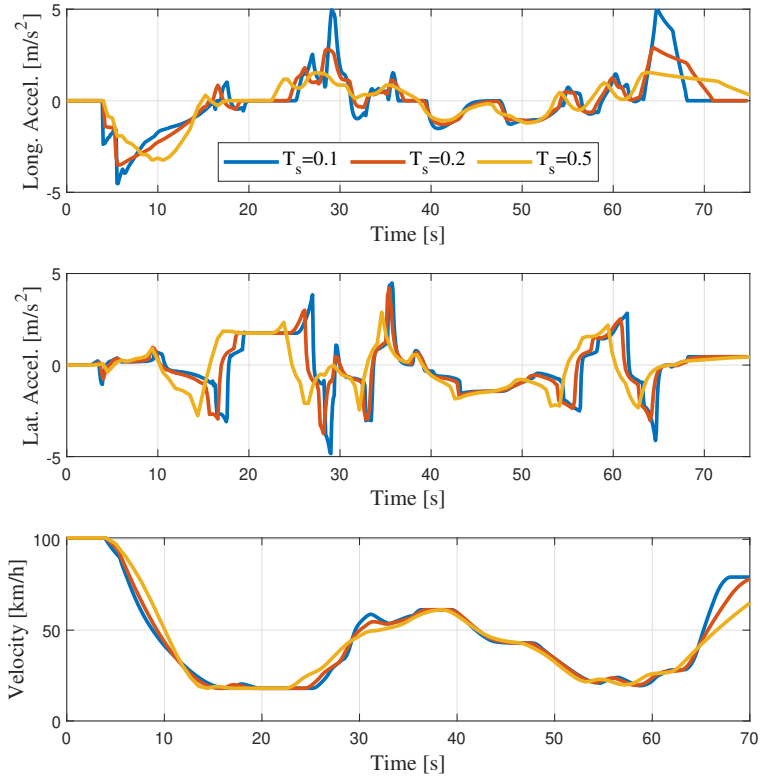

Figure 3.6: Comparison of motion profiles of the receding-horizon motion planner aimed at motion sickness mitigation using different sampling times.

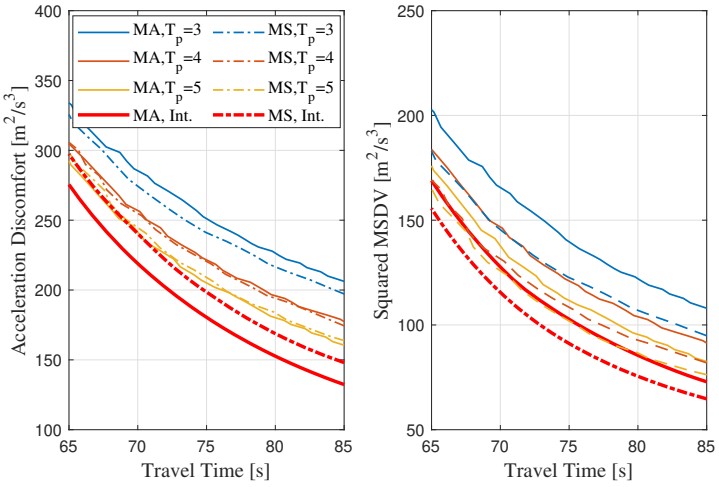

Figure 3.7: Demonstration of performance loss of the receding-horizon approach over the integral approach.

sickness-mitigating planner shows a squared MSDV 7.5-11.3% lower than the minimal-acceleration planner across the range of reasonable travel time. At the same time, the MS planner causes an increase of approximately 8.3-11.7% in acceleration discomfort over the MA planner. This observation suggests a potential conflict of interest between mitigating motion sickness and improving general motion comfort.

3.3.4. ACCELERATION MAGNITUDES AND FEASIBILITY

The optimization scheme does not impose any explicit constraint on the aggressiveness of the planned motion. The physical feasibility of the planned motion is verified by the peak acceleration magnitude. Fig. 3.8 shows the maximum absolute acceleration to be experienced by the vehicle with the MS planners, while Fig. 3.9 shows that of the MA planners. The former exhibits slightly higher combined acceleration in general. The values observed here are well aligned with the findings in [18] where a peak acceleration of around 6.0 m/s^2 for urban driving is observed from naturalistic driving data. It can be seen from the receding-horizon approaches using either of the objectives that the peak combined acceleration is closely following the peak longitudinal acceleration for more gentle driving and switches to the peak lateral acceleration in between. When time efficiency receives a smaller weight, the vehicle reduces its speed so much as to achieve smaller lateral acceleration throughout the turns. A larger weight, on the other hand, causes the planner to prefer cornering faster to save time, consequently leading to a higher peak value in lateral acceleration.

3.3.5. COMPUTATION TIME

The receding-horizon approach is expected to have a lower computation complexity and to be capable of real-time implementation. We collected the computational time when the algorithm runs as MATLAB scripts on a desktop PC. The computation is limited to a

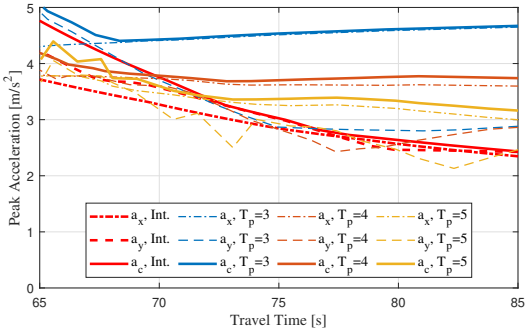

Figure 3.8: Maximum magnitude of longitudinal, lateral, and combined acceleration observed from the MS planner variants. The preview time is varied from 3s to 5s while the sampling time is fixed at 0.5s.

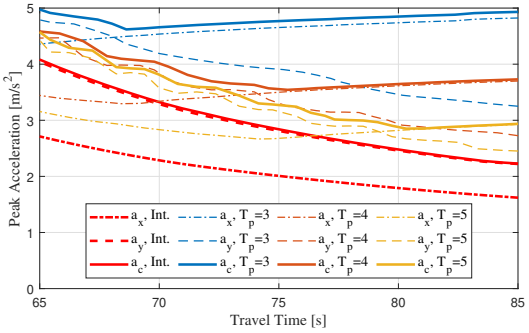

Figure 3.9: Maximum magnitude of longitudinal, lateral, and combined acceleration observed from the MA planner variants. The preview time is varied from 3s to 5s while the sampling time is fixed at 0.2s.

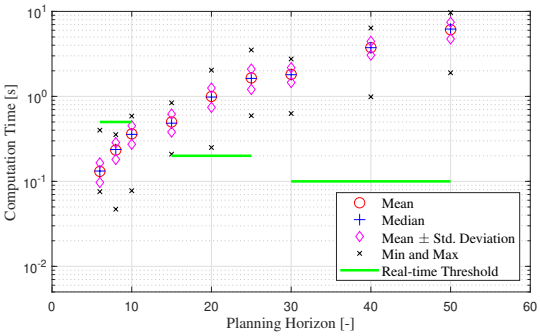

Figure 3.10: Computation time of receding-horizon MS planners using different preview times and sampling times.

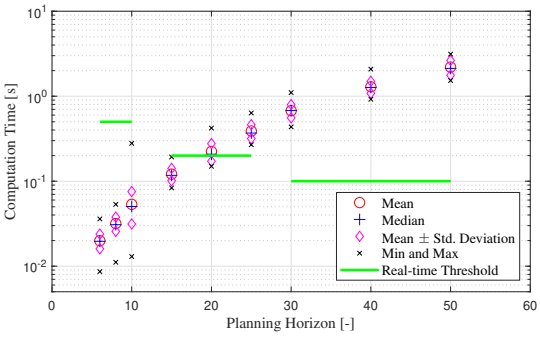

Figure 3.11: Computation time of receding-horizon MA planner using different preview times and sampling times.

single CPU core with a clock frequency of 4.1 GHz. Fig. 3.10 and 3.11 show the variation in computation time with different N_p. With the same T_p, increasing T_s from 0.1 s to 0.2 s reduces computation time by a factor of 5-6. An extra 5-fold reduction can be observed when T_s increases to 0.5 s. With $T_s = 0.5$ s, the MS planner is marginally capable of operating at T_p =5 s. We expect that performing only a limited number of iterations and easing the termination criteria could guarantee that the peak computation time is below the real-time threshold. The algorithm may also be accelerated when running as compiled code instead of MATLAB script. The computation time of the MA planner is approximately 25% to 30% of the MS planner. This allows for a wider margin from the real-time threshold. Alternatively, it could be feasible to use the setting of $T_p = 5$ s and $T_s = 0.2$ s if the algorithm can indeed run faster after the modifications proposed above. The comparison between Fig. 3.10 and 3.11 highlights the complexity of incorporating the frequency sensitivity in motion sickness. It remains an open question whether the MS planner's effectiveness in mitigating motion sickness is worth the extra computation. This needs to be investigated further with experimental studies on human subjects.

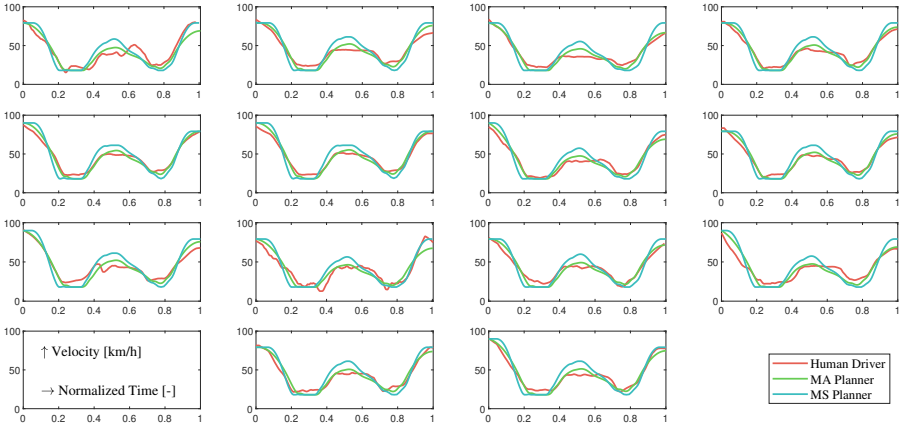

Figure 3.12: A collection of velocity profiles in normalized time, where the human driving data is compared with the optimized motion plans that have the same duration.

3.4. COMPARISON WITH HUMAN DRIVERS

3.4.1. COMPARISON WITH INDIVIDUALS

For each valid test run, we generated optimization-based motion profiles using the motion planning algorithm described in Section 3.2 with the two different objective functions. The weight on duration has been adjusted accordingly in order to obtain an approximate matching of travel time between the human driver and the motion planner. Because minimal instructions were given to the participants regarding how they should drive, the initial velocities at the start of the run are different. Hence we also adjusted the initial velocity in the motion planner to ensure a fair comparison.

The velocity profiles of human drivers and motion planners are provided in Fig. 3.12. Several differences between human drivers and our motion planners can be observed in multiple examples. First, most human-driven runs exhibit a more significant speed reduction at the beginning of the run. This is because of the drivers' attempt to save control effort by letting the vehicle coast for a reasonable distance ahead of an intersection as long as it does not impede other road users. Another potential cause of this difference is that the drivers were maintaining a wider safety margin when approaching an intersection with a higher initial speed. At the end of this braking period, the vehicle would enter RB1 where it needs to give way to vehicles traveling inside. By reducing speed in advance, the drivers have more time to observe the traffic situation and react safely. This is especially relevant because of the poor visibility at this roundabout as depicted by Fig. 3.13. It is hardly possible for the drivers following our test route to detect other road users entering the roundabout from behind occlusions. Therefore, the participants could have decided to decelerate earlier to ensure comfort for the unforeseen case where they need to come to a full stop at the entry to RB1. Inside RB1, however, most drivers adopted a higher speed than the motion planners. The drivers might have overestimated the time loss or they were concerned about the following vehicle. Alternatively, they subconsciously tried to minimize fuel consumption and mechanical wear in

Figure 3.13: The visibility condition when entering the first roundabout on the test route. Vehicles entering from two other directions, represented by the arrows, only become visible at a distance of approximately 30 m. Image source: Google Street View

the braking system. Again, the driving effort could have also played a role here because passing the roundabout with a lower speed means more pedal inputs.

In the RLR sector, the human drivers reached a lower top speed that is well below the imposed limit of 60 km/h. We believe this difference is primarily caused by the damaged pavement at the left-hand turn. The participants drove here at a lower speed in order to maintain good vertical comfort while the motion planners are developed under the assumption of ideal pavement conditions. Limited by this, the drivers would not attempt to reach the speed limit before the next right-hand turn that lies less than 100 m ahead, where the vehicle needs to slow down again.

Finally, upon entering RB2, the participants often chose to decelerate later and more aggressively. In contrast to the first one, the second roundabout is located in an open area where oncoming traffic can be observed with little obstruction. This supports the discussion above that the visibility condition at an intersection may influence human drivers' choices of speed. Meanwhile, the feature of a higher speed by human drivers inside RB2 is similar to what was observed at RB1. After leaving RB2, most participants commanded a less aggressive acceleration than the motion planners. This could be relevant to the arguments above that human drivers may consider fuel consumption in their decision-making.

3.4.2. GROUP PERFORMANCE

The performance of human drivers is evaluated with the objectives of the motion planners: travel time and acceleration energy with or without frequency weighting. On average, the participants took 76.5 s to complete the test run while the average acceleration energy is 211.4 m^2/s^3 and the average frequency-weighted acceleration energy is 147.1 m^2/s^3. In Fig. 3.14, the human driving performance is compared with the MA planner with the acceleration energy being the comfort criterion. The participants exhibited up to 50% more discomfort than the MA planner when consuming the same amount of time. The average disadvantage is 23.5% with the majority (11 out of 14) lying between 0 and 30%. It suggests that human drivers are reasonably good at planning vehicle motions that reduce the accelerations when they are experienced with the route. In contrast, human drivers' performance in mitigating motion sickness is significantly

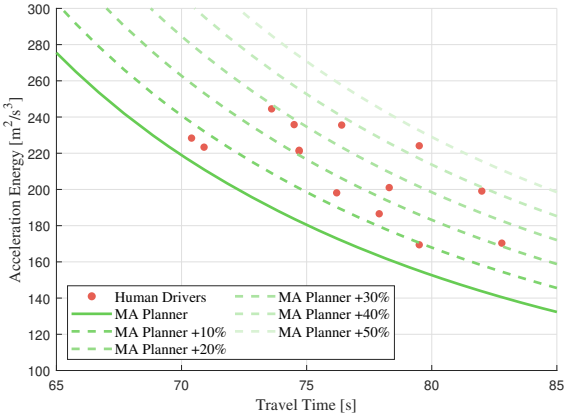

Figure 3.14: The performance of human drivers in improving acceleration comfort and minimizing travel time. The motion planner optimizing these two factors is visualized for comparison purposes. The dash lines are the contours corresponding to amplified discomfort when consuming the same amount of time.

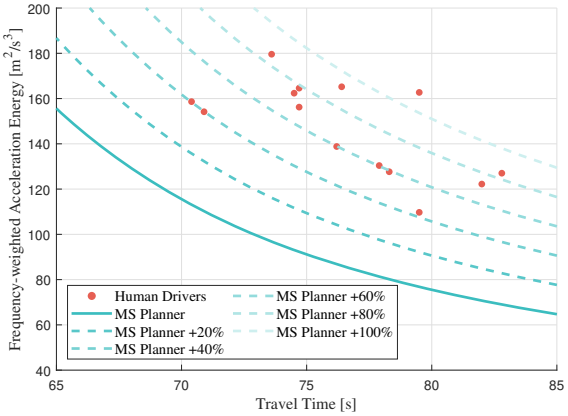

Figure 3.15: The performance of human drivers in mitigating motion sickness and minimizing travel time. The motion planner optimizing these two factors is visualized for comparison purposes. The dash lines are the contours corresponding to amplified predicted sickness levels when consuming the same amount of time.

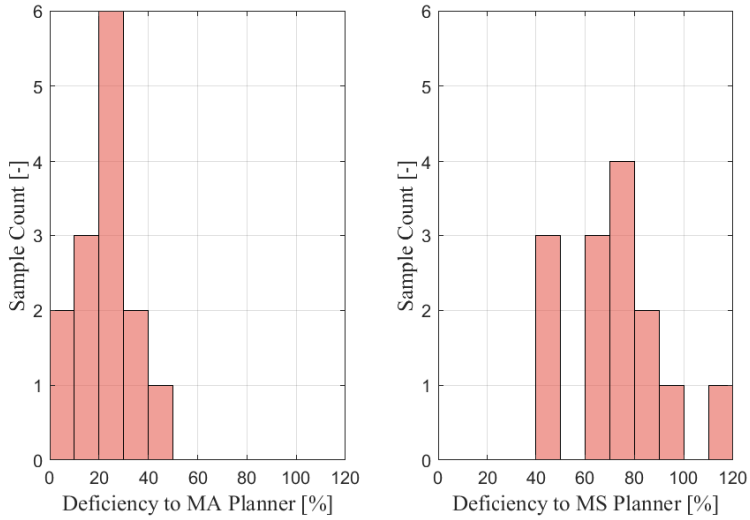

Figure 3.16: Distribution of human drivers' performance deficiency to the corresponding optimization-based motion planners.

worse as suggested by Fig. 3.15. The best-performing human driver still inflicted 20% higher frequency-weighted acceleration energy than the MS planner while the average deficiency is 70.2%. We highlight the distribution of performance deficiency with Fig. 3.16. The more significant difference in mitigating motion sickness is probably caused by the human driver's lower susceptibility to motion sickness due to their active engagement in vehicle control. When they cannot sense certain driving behaviors that give rise to motion sickness among the passengers, it is unlikely that they are able to avoid such behaviors.

3.4.3. FREQUENCY-DOMAIN COMPARISON

The distribution of acceleration energy in the frequency domain is closely related to the incidence of motion sickness. The frequency components in the acceleration data from human drivers are presented in Fig. 3.17, 3.18 in comparison with the motion plans from our optimization-based motion planners. Human drivers have more longitudinal acceleration energy distributed in the range above 0.2 Hz, which reflects more fluctuations in speed. These fluctuations could be perceived as uncomfortable or disturbing rather than nauseogenic because they are outside the most sensitive frequency range. We suspect that smooth control of vehicle speed is challenging for human drivers. Intuitively, it is physically demanding for human drivers to ensure smooth pedal inputs. As discussed before, they may attempt to save input effort when it does not significantly hamper comfort. Moreover, smooth input does not necessarily mean smooth vehicle speed because of the characteristics of the powertrain and the braking system. For example, when the transmission controller selects a higher gear, more throttle input is required in order to maintain the previous acceleration level. The driver has to sense a drop in acceleration

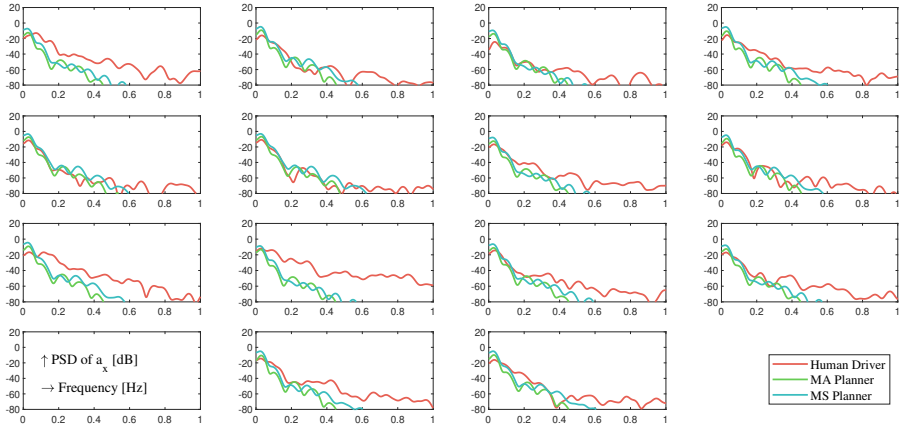

Figure 3.17: A collection of power spectral density in longitudinal accelerations, where the human driving data is compared with the optimized motion plans that have the same duration.

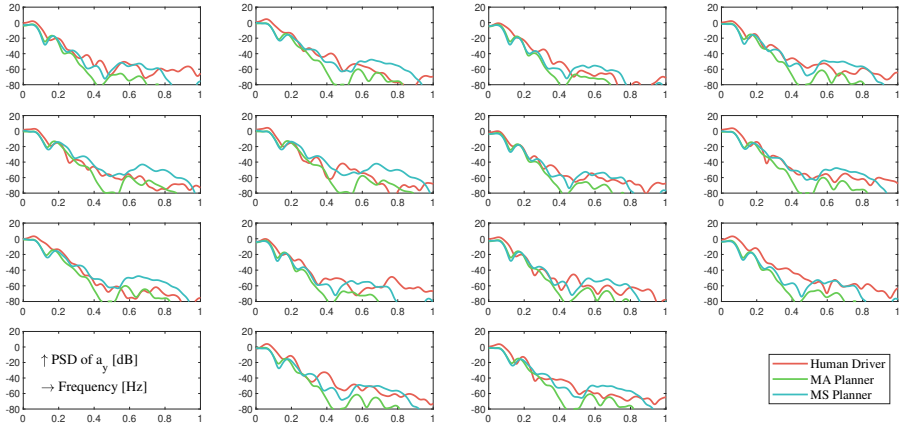

Figure 3.18: A collection of power spectral density in lateral accelerations, where the human driving data is compared with the optimized motion plans that have the same duration.

before starting to adjust his throttle input. It is possible that they would accept a drop in acceleration and keep the input unchanged.

In lateral acceleration, the difference between human drivers and motion planners appears to be less significant. A higher magnitude can be seen from most human drivers for the frequency range below 0.2 Hz. This is mainly due to their choice of a higher speed when driving inside RB1 and RB2 because the low-frequency range is more reflective of the sustained accelerations. Given the frequency sensitivity in motion sickness, this difference could contribute significantly to motion sickness among passengers. In the higher frequencies, however, human drivers did not exhibit significantly more energy. The characteristics of the steering system could be one of the reasons. In general, the lateral acceleration of the vehicle is approximately linear with respect to the steering wheel input for the most common range of dynamics in daily driving, given that the tires are in the linear range. The steering ratio further reduces the scaling ratio between the steering wheel input and the resulting lateral and yaw motion of the vehicle. The haptic feedback is another factor that facilitates the lateral control task. The drivers can feel the torque on the steering wheel, which is indicative of lateral acceleration. Although a similar relationship exists between the brake pedal force and longitudinal acceleration, human beings are in general more sensitive with their hands than feet. Hence is lateral acceleration more smoothly controlled than longitudinal acceleration.

3.5. CONCLUDING REMARKS

This chapter introduced a novel formulation for incorporating the frequency sensitivity to accelerations in the development of a comfort-oriented optimization-based motion planning framework. The proposed method reduced the squared MSDV, an indicator of motion sickness, by up to 11.3% compared with minimizing accelerations in general. A receding-horizon formulation of the optimal planning problem is compared with optimizing for a complex driving scenario in an integral manner. The performance difference from the integral planning approach is quantified for a variety of combinations of the preview parameters in the receding-horizon planner. We consider a preview time of 3 s as the lower limit since this leaves the vehicle with limited time to prepare for a corner entry, resulting in worse motion comfort and a higher chance of motion sickness. We found a longer nominal sampling time of 0.5 s beneficial for the purpose of mitigating motion sickness due to the slow dynamics in the frequency-weighting filter. On the other hand, a nominal sampling time of 0.2 s is sufficiently short for optimizing acceleration comfort. We further investigated the computation time of the receding-horizon planners. The algorithm is close to achieving real-time capability if it could be compiled as machine code and certain parameters of the optimization solver could be adjusted. Furthermore, on-road experiments revealed a performance gap between human drivers and the optimization-based planners described in this study. The proposed sickness-mitigating method achieved a reduction in frequency-weighted accelerations by 32% from the best-performing human driver, while its counterpart without considering the frequency sensitivity improves general acceleration comfort by 19%. The difference suggests that automated vehicles can be even more effective in mitigating motion sickness than in improving general motion comfort.

The motion profiles are compared to two optimization-based motion planners from

our previous research that aim to improve motion comfort by minimizing acceleration discomfort or the predicted incidence of motion sickness. In the time domain, we observed certain differences between human drivers and motion planners and analyzed the potential reasons leading to such differences. The performance deficiency of human drivers may not be solely to blame on their inferior capability in planning and controlling vehicle motion. Rather, they may have included other factors such as input effort and fuel consumption in their decision-making. Nevertheless, their driving behavior could potentially lead to a significantly higher level of motion sickness than the corresponding motion planner. We assert that this phenomenon is related to their lower susceptibility to motion sickness, which means they are not sensitive to the features in vehicle motion that are perceived by passengers as nauseogenic. In terms of the average performance, the participants show approximately 23.5% more acceleration energy or 70.2% more frequency-weighted acceleration energy than the motion planners. These values are calculated with identical travel times. The findings in this study suggest that AVs could potentially overcome the challenges posed by motion sickness by significantly improving their level of motion comfort over average human drivers without sacrificing time efficiency.

Nonetheless, this study relies primarily on the conclusion from past studies that motion sickness has a strong correlation with accelerations in certain frequency ranges. In the literature, there are more complex numerical models to predict motion sickness. We expect that including such models in the motion planning algorithm would require more intensive computation, making it more difficult to implement such approaches in real time. Alternatively, one may explore learning-based approaches to shift the computation offline and achieve real-time sub-optimal planning. Besides, the actual effect of the proposed method on the development of motion sickness among passengers in an automated vehicle remains to be validated. If an on-road experiment is to be performed, a closed track would be needed as motion sickness develops rather slowly and an instrumented vehicle needs to complete multiple laps to observe a difference. Lastly, this work includes only a small number of participants for the evaluation of human driving performance. This limits our ability to generalize the conclusions above to average human drivers. Instead, only the advantage over the best-performing participant was emphasized. We plan to test human drivers on a larger scale on public roads to solidify the baseline performance. This would contribute not only to the evaluation of motion planning and control methods in automated driving but also to quantifying their potential advantage over human drivers.

Besides, the performance deficiency of human drivers might be overestimated. The elevation change and pavement conditions faced by the participants are not considered by the motion planners. Meanwhile, the accelerations might be underestimated when processing the measurement data. The actual extent of how these two factors influence the suggested performance difference could not be verified. On the test route, the use of a GPS sensor alone as a source of position information is insufficient due to the unstable satellite connection. In future research, we recommend measuring the vehicle's relative position within the lane as an additional source of positional information, which could improve the estimation quality of the vehicle trajectory. This could be done by, for example, mounting cameras on the sides of the test vehicle and calculating the distance

with intrinsic camera parameters. Lastly, we recommend the experimental validation of the findings from this study in terms of subjective comfort evaluation. The demonstrated advantage of AVs in mitigating motion sickness is based on empirical prediction methods of motion sickness. It is highly helpful in promoting AVs if the benefit could be reproduced in a real-world setup with human subjects.

BIBLIOGRAPHY

[1] J. A. Silva and V. Grassi, "Clothoid-based global path planning for autonomous vehicles in urban scenarios", in *Proc. IEEE Int. Conf. Robot. and Automat. (ICRA)*, IEEE, 2018, pp. 4312–4318.

[2] S. Zhang, Y. Chen, S. Chen, and N. Zheng, "Hybrid A*-based curvature continuous path planning in complex dynamic environments", in *Proc. IEEE Intell. Transp. Syst. Conf. (ITSC)*, IEEE, 2019, pp. 1468–1474.

[3] X. Qian, I. Navarro, A. de La Fortelle, and F. Moutarde, "Motion planning for urban autonomous driving using bézier curves and mpc", in *Proc. IEEE 19th Int. Conf. Intell. Transp. Syst. (ITSC)*, Ieee, 2016, pp. 826–833.

[4] A. Artunedo, J. Villagra, and J. Godoy, "Real-time motion planning approach for automated driving in urban environments", *IEEE Access*, vol. 7, pp. 180 039–180 053, 2019.

[5] R. Lattarulo, L. González, and J. Perez, "Real-time trajectory planning method based on n-order curve optimization", in *Proc. 24th Int. Conf. Syst. Theory, Control and Computing (ICSTCC)*, IEEE, 2020, pp. 751–756.

[6] H. Cao and M. Zoldy, "Implementing B-spline path planning method based on roundabout geometry elements", *IEEE Access*, vol. 10, pp. 81 434–81 446, 2022.

[7] C. L. Bottasso, D. Leonello, and B. Savini, "Path planning for autonomous vehicles by trajectory smoothing using motion primitives", *IEEE Trans. Control Syst. Technol.*, vol. 16, no. 6, pp. 1152–1168, 2008.

[8] M. McNaughton, C. Urmson, J. M. Dolan, and J.-W. Lee, "Motion planning for autonomous driving with a conformal spatiotemporal lattice", in *Proc. IEEE Int. Conf. Robot. and Automat. (ICRA)*, IEEE, 2011, pp. 4889–4895.

[9] M. Mischinger, M. Rudigier, P. Wimmer, and A. Kerschbaumer, "Towards comfort-optimal trajectory planning and control", *Veh. Syst. Dynamics*, vol. 57, no. 8, pp. 1108–1125, 2019.

[10] M. R. Siddiqi, S. Milani, R. N. Jazar, and H. Marzbani, "Ergonomic path planning for autonomous vehicles-an investigation on the effect of transition curves on motion sickness", *IEEE Trans. Intell. Transp. Syst.*, vol. 23, no. 7, pp. 7258–7269, 2022.

[11] H. Shin, D. Kim, and S.-E. Yoon, "Kinodynamic comfort trajectory planning for car-like robots", in *Proc. IEEE/RSJ Int. Conf. Intell. Robots and Syst. (IROS)*, IEEE, 2018, pp. 6532–6539.

[12] Y. Zheng, B. Shyrokau, and T. Keviczky, "Comfort and time efficiency: A roundabout case study", in *Proc. IEEE Int. Intell. Transp. Syst. Conf. (ITSC)*, IEEE, 2021, pp. 3877–3883.

[13] Y. Zheng, B. Shyrokau, and T. Keviczky, "3DOP: Comfort-oriented motion planning for automated vehicles with active suspensions", in *Proc. IEEE Intell. Veh. Symp. (IV)*, IEEE, 2022, pp. 390–395.

[14] Z. Htike, G. Papaioannou, E. Siampis, E. Velenis, and S. Longo, "Fundamentals of motion planning for mitigating motion sickness in automated vehicles", *IEEE Trans. Veh. Technol.*, vol. 71, no. 3, pp. 2375–2384, 2021.

[15] D. Li and J. Hu, "Mitigating motion sickness in automated vehicles with frequency-shaping approach to motion planning", *IEEE Robot. and Automat. Lett.*, vol. 6, no. 4, pp. 7714–7720, 2021.

[16] Y. Kuwata, J. Teo, G. Fiore, S. Karaman, E. Frazzoli, and J. P. How, "Real-time motion planning with applications to autonomous urban driving", *IEEE Trans. Control Systems Technology*, vol. 17, no. 5, pp. 1105–1118, 2009.

[17] Z. Htike, G. Papaioannou, E. Siampis, E. Velenis, and S. Longo, "Minimisation of motion sickness in autonomous vehicles", in *Proc. IEEE Intell. Veh. Symp. (IV)*, IEEE, 2020, pp. 1135–1140.

[18] R. Liu and X. Zhu, "Driving data distribution of human drivers in urban driving condition", in *Proc. IEEE 20th Int. Conf. Intell. Transp. Syst. (ITSC)*, IEEE, 2017, pp. 1–6.

4

NONLINEAR MODEL PREDICTIVE CONTROL FOR CURVE TILTING

If everything seems under control, you're just not going fast enough.

Mario Andretti

Parts of this chapter have been published in IEEE Transactions on Control Systems Technology [1].

4.1. INTRODUCTION

The attractive advantages of active suspension have promoted its continuous development. The active force generation in the suspension system allows the decoupling of the control of wheel and vehicle body motion, making it feasible to improve the ride quality and the road holding performance simultaneously [2]. Moreover, it enables the control of the vehicle's body attitude, which could be helpful when for example, the vehicle is subjected to a side collision. The vehicle body could be rolled away from the side of impact, absorbing more energy with the mechanical structure and hence providing the occupants with better protection. Besides, active suspension unlocks further potential in enhancing motion comfort in other motion regimes than the vertical. The tilting car concept invented for railroad vehicles [3] could now be brought onto road vehicles. This was first seen on production passenger vehicles under the name of curve tilting. Two major challenges need to be tackled for a useful implementation of the tilting concept: predicting the driving action and accommodating the dynamic vehicle motion. The former is essential for determining the reference tilting angle that leads to a reduction in lateral acceleration. Meanwhile, the coupled roll-yaw rotation that amplifies motion sickness should be avoided in this reference generation process. Desirably, the roll angle should have a phase lead over the yaw motion [4]. Hence the tilting must have started before the driver applies a steering input. This is usually achieved with the camera-based road preview that detects the lane marks and estimates the curvature and has seen successful experimental implementation in a motorway driving scenario. However, this is complicated by adding the longitudinal motion into consideration. In a more dynamic scenario, predicting driver input and vehicle motion becomes more difficult when significant speed changes are present. The actual speed adopted by the driver determines the magnitude of the lateral acceleration. This uncertainty causes difficulty not only in generating a reference roll angle but also in the control. The inertial accelerations exerted on the vehicle body are countered by the redistribution of vertical loads among the four wheels. The change in vertical load should be compensated for by the active suspensions in order to maintain a stable body attitude. Without an accurate estimate of the load transfer, it is difficult to achieve satisfactory control quality.

The state-of-the-art approach of the active curve tilting functionality is based on the preview of road curvature using stereo cameras, combined with PID control [5] which is widely implemented in industrial applications. Previewing curvature alone is not sufficient for predicting the vehicle's planar motion and is a compromised solution for vehicles with little to no automation. With the human driver in the loop, the longitudinal velocity can only be predicted by understanding the driver's intention and the surrounding traffic situation. However, this cannot provide a precise value of the velocity at a certain time ahead. Similarly, the steering action may be presumed by the lane mark and the usage of turning indicators, as implemented in lane-keeping assistance [6]. Nevertheless, such estimation has limited precision and the actual moment and magnitude of the steering input remain uncertain. With these uncertainties in predicting the steering action, it is difficult to determine the tilting manner of the vehicle body in order to effectively minimize the lateral disturbance exerted on the occupants. Meanwhile, these uncertainties also harm the control quality of the roll motion. The acceleration (or deceleration) and steering inputs influence the attitude of the vehicle body by causing

longitudinal and lateral load transfer, which further exerts additional vertical forces on the suspensions at different locations. Only with reliably predicted planar motion can such forces be estimated in advance and requested from the active suspensions in order to prevent the vehicle body's attitude from being disturbed. The PID control method exhibits certain disadvantages in this specific application. In order to maximize the utilization of the stroke length available, the system inevitably operates in the nonlinear range of the spring where linear methods are perceived as less capable. When operating close to certain constraints (e.g., physical limit, actuator's capability) in the system, PID cannot explicitly avoid violations, potentially causing damages to the suspension system in the long term and raising the operational cost of the vehicle.

Alternatively, nonlinear model predictive control (NMPC) is known for its capability of explicitly handling nonlinear system dynamics and constraints. Model predictive control is an optimization-based control method that determines the control input by minimizing a cost function while satisfying certain constraints. Based on the prediction with a model of the system's dynamics throughout a certain prediction horizon, the cost function accumulates the control effort and the consequential error. By minimizing the cost function, the controller computes the control input that yields an optimal trade-off solution between quality and actuation expenses. Nonlinear MPC is a branch of MPC that allows predicting with nonlinear models and can handle nonlinear constraints if necessary. The underlying numerical optimization problem is more complex than in a linear MPC, where the prediction model and constraints are linear and the cost function is typically quadratic. With few exceptions (e.g., quadratic programming as in a linear MPC), optimization of a nonlinear non-convex cost function requires intensive computation. The main contributor to the computational burden is the complexity of the prediction model that allows the evaluation of the cost function. The evaluation of the cost function is done by simulating the system behavior with the prediction model by means of numerical integration. On top of that, most nonlinear optimization algorithms, including gradient descent, sequential quadratic programming, interior-point method, etc., utilize the gradient information of the cost function, which is determined numerically if the analytic form of the gradient function is unavailable. The numerical differentiation method further increases the computational cost. Hence, the dimensionality of the input also plays a role. Another contributing factor to the complexity is the non-convexity of the cost function. In practice, it is difficult to verify the convexity of a cost function. Hence, the number of local optima in the function should be considered unknown.

Running the aforementioned nonlinear optimization algorithms for one time without proper initialization is at the risk of converging to a local minimum that does not yield a reasonable control input. This problem could be tackled with global optimization heuristics, for example, multi-start local search, evolutionary algorithms, simulated annealing, etc. Such approaches are successful in raising the chance of avoiding local minima but are computationally less efficient. In the case of vehicle dynamics, some studies run NMPC controllers at 20 Hz [7], [8], while linear controllers such as PID and linear quadratic regulator (LQR) can operate at 100 Hz. This makes the aforementioned heuristics that demand heavy computation less desirable in this specific application. Instead, the warm-start technique has been explored to enable real-time implementation

of NMPC in vehicle dynamics control. One of the approaches is to initialize the upcoming optimization process using the results of the previous step [9]. The method is effective if the plant is modeled with sufficient accuracy and the magnitude of the disturbance is limited. Only under such conditions, the prediction coincides with the actual behavior of the system and the previous result is still feasible, although not necessarily optimal due to the shift in the prediction horizon. Otherwise, the actual state at the next step may deviate largely from what is predicted and the corresponding control input does not yield a good initial guess anymore. Instead, some studies propose to initialize online optimization with an explicit control law [10]. The explicit control law is computed offline by approximating the optimal solution of the optimization problem with PWA functions. The approach of explicitly initializing the NMPC with an alternative sub-optimal controller has been proposed in [11] and tested with an arbitrary mathematical model. A similar method was implemented in [12], where the explicit controller is computed by solving a comparable hybrid MPC problem offline. The controller aims to stabilize the excessive yaw and lateral motion of a passenger vehicle in case of a rear-end traverse impact. Such approaches effectively move a portion of the computational effort offline and better utilize the onboard storage resource.

4.2. CONTROL METHOD

This section presents in detail the control approach to the curve tilting application. The control system's main objective is to ensure that the vehicle body's roll angle accurately follows the reference value. The functionality is enabled by active suspension actuators that generate the desired amount of additional vertical force, as commanded by the controller. The force commands are computed under the framework of nonlinear model predictive control. The underlying numerical optimization process is accelerated with a novel explicit initialization method. The control scheme is explained in Fig. 4.1 and the components will be explained in Subsections 4.2.1-4.2.5.

4.2.1. REFERENCE MOTION

The desired manner of active roll motion is designed according to comfort-related requirements and physical limitations. The reference roll angle is a function of previewed lateral acceleration on the vehicle chassis at 1 second ahead. The permissible roll angle can reduce the lateral acceleration by at most $0.5\,\mathrm{m/s^2}$ from what is exerted on the passenger. As the lateral acceleration builds up, it would be undesirable if the roll angle approaches the saturation value with a high velocity. Hence, we adopted a smooth curve shape for the transition (Fig. 4.2). A half period of a sinusoid is placed at the origin, connecting two linear sections with a constant value:

$$\phi_{ref}^{\mathrm{ss}} = \begin{cases} k_1 \sin\left(k_2 a_{y,\mathrm{prev}}\right), & \left|k_2 a_{y,\mathrm{prev}}\right| \leq \pi/2 \\ k_1, & \left|k_2 a_{y,\mathrm{prev}}\right| > \pi/2 \end{cases} \tag{4.1}$$

The parameter k_1 is set to equal the maximum permissible roll angle ϕ_{max}. The parameter k_2 is chosen to meet the following boundary condition:

$$\frac{\mathrm{d}\phi_{\mathrm{ref}}^{\mathrm{ss}}}{\mathrm{d}a_{y,\mathrm{prev}}^{\mathrm{ss}}}\bigg|_{a_{y,\mathrm{prev}}^{\mathrm{ss}}=0} = k_1 k_2 = \frac{1}{g} \tag{4.2}$$

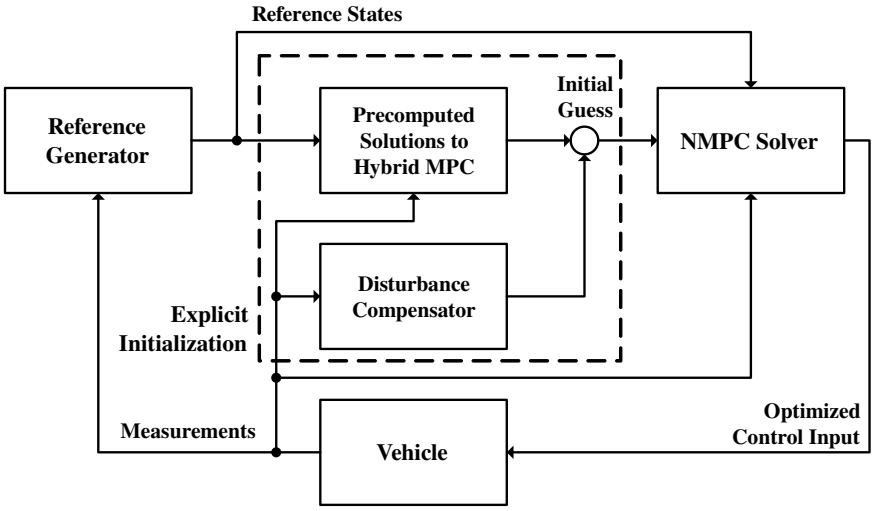

Figure 4.1: A schematic drawing of the proposed control approach. The components inside the dashed rectangle belong to the explicit initialization scheme. The NMPC solver takes inputs from the reference generator, the vehicle's onboard sensors, and the output of the initialization to compute an optimal control input to the active suspension actuators.

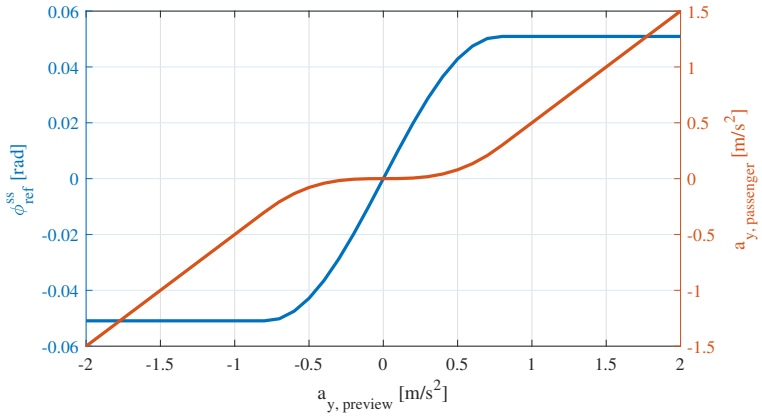

Figure 4.2: The reference motion and resultant lateral acceleration sensed by the passenger are plotted versus the previewed lateral acceleration. The previewed lateral acceleration is estimated with the current velocity and the curvature of the lane center at 1 second of time ahead.

where g is the gravitational acceleration. This equation expresses the requirement that the slope of the tangent line of the curve at the origin should result in zero lateral acceleration to be sensed by the passenger. It ensures that the minor lateral disturbances are fully compensated for. In addition to the smooth steady-state reference curve, we further applied a low-pass filter on the previewed acceleration, in order to generate feasible and comfortable reference motion even when the curvature changes abruptly. The filter is defined as:

$$a_{y,\mathrm{prev}}(s) = \frac{\omega_n^2}{s^2 + 2\zeta\omega_n s + \omega_n^2} a_{y,\mathrm{prev}}^{\mathrm{ss}}(s) \tag{4.3}$$

where ω_n and ζ are the natural frequency and the damping coefficient of the filter, respectively. A second-order filter is chosen such that the roll acceleration is bounded and the roll velocity is continuous. The filter exhibits an over-damped behavior (i.e., $\zeta > 1$), which eliminates overshoot and residual oscillations in the reference motion.

4.2.2. PREDICTION MODEL

The motion regimes of interest include the vehicle body's roll, pitch, and heave, noted by ϕ, θ, and z, respectively. They must be modeled as a whole as these motions interact with each other through the rigid vehicle body. The equations of motion are as follows [13]:

$$\begin{aligned} I_{xx}\ddot{\phi} &= \left(F_{z,\mathrm{FL}} + F_{z,\mathrm{RL}} - F_{z,\mathrm{FR}} - F_{z,\mathrm{RR}}\right) B/2 \\ &\quad - m_{\mathrm{spr}} a_y \left(h_{\mathrm{cg}} - h_{\mathrm{cr}}\right) - \left(I_{zz} - I_{yy}\right)\dot{\theta}\dot{\psi} \\ I_{yy}\ddot{\theta} &= \left(F_{z,\mathrm{RL}} + F_{z,\mathrm{RR}}\right) L_{\mathrm{R}} - \left(F_{z,\mathrm{FL}} + F_{z,\mathrm{FR}}\right) L_{\mathrm{F}} \\ &\quad - m_{\mathrm{spr}} a_x \left(h_{\mathrm{cg}} - h_{\mathrm{cp}}\right) + \left(I_{xx} - I_{zz}\right)\dot{\psi}\dot{\phi} \\ m_{\mathrm{spr}}\ddot{z} &= F_{z,\mathrm{FL}} + F_{z,\mathrm{FR}} + F_{z,\mathrm{RL}} + F_{z,\mathrm{RR}} \end{aligned} \tag{4.4}$$

where h_{cg} is the static height of the center of gravity and h_{cp}, and h_{cr} stand for the static heights of the instant centers of pitch and roll rotations, respectively. The longitudinal distances from the center of gravity of the sprung mass m_{spr} to the front and rear axle are denoted by L_{F} and L_{R}, whereas the track width of the vehicle is represented by B. The vertical force at each wheel, $F_{z,*}$ (where $* \in \{\mathrm{FL}, \mathrm{FR}, \mathrm{RL}, \mathrm{RR}\}$ stands for wheel locations) is a function of the motion states plus the control input from the active suspension actuator $F_{\mathrm{act},*}$:

$$F_{z,*} = f_*\left(\phi, \dot{\phi}, \theta, \dot{\theta}, z, \dot{z}\right) + F_{\mathrm{act},*} \tag{4.5}$$

The planar motions (i.e., longitudinal, lateral, and yaw) are excluded as they are governed by either a human driver or the motion planning and control on an automated vehicle. Still, the planar motions have a strong influence on these modeled motions. The inertial acceleration causes load transfer in longitudinal and lateral directions, exerting additional pitch and yaw moments on the vehicle body. The yaw motion is coupled with pitch and roll according to the rotational dynamics of a rigid body governed by Euler's equations.

Suspension forces are the key characteristics to describe in the prediction model. The typical approach to suspension control assumes constant spring stiffness and damping coefficient, in order to obtain a linear model [14], [15]. Since we aim to maximize the utilization of wheel travel for the tilting, the suspension is stretched or compressed to an extent that the linear approximation is no longer valid. On one hand, the kinematics of the suspension system is constrained by its geometry, which is optimized for a linear relationship around the neutral position. As the wheel moves farther away from the neutral position, the control arms rotate largely so that the validity of the small-angle approximation no longer holds. Consequently, the compression or stretching of the spring and damper is not proportional to the wheel displacement. In addition, the forces on the spring and damper are not proportional to their displacement or velocity, either. In practice, the spring has a stiffness that gradually increases when compressed, which together with the buffer block, protects the components from physical damage due to excessive wheel movements. Meanwhile, the dampers usually exhibit degressive characteristics (i.e., the force-to-velocity ratio decreases as the velocity increases) which prevent the hydraulic cylinder from over-pressurization. Besides, the damper generates less force in the compression stroke than in the stretching stroke. This is mainly done to minimize the transmission of road disturbance in case of an upward impact is exerted on the wheel (e.g., when driving over speed bumps or debris), which is more frequently experienced [16]. These nonlinearities can be captured at once by determining the function of force-to-displacement and force-to-velocity relationships. The relevant data can be obtained from the simulation model.

4.2.3. OPTIMAL CONTROL PROBLEM

The MPC determines the control input by solving an optimal control problem (OCP) at each time step. An optimal control input sequence of finite length is calculated by minimizing a cost function and the first input in the sequence is forwarded to the controlled system. The OCP is formulated as:

$$\begin{aligned} \min_{\boldsymbol{u}} \quad & J_{\mathrm{NMPC}}(\boldsymbol{u}) \\ \text{s.t.} \quad & \boldsymbol{u}_{\min} \leq \boldsymbol{u} \leq \boldsymbol{u}_{\max} \end{aligned} \tag{4.6}$$

The cost function J reflects the priorities of the state tracking errors and control efforts and focuses on a finite horizon from the current moment. In this study, we use a quadratic cost function integrated through the prediction horizon:

$$J = \int_{t_0}^{t_0+t_\mathrm{p}} \left((\boldsymbol{x_t} - \boldsymbol{x}_{\mathrm{ref}})^T \boldsymbol{Q} (\boldsymbol{x_t} - \boldsymbol{x}_{\mathrm{ref}}) + \boldsymbol{u_t}^T \boldsymbol{R} \boldsymbol{u_t} \right) dt \tag{4.7}$$

where the states, reference states, and inputs are defined as:

$$\begin{aligned} \boldsymbol{x} &= \left(\phi, \dot{\phi}, \theta, \dot{\theta}, z, \dot{z}\right)^T \\ \boldsymbol{x}_{\mathrm{ref}} &= \left(\phi_{\mathrm{ref}}, 0, 0, 0, 0, 0\right)^T \\ \boldsymbol{u_t} &= \left(F_{\mathrm{act,FL}}, F_{\mathrm{act,FR}}, F_{\mathrm{act,RL}}, F_{\mathrm{act,RR}}\right)^T \end{aligned} \tag{4.8}$$

Table 4.1: Weighting parameters of the NMPC

Variable	Unit	Weight
Roll angle	rad	12
Roll rate	rad/s	0.4
Pitch angle	rad	2
Pitch rate	rad/s	0.1
Heave	m	2
Heave rate	m/s	0.1
Actuation force	kN	0.0001

The cost function is evaluated by means of numerical integration with an Euler step of 50 ms. The control input is fixed through the prediction horizon t_p, i.e. the number of decision variables is 4. The inputs are bounded within the capability of the actuators. Due to the limited information available for predicting the vehicle's planar motion, the exogenous disturbances are assumed constant through the prediction horizon of 0.4 s. The assumption may not be valid for more dynamic situations and could be improved when combined with a motion planner. Minimizing the aforementioned cost function results in an optimal control input that ensures that the reference roll angle is tracked with a minimal error while the influence of the active suspension forces on the pitch (θ and $\dot{\theta}$) and heave (z and $\dot{z}$) motions and the control efforts are kept reasonably low. The values of the weighting parameters are presented in Table 4.1.

4.2.4. EXPLICIT INITIALIZATION

The numerical optimization process for solving the OCP described above is accelerated with an explicit initialization technique. A hybrid MPC is developed for this purpose. By approximating the nonlinear dynamics with multiple linear modes under a piecewise affine (PWA) formulation, we formulate the OCP as a mixed-integer quadratic programming (MIQP) problem that can be solved efficiently [17]. Given finite modes and prediction steps, the MIQP problem contains finite binary and continuous variables. It is therefore possible to solve the problem in finite time by naive enumeration of all combinations of the binary variables. The branch-and-bound algorithm only has to do so in the worst case [18]. This feature allows the MIQP problem to be solved with guaranteed global optimality given sufficient computational effort, which is not a problem for offline preparation. Nevertheless, the formulation of a hybrid model of the roll, pitch, and heave motion is complex due to a large number of modes. To overcome this, we divide the whole vehicle body into four separate sprung masses, each suspended above the corresponding wheel. Such dynamics are described with a quarter-car model:

$$\begin{aligned} \begin{bmatrix} z_{*,k+1} \\ \dot{z}_{*,k+1} \end{bmatrix} &= A_{*,j} \begin{bmatrix} z_{*,k} \\ \dot{z}_{*,k} \end{bmatrix} + B_{*,j} F_{\text{act},*,k} + f_{*,j} \\ \begin{bmatrix} z_{*,j,lb} \\ \dot{z}_{*,j,lb} \end{bmatrix} &\leq \begin{bmatrix} z_k \\ \dot{z}_k \end{bmatrix} \leq \begin{bmatrix} z_{*,j,ub} \\ \dot{z}_{*,j,ub} \end{bmatrix} \end{aligned} \tag{4.9}$$

where j denotes the mode that the system operates in at step k. For each mode j, a

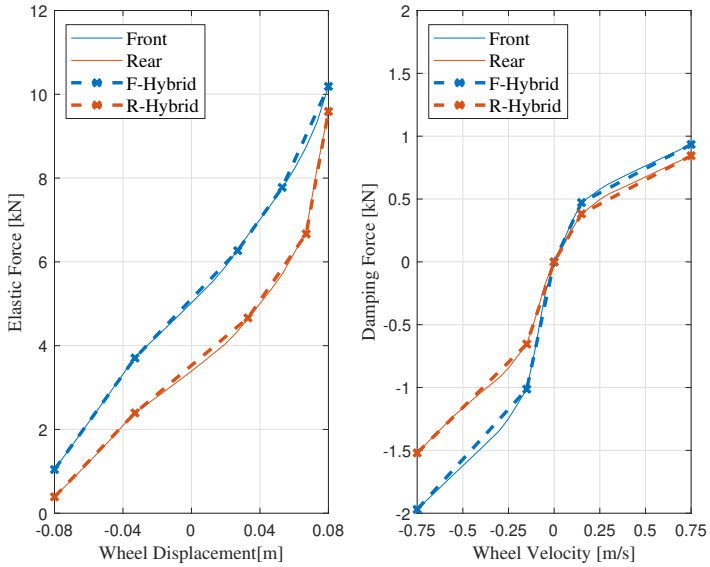

Figure 4.3: The suspension force characteristics according to the actual multi-body model and the hybrid model for quarter-car dynamics.

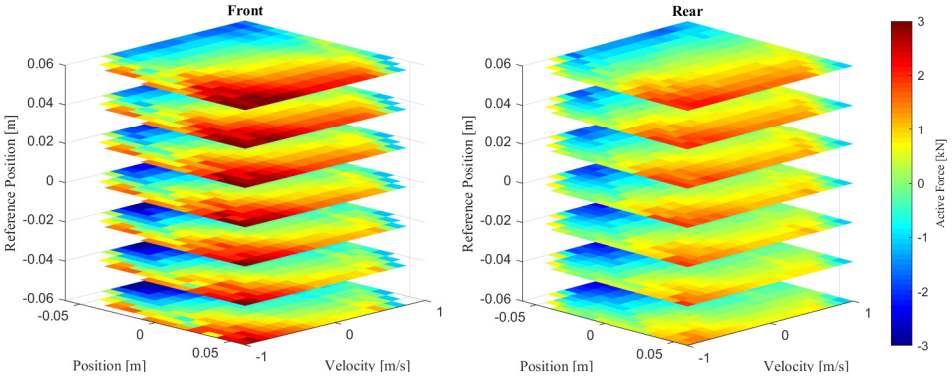

Figure 4.4: Slices of the 3-D look-up table for the purpose of explicitly initializing the optimization problem in NMPC.

corresponding set of A, B, and f is defined based on the PWA approximation of the suspension forces. As Fig. 4.3 shows, the forces on the front and rear springs and dampers are each divided into 4 sectors. Given the independence between the spring and the damper, the hybrid quarter-car model contains 16 modes. The decision is based on the fact that most hydraulic dampers on passenger vehicles have 4 operating modes, namely the slow bump, fast bump, slow rebound, and fast rebound. For sake of convenience, we also divide the spring characteristics into 4 pieces. In the hybrid model, the dynamics of the unsprung mass, including the tire, wheel, and wheel hub, are neglected because of the high modal frequency (100 Hz according to [19]) as a result of the high stiffness-to-mass ratio. The sampling frequency of the MPC, 20 Hz in our case, is too low to capture such dynamics without aliasing according to the Nyquist–Shannon sampling theorem. Increasing the sampling frequency of the MPC to 200 Hz is unfavorable from the perspective of computational complexity. The higher frequency vibration is outside the frequency range of interest and has a limited impact on the aspect of comfort that this paper focuses on. Thus the radial dynamics of the tire is neglected. The OCP in the hybrid MPC is formulated as:

$$\begin{aligned} \min_{F_{act,*}} \quad & J_{hyb}(F_{act,*}) \\ s.t. \quad & F_{\min} \leq F_{act,*} \leq F_{\max} \end{aligned} \tag{4.10}$$

where the cost function J_{hyb} is:

$$J = \sum_{i=1}^{k} q_z \left(z_* - z_{\text{ref},*}\right)^2 + r_{\text{hyb}} F_{\text{act},*}^2 \tag{4.11}$$

The resemblance of the OCP in the hybrid MPC to the one in the NMPC is achieved by choosing the proper reference and weightings. The hybrid MPC controls the height of the sprung mass to follow a reference:

$$\begin{aligned} z_{\text{FL,ref}} &= z_{\text{RL,ref}} = \phi_{\text{ref}} \cdot B/2 \\ z_{\text{FR,ref}} &= z_{\text{RR,ref}} = -\phi_{\text{ref}} \cdot B/2 \end{aligned} \tag{4.12}$$

If all four suspensions track their reference height, the vehicle body would consequently track the reference roll angle. The equivalence of weighting is given by:

$$\begin{aligned} q_{z,\text{hyb}} \cdot z_{*,\text{ref}}^2 &= q_{\phi,\text{NMPC}} \cdot \phi_{\text{ref}}^2 \\ r_{\text{hyb}} \cdot F_{\text{act},*}^2 &= r_{\text{NMPC}} \cdot F_{\text{act},*}^2 \end{aligned} \tag{4.13}$$

Given the identical penalty on the control effort in both OCPs, the penalty on height tracking error should equal the penalty on the consequent roll tracking error. The hybrid MPC is implemented using the Multi-parametric Toolbox [20] and the OCP is solved on a uniform grid of the 3-dimensional space of z_*, $\dot{z}_*$, $z_{\text{ref},*}$ and the initial output is evaluated by linear interpolation (see Fig. 4.4). In total, the OCP is solved 3,549 times. Using multi-parametric optimization for generating the explicit control low would reduce the loss optimality than the grid approach but the computational time is observed to be too high

Table 4.2: Comparison of roll and pitch moment of inertia

Moment of Inertia	Roll	Pitch
Rigid Body [kg m^2]	718.2	2783.8
4 Point Masses [kg m^2]	1020.1	3341.1
Difference [%]	42.0	20.0

even for offline processing. Instead, we expect online optimization to compensate for the loss of optimality.

Nevertheless, there are further fundamental differences when modeling a rigid body with four separate point masses. They should be carefully considered to avoid invalidating the initialization scheme. Firstly, the four sprung masses do not yield precisely the actual moment of inertia of roll and pitch when connected with rigid links. The comparison is given in Table 4.2. The mismatch in moments of inertia may cause the hybrid MPC to demand a larger force than the actual optimal force according to the NMPC's OCP. Moreover, the quarter-car models alone can by no means capture the load transfer caused by planar accelerations. The load transfer influences each individual quarter-car model as an external disturbance and should be compensated for with:

$$\begin{aligned} F_{\text{comp},*} &= m_s a_y \big(h_{\text{cg}} - h_{\text{cr}}\big)/(2B) \cdot s_{\text{side}} \\ s_{\text{side}} &= \begin{cases} 1, * \in \{\text{FR,RR}\} \\ -1, * \in \{\text{FL,RL}\} \end{cases} \end{aligned} \tag{4.14}$$

The compensatory component is added to the initial output by interpolating the hybrid OCP solutions to eventually construct the starting point as:

$$F^{\text{init}}_{\text{act},*} = F_{\text{interp},*} + F_{\text{comp},*} \tag{4.15}$$

The eventual starting point is expected to reduce the online computational load as well as to serve as a valid control input by itself. Relevant results will be presented in Section 4.4.

4.2.5. NONLINEAR PROGRAMMING SOLVER

From the starting point described above, local optimization is further performed to find the optimal control input. We implemented the gradient descent method with inexact (backtracking) line search [21]. To incorporate the constraints on control inputs, a shrinkage of the step length also happens when the current step size causes a violation. The algorithm stops when the norm of the local gradient is below a certain threshold, or when the number of iterations exceeds a certain limit. The latter allows us to balance the performance gain and the computational load, which can be exploited when running the controller with limited computational resources.

4.3. SIMULATION SETUP

The proposed control strategy is examined in a virtual environment in multiple scenarios. The simulation platform is IPG CarMaker, in which a passenger car's dynamics are modeled in detail and experimentally validated by DRiV Incorporated, which includes

validated sub-models of the active suspension actuators. A virtual driver model controls the vehicle's longitudinal and lateral motion to follow the desired route. It allows deviating from the lane center in order to reduce the curvature of the path and the velocity is regulated such that the acceleration stays within a predefined envelope. In the simulation, the velocity-dependent curvature preview is implemented with a virtual road sensor, while in reality this may be enabled by high-precision road maps and/or the environmental perception systems on automated vehicles. The simulation is initially executed on a desktop PC (3.7 GHz Hexa-core CPU plus 64 GB DDR4 RAM) for understanding the behavior of the system and tuning the parameters before moving to a hard real-time platform (see details in 4.3.3).

4.3.1. SCENARIOS

The system is supposed to operate on well-paved roads only. We adopted three typical scenarios that are commonly experienced in daily driving, namely the highway, rural, and urban scenarios. Highway driving mainly features sustained cornering motion that changes gradually and the peak magnitude of the acceleration is rather low, too. The longitudinal velocity would stay mostly constant. This scenario mainly tests the system's performance in terms of steady-state tracking. Driving in urban areas is the exact opposite as it involves sharp turnings with shorter duration and moderate magnitude, in addition to the frequent changing of direction and speed. It examines the system's dynamic response to quick-changing references. In between is the rural scenario where mid- to high-speed corners are common. The corners can be closely adjacent to each other and the curvature is varying continuously. A higher magnitude of lateral acceleration than the other scenarios may be observed. The paths of the vehicle in the proposed scenarios are shown in Fig. 4.5.

4.3.2. EVALUATION

The simulation study aims to evaluate the proposed system from two perspectives: control quality and motion comfort. For control quality, we focus on the tracking error of the roll angle, specifically, the root-mean-square (RMS) value of the error signal. Motion comfort, on the other hand, is a more comprehensive quality to quantify and measure. Extensive guidelines for comfort evaluation subject to mechanical vibrations can be found in ISO 2631-1 [22]. However, the proposed method only aims to reduce the lateral acceleration exerted on the occupant in order to mitigate motion sickness. Thus we adopt the frequency weighting proposed in [23] for motion sickness induced by lateral oscillations. A virtual inertial measurement unit (IMU) is placed at the approximate position of the otolith organs of the occupant. The IMU's orientation is fixed to the vehicle body, assuming that the occupant is relevantly static to the vehicle. In addition to examining the RMS value of the sensed lateral acceleration, we further take into account the human body's sensitivity to vibrations with different frequencies. The lateral acceleration signal's power distribution (PSD) is calculated first before the aforementioned weighting is applied. To help demonstrate the performance of the NMPC method, we also included a PID-based curve tilting controller as the baseline. The PID controller is accompanied by the same disturbance-compensating input as a feed-forward term that counteracts lateral load transfer. The PID output is bounded according to the actuators'

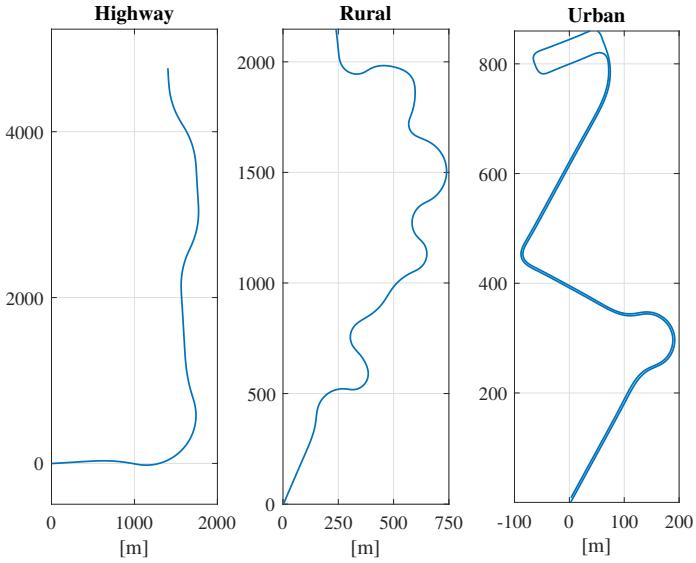

Figure 4.5: Road profiles of the proposed scenarios for the simulation study.

capability and its integral component resets to zero once the reference roll angle starts to change. This helps combat the windup issue due to the relatively large integral gain. The PID controller is tuned per scenario to maximize its performance while the weighting parameters in the NMPC remain constant. Additional simulation runs are performed by using the output of the explicit initialization as control input such that the validity of the initialization scheme is verified.

4.3.3. HIL SETUP

In order to further validate whether the control method is efficient enough for real-time implementation with limited computational resources, the simulation runs have been repeated on a hardware-in-the-loop setup (Fig. 4.6). The controller is compiled on a dSPACE MicroAutoBox II, which carries a single-core 900 MHz processor and 16 MB random memory. This device has been widely used in the industry to test prototype control algorithms. It yields a feasible performance for industrial microprocessors targeting highly automated vehicles (e.g., the quad-core 800 MHz NXP S32S247). The simulation environment is compiled on the dSPACE DS1006 processing board (quad-core 2.8 GHz CPU, 1 GB DDR2 RAM). The two devices communicate via a CAN bus, on which the virtual vehicle exchanges the controller's command with the necessary measurements. The communication operates at 20 Hz, identical to the controller's sampling frequency, while the vehicle dynamics are updated at 1 kHz. Also included in the HIL setup is the Delft Advanced Driving Simulator (DAVSi) [24], which mainly consists of a mock-up of the front half of a Toyota Yaris and a hexapod motion platform driven by six electric motors. The experiment runs in hard real-time mode, where if the turnaround time of the controller

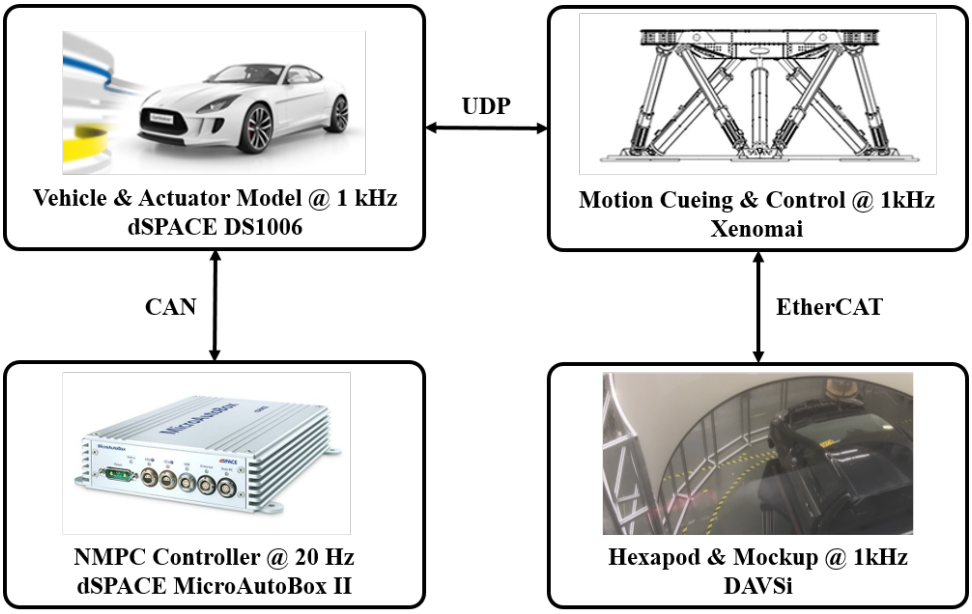

Figure 4.6: A schematic drawing of the HIL experiment setup explaining the functions of each platform and the communications between the platforms.

exceeds the sampling time, the simulation is terminated immediately.

4.4. RESULTS

4.4.1. NUMERICAL PERFORMANCE

The NMPC's solver settings influence the trade-off between computational effort and performance. The key parameter in our case is the number of iterations. This parameter is varied between 2 and 64. The corresponding performance indicators are shown in Fig. 4.7. The contribution of the initialization scheme is apparent. After a small number of iterations, the tracking error and the resultant lateral acceleration are not decreasing steeply anymore. Performing more iterations is not significantly beneficial, especially when considering the limited computational resource for real-time implementation. In the more dynamic scenarios, the tracking error starts to grow at a larger number of iterations. This is partly due to the assumption that the disturbances are constant throughout the prediction horizon whose validity diminishes in this scenario. Another part of the contribution comes from the potential model mismatch. It is nevertheless challenging to formulate a compact prediction model to capture all the complex multibody dynamics of a passenger vehicle. Because the equivalent moments of inertia in the initialization scheme are higher, the starting point of the optimization is likely to yield a higher control effort. This is on some occasions helpful in reducing the tracking error. By further optimizing the control inputs, the control effort would decrease while allowing marginally larger tracking errors. The trend is different when the NMPC solver starts from all ze-

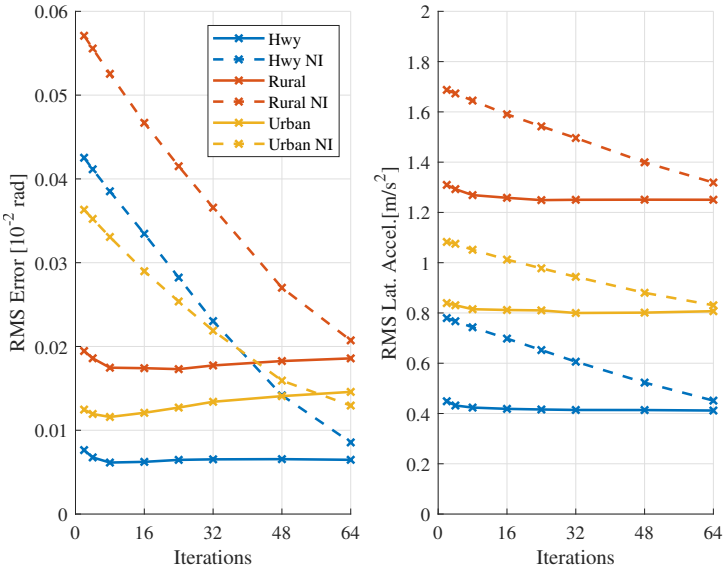

Figure 4.7: Variation of the comfort and control performance indicators when different numbers of iterations in the nonlinear optimization are performed. The term NI in the legends stands for 'No Initialization', meaning the optimization process starts from zeros.

ros, where both indicators keep decreasing up to 64 iterations. Though a comparable performance level is only achieved at 64 iterations, illustrating the contribution of the initialization scheme. Eventually, 8 iterations are chosen for further analysis. With this setting, a worst-case turnaround time of 43 ms has been observed in the HIL experiment. This is lower than the sampling time of the controller, 50 ms, proving that the proposed NMPC controller is capable of real-time implementation.

4.4.2. CONTROL QUALITY

The simulation results for the three scenarios in terms of roll tracking are shown in Fig. 4.8. The RMS tracking error per control method per scenario is compared in Table 4.3. In the highway scenario, the reference roll angle stays constant for long periods of time, allowing the integral action of PID to correct the error. The model-based approaches, i.e. the explicit control and NMPC, yield a constant tracking error due to potential model mismatch. This disadvantage becomes less obvious in rural and urban scenarios, where the reference roll angle varies more frequently. The integral action is not given sufficient time to bring down the error before the reference value changes. The quicker response of explicit control and NMPC contributes in these situations to the reduction of the error, demonstrating the superiority of the prediction over the reaction in a more dynamic environment. These two methods show minor non-minimum-phase behavior at the beginning of a changed reference, though. Because when the vehicle leaves a steady-state cornering motion, the assumption of constant lateral acceleration through the prediction horizon does not hold. The actual lateral acceleration experienced by the vehicle is

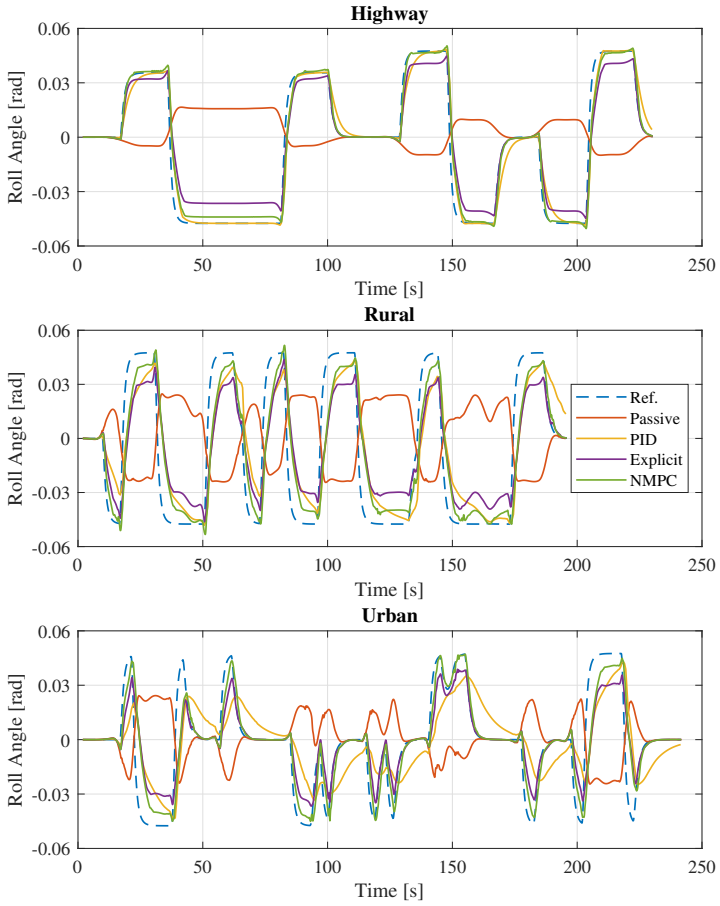

Figure 4.8: Roll angles of the vehicle body per simulation scenario. In each sub-graph, the roll angles of a vehicle with passive suspension and active suspension using different methods are compared against the reference value.

lower than what the controller expects. Hence the controller commands a larger force than the actual need.

Table 4.3: Comparison of the tracking performance of the control methods used in the simulation.

Controller	Tracking Error	Highway	Rural	Urban
PID	RMS [10^{-2} rad]	0.706	2.090	1.868
Explicit	RMS [10^{-2} rad]	0.881	2.053	1.330
	Difference [%]	+24.8	-1.8	-28.8
NMPC	RMS [10^{-2} rad]	0.615	1.747	1.159
	Difference [%]	-12.9	-16.4	-38.0

4.4.3. MOTION COMFORT

The lateral acceleration sensed by the occupants is shown in Fig. 4.9, indicating their level of discomfort. Table 4.4 compares the lateral acceleration sensed by the occupant, with and without the curve tilting function, and using different control methods. The body of a passive vehicle leans away from the curvature center when cornering, slightly magnifying the lateral acceleration on the occupant. The effectiveness of the tilting functionality is significant in the highway scenario where all control methods achieved a reduction of lateral acceleration by 40%. In rural and urban scenarios, the benefit of the system decreases to the range of 20-25% due to multiple reasons. On one hand, the absolute magnitude of the reduction in lateral acceleration is limited by the roll angle available. The same amount of reduction becomes less obvious on a relative scale when the actual magnitude is larger. On the other hand, the system is not able to respond sharply to the highly dynamic planar motion. Roll velocity is penalized to ensure a gentle transition and avoid introducing another source of discomfort. And even the predictive control methods are only reacting to a change of reference. Though according to the RMS acceleration, the advantage of using NMPC over PID is only marginal, in contrast with the more visible improvement in terms of tracking accuracy. This is primarily because the RMS value is more sensitive to the higher-amplitude part of the signal. The higher amplitude is usually coupled with steady-state tracking of the saturated reference roll angle, which is a result of the limited roll angle allowed by the suspension geometry. NMPC

Table 4.4: Comparison of the motion comfort in terms of RMS lateral acceleration using different control methods used in the simulation.

Controller	Acceleration	Highway	Rural	Urban
Passive	RMS [m/s^2]	0.796	1.710	1.103
PID	RMS [m/s^2]	0.414	1.300	0.882
	Difference [%]	-47.8	-23.6	-19.3
Explicit	RMS [m/s^2]	0.465	1.326	0.856
	Difference [%]	-41.3	-22.1	-21.7
NMPC	RMS [m/s^2]	0.424	1.269	0.815
	Difference [%]	-46.5	-25.4	-25.4

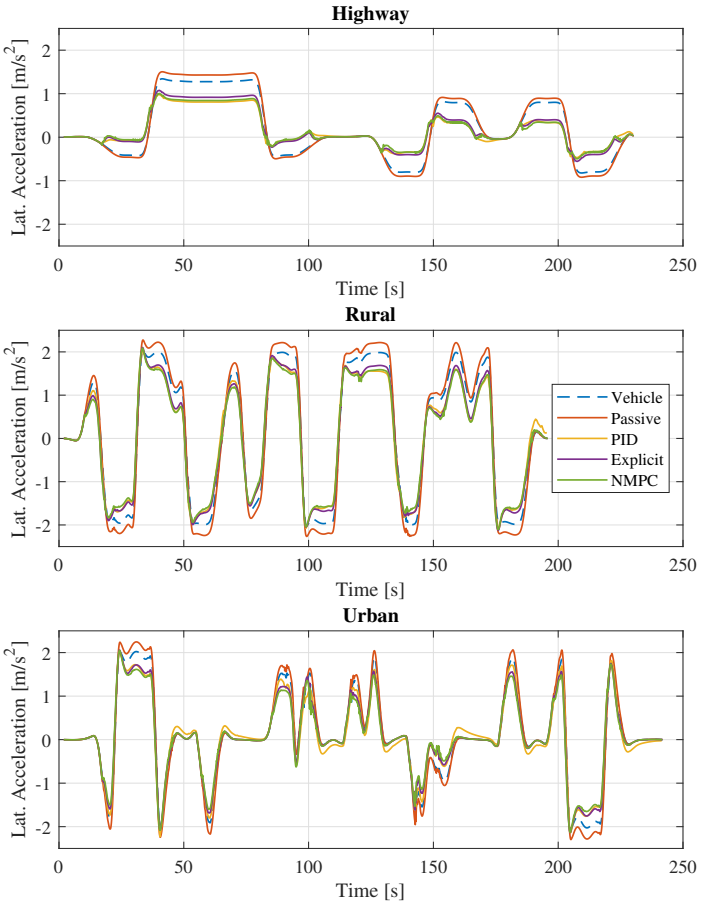

Figure 4.9: Lateral accelerations per simulation scenario. In each sub-graph, the lateral acceleration exerted on the occupants of a vehicle with passive suspension and with active suspension using different methods are compared against the lateral acceleration of the vehicle body.

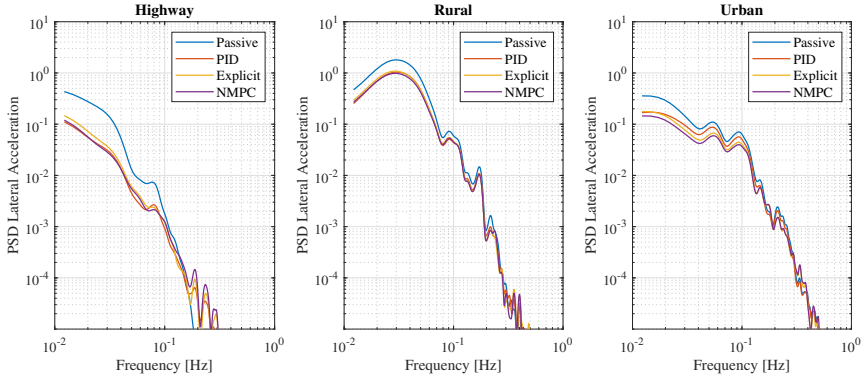

Figure 4.10: Frequency-domain power distribution of the lateral acceleration sensed by the occupant.

outperforms PID mainly in transient response when the actual lateral acceleration is relatively low. The phase lead of the reference generator also helps mitigate the negative impact of the PID's slower response on the resulting comfort quality. Nevertheless, the trend is consistent between Table 4.3 and 4.4 that NMPC's advantage over PID is more obvious in more dynamic driving scenarios. In addition to the RMS value of the sensed acceleration, we further analyzed the results in the frequency domain. The power spectral density is computed and weighted according to the recommendations in [23], which indicates a higher influence in the low-frequency range up to 0.25 Hz. The weighted PSDs resulting are displayed in Fig. 4.10. With the actively controlled roll motion, a significant improvement is observed in the frequency range of up to approximately 0.1 Hz in all three scenarios. Though the active control of the roll motion slightly elevates the high-frequency components in the highway scenario where the passive motion is steady.

4.5. CONCLUDING REMARKS

This Chapter presents an NMPC strategy for the curve tilting functionality using active suspensions. To tackle the commonly reported challenge of reducing the computational load for solving the OCP online, we proposed an explicit initialization scheme. By precomputing a look-up table offline, the starting point of the nonlinear optimization is quickly determined by 3-dimensional linear interpolation. The lookup table results from a hybrid modeling method of the quarter-car dynamics with highly nonlinear suspension forces. Based on this model, a hybrid MPC problem has been formulated, reflecting the same objectives and weightings as in the NMPC. The alternative OCP is solved on a wide range of initial and reference states to form a look-up table. The output of the interpolation is further combined with disturbance compensation, which estimates and counteracts the influences of load transfer that are not captured by the quarter-car model. The eventual starting point is supposed to yield a valid control input. Simulation shows that controlling the suspensions with the initialization scheme already enables the desired functionality. Further performing the online optimization in NMPC improves the transient response and reduces the tracking error. The NMPC approach yields

a better overall tracking performance in all three driving scenarios (12.9%, 16.4%, and 38.0% smaller, respectively) albeit being slightly outperformed by PID in steady-state tracking where the integral action is highly beneficial. HIL experiment on limited computational resources confirms the real-time capability of the proposed method, whose parameters are chosen to balance the additional computational effort and the marginal performance gain. Also, thanks to the explicit initialization scheme, the NMPC solver's computational load is reduced significantly compared to starting the optimization from zeros.

Meanwhile, the current study shows certain disadvantages. Neglecting the dynamics of the unsprung masses implies that the performance may not be as satisfactory when driving on a rough road. Nevertheless, the major source of discomfort under such circumstances would be vertical excitation instead of lateral acceleration. The HIL simulation reveals that the full capability of the NMPC scheme is not yet fully realized with the hardware available to us. The computational capability of the HIL hardware, released in 2010, is not representative of what could be available on the latest highly automated vehicles, given the rapid development in high-performance automotive microcontrollers. It is interesting to investigate if the numerical efficiency could be boosted with parallel computing on multi-core microcontrollers. For industrial applications, the code would be further optimized for efficiency and could run faster than in the rapid-prototyping phase. Such advances may allow a more complex prediction model in the NMPC although the model validation process would become more challenging, too. The full potential of the current implementation could be realized on automated vehicles where the predictive feature of the NMPC can be joined by the motion planning algorithm. The idea will be explored in the upcoming Chapter 5.

BIBLIOGRAPHY

[1] Y. Zheng, B. Shyrokau, T. Keviczky, M. Al Sakka, and M. Dhaens, "Curve tilting with nonlinear model predictive control for enhancing motion comfort", *IEEE Transactions on Control Systems Technology*, vol. 30, no. 4, pp. 1538–1549, 2021.

[2] H. E. Tseng and D. Hrovat, "State of the art survey: Active and semi-active suspension control", *Vehicle system dynamics*, vol. 53, no. 7, pp. 1034–1062, 2015.

[3] D. Boocock and B. King, "The development of the prototype advanced passenger train", *Proceedings of the Institution of Mechanical Engineers*, vol. 196, no. 1, pp. 35–46, 1982.

[4] J. A. Joseph and M. J. Griffin, "Motion sickness from combined lateral and roll oscillation: Effect of varying phase relationships", *Aviation, space, and environmental medicine*, vol. 78, no. 10, pp. 944–950, 2007.

[5] M. Bär, *Vorausschauende Fahrwerkregelung zur Reduktion der auf die Insassen wirkenden Querbeschleunigung*. Forschungsges. Kraftfahrwesen (fka), 2014.

[6] T. Pilutti and A. G. Ulsoy, "Identification of driver state for lane-keeping tasks", *IEEE transactions on systems, man, and cybernetics-Part A: Systems and humans*, vol. 29, no. 5, pp. 486–502, 1999.

[7] F. Borrelli, P. Falcone, T. Keviczky, J. Asgari, and D. Hrovat, "Mpc-based approach to active steering for autonomous vehicle systems", *International journal of vehicle autonomous systems*, vol. 3, no. 2-4, pp. 265–291, 2005.

[8] E. Siampis, E. Velenis, S. Gariuolo, and S. Longo, "A real-time nonlinear model predictive control strategy for stabilization of an electric vehicle at the limits of handling", *IEEE Transactions on Control Systems Technology*, vol. 26, no. 6, pp. 1982–1994, 2017.

[9] M. Diehl, H. G. Bock, and J. P. Schlöder, "A real-time iteration scheme for nonlinear optimization in optimal feedback control", *SIAM Journal on control and optimization*, vol. 43, no. 5, pp. 1714–1736, 2005.

[10] M. N. Zeilinger, C. N. Jones, and M. Morari, "Real-time suboptimal model predictive control using a combination of explicit mpc and online optimization", *IEEE Transactions on Automatic Control*, vol. 56, no. 7, pp. 1524–1534, 2011.

[11] M. S. Darup and M. Mönnigmann, "Explicit feasible initialization for nonlinear mpc with guaranteed stability", in *2011 50th IEEE Conference on Decision and Control and European Control Conference*, IEEE, 2011, pp. 2674–2679.

[12] Y. Zheng and B. Shyrokau, "A real-time nonlinear mpc for extreme lateral stabilization of passenger vehicles", in *2019 IEEE International Conference on Mechatronics (ICM)*, IEEE, vol. 1, 2019, pp. 519–524.

[13] M. Kissai, B. Monsuez, X. Mouton, D. Martinez, and A. Tapus, "Adaptive robust vehicle motion control for future over-actuated vehicles", *Machines*, vol. 7, no. 2, p. 26, 2019.

[14] S. Ikenaga, F. L. Lewis, J. Campos, and L. Davis, "Active suspension control of ground vehicle based on a full-vehicle model", in *Proceedings of the 2000 American Control Conference. ACC (IEEE Cat. No. 00CH36334)*, IEEE, vol. 6, 2000, pp. 4019–4024.

[15] M. Zapateiro, F. Pozo, H. R. Karimi, and N. Luo, "Semiactive control methodologies for suspension control with magnetorheological dampers", *IEEE/ASME Transactions on mechatronics*, vol. 17, no. 2, pp. 370–380, 2011.

[16] W. F. Milliken, D. L. Milliken, *et al.*, *Race car vehicle dynamics*. Society of Automotive Engineers Warrendale, PA, 1995, vol. 400.

[17] A. Bemporad, D. Mignone, and M. Morari, "An efficient branch and bound algorithm for state estimation and control of hybrid systems", in *1999 European Control Conference (ECC)*, IEEE, 1999, pp. 557–562.

[18] D. Axehill and M. Morari, "Improved complexity analysis of branch and bound for hybrid mpc", in *49th IEEE Conference on Decision and Control (CDC)*, IEEE, 2010, pp. 4216–4222.

[19] L. Yam, D. Guan, and A. Zhang, "Three-dimensional mode shapes of a tire using experimental modal analysis", *Experimental mechanics*, vol. 40, no. 4, pp. 369–375, 2000.

[20] M. Herceg, M. Kvasnica, C. N. Jones, and M. Morari, "Multi-parametric toolbox 3.0", in *2013 European control conference (ECC)*, IEEE, 2013, pp. 502–510.

[21] L. Armijo, "Minimization of functions having lipschitz continuous first partial derivatives", *Pacific Journal of mathematics*, vol. 16, no. 1, pp. 1–3, 1966.

[22] "Mechanical vibration and shock — evaluation of human exposure to whole-body vibration — part 1: General requirements", International Organization for Standardization, Geneva, CH, Standard, May 1997.

[23] B. E. Donohew and M. J. Griffin, "Motion sickness: Effect of the frequency of lateral oscillation", *Aviation, Space, and Environ. Medicine*, vol. 75, no. 8, pp. 649–656, 2004.

[24] Y. R. Khusro, Y. Zheng, M. Grottoli, and B. Shyrokau, "Mpc-based motion-cueing algorithm for a 6-dof driving simulator with actuator constraints", *Vehicles*, vol. 2, no. 4, pp. 625–647, 2020.

5

Motion Planning for Curve Tilting Using Active Suspensions

Every day is a major balancing act that I have to figure out and coordinate.

Jocko Willink

Parts of this chapter have been published in IEEE International Conference on Intelligent Transportation Systems [1].

5.1. INTRODUCTION

Considerable potential in improving motion comfort and reducing motion sickness has been suggested by the findings in Chapter 3 thanks to the automated vehicle's advantages in precise perception and motion control. While staying safely within the permissible driving space, the lane width could be better utilized than averagely capable human drivers. Meanwhile, the possibility of reducing perceived lateral acceleration with active suspensions has been explored in Chapter 4. When designed to cooperate with or assist human drivers, the idea of actively tilting the vehicle body is hindered by the difficulty in predicting vehicle motions. It is possible to anticipate driver action under certain circumstances but more often only on a behavior level. For example, one may be certain about the driver commanding a deceleration when approaching a red traffic light. However, this is insufficient for facilitating the planning and control of vehicle body attitude. The roll and pitch of the vehicle body are under constant influences of the longitudinal and lateral vehicle motions, primarily due to the load transfer effect. It is difficult to achieve accurate body attitude control without reliably predicting the exact motion pattern to be commanded. More significant challenges for implementing roll compensation for lateral acceleration in road vehicles lie within the decision on the timing and amplitude of the active roll motion. The combination of roll and lateral motion could cause diverse intensities of motion sickness. Past experiments showed that the exact magnitude depends on a variety of factors including motion amplitude, frequency, percentage of compensation, phase relations, as well as the location of the rotation axis [2]–[6]. When the lateral acceleration is fully compensated by a corresponding roll motion, the development of motion sickness appears to be faster than in the case of a 25% compensation. The findings apply to an excitation frequency of 0.1 and 0.2 Hz while for a lower frequency, a high percentage of roll compensation may contribute more to improving physical comfort. The recommended range of compensation ratio partly overlaps what is actually achievable by using active suspensions on passenger vehicles, according to the simulation data presented in Chapter 4 and depending on the driving scenario. Meanwhile, the phase relation between the roll motion and lateral acceleration is found to be significantly influential to the effect of the compensation. It is suggested that a phase lead in the roll motion, i.e. the roll angle preceding lateral acceleration, would cause less motion sickness than vice versa. However, the case of no phase difference examined in the literature was combined with full compensation while the others were with partial compensation. The uncontrolled differences in the experiment conditions complicate the task to provide solid recommendations on how the roll motion should be designed.

This chapter introduces a motion planning algorithm extended from what was described in Chapter 3 in order to coordinate the roll motion with the planar motions. Despite the difficulties in predicting the sickness level to be caused by the combined motion, it still could reveal the unique advantages of combining automated vehicles with active suspensions. In understanding such advantages, it could be justified whether the idea of reducing lateral acceleration with roll compensation is a viable solution for passenger vehicles.

5.2. OPTIMIZATION PROBLEM

5.2.1. MOTION DEFINITION

The proposed planning algorithm, referred to as '3DOP', considers the roll motion of the vehicle in addition to its longitudinal and lateral motions. It outputs desired vehicle motions in the three regimes to be fulfilled by chassis actuators and controllers. As has been described in Chapter 3-3.2.1, the road profile is described with straight and curved segments, each assigned a curvature (0 for straight segments) and a length. The segments are further discretized into a string of reference stations distributed along the lane center. At each station, a local lateral axis is defined along the curvature radius, with the left-hand side of the driving direction being positive. The vehicle's path is then constructed with a set of waypoints, each located relative to the corresponding station with a lateral position y. The vehicle's velocity v and roll angle ϕ when passing a waypoint are directly assigned by the motion planner and the accelerations are calculated accordingly.

5.2.2. OBJECTIVE FUNCTION

The purpose of 3DOP is to improve comfort while preserving time efficiency for passengers traveling in an automated vehicle. We choose to minimize the weighted sum of discomfort D and maneuver time T:

$$J = W_{\text{time}} T + D \tag{5.1}$$

Where a relative weighting factor W_{time} is used for maneuver time T and is varied to cover a wide spectrum of user preferences. A small weight suits those highly susceptible to motion sickness, whereas a larger weight can be selected by those in urgent transit. Although maneuver time is straightforward to calculate, comfort is a more abstract concept to measure. We choose to characterize the major discomfort indicator in (5.2), as the integral of squared accelerations along the passenger's perceived horizontal plane. In this way, the effect of vehicle body tilt on the lateral acceleration sensed by the passenger is incorporated. It differs from the MSDV used in [7]. It remains uncertain whether the MSDV concept could be generalized to combined longitudinal and lateral accelerations whereas the computation of relative quantities increases the complexity of the problem.

$$D_{\text{acc}} = \int_0^T \left(a_x^2 + a_y^2\right) dt \tag{5.2}$$

The roll motion is an additional source of discomfort that should be considered. Experiments suggest a perception threshold of 0.5 deg/s for the frequency component of 1 Hz [8]. This is far below the roll rate observed on curve tilting systems [9], meaning that the roll motion could be perceived in most situations. The contribution of roll motion to motion sickness has also been suggested by past studies. Hence, we penalize the absolute roll motion in an additional roll-related discomfort term (5.3). The total discomfort is then given by (5.4), which is the sum of acceleration-related discomfort and roll-related discomfort scaled with weighting factor W_{roll}.

$$D_{\text{roll}} = \int_0^T \left|\dot{\phi}\right| dt \tag{5.3}$$

$$D = D_{\text{acc}} + W_{\text{roll}} D_{\text{roll}} \tag{5.4}$$

The entire motion consists of $M = N - 1$ segments connecting two adjacent waypoints, with N being the total number of waypoints. The integral form of the objective function is equivalent to the sum of segment values:

$$J = \sum_{k=1}^{M} \left(W_{\text{time}} \Delta T_k + \Delta D_{\text{acc},k} + W_{\text{roll}} \Delta D_{\text{roll},k} \right) \tag{5.5}$$

The segment values are calculated as:

$$\begin{aligned} \Delta D_{\text{acc},k} &= \int_{T_k}^{T_{k+1}} \left(a_{x,k}^2 + a_{y,k}^2 \right) dt \\ \Delta D_{\text{roll},k} &= \int_{T_k}^{T_{k+1}} \left| \dot{\phi} \right| dt \end{aligned} \tag{5.6}$$

Within a segment, we consider the velocity and roll angle to change linearly with respect to time. Knowing the distance between the two waypoints d_k (1 m in our case) gives the following:

$$\begin{aligned} \Delta T &= \tfrac{2 d_k}{v_k + v_{k+1}} \\ a_{x,k} &= (v_{k+1} - v_k) / \Delta T \\ \dot{\phi}_k &= (\phi_{k+1} - \phi_k) / \Delta T \end{aligned} \tag{5.7}$$

Further, we assume the curvature remains constant within the segment, calculated as:

$$\kappa_k = (\psi_{k+1} - \psi_k) / d_k \tag{5.8}$$

The lateral acceleration within the segment is hence approximated as:

$$\begin{aligned} a_{y,k} &= \kappa_k \bar{v}_k^2 - g \sin \bar{\phi}_k \\ \bar{v}_k &= (v_k + v_{k+1}) / 2 \\ \bar{\phi}_k &= (\phi_k + \phi_{k+1}) / 2 \end{aligned} \tag{5.9}$$

Combining these equations allows determining the value of J from a given motion plan.

5.2.3. CONSTRAINTS AND INITIALIZATION

The comfort vs time-efficiency optimization produces reasonable results only when constrained properly. In our case, box constraints are placed on all motion variables. For lateral position, the bounds are determined by the width of the lane and the vehicle body. A typical lane width of 3.75 m is found in most European countries, outside populated areas. A representative width of a D-segment passenger vehicle including mirrors is under 2.10 m. Hence the vehicle is allowed to deviate from the lane center by up to 0.75 m on each side and the remaining centimeters are left as a safety margin. The vehicle's forward velocity is constrained according to local policies. In the Netherlands, a speed limit of 80 km/h is found on most of the distributor (rural) roads. The roll angle of the vehicle body is constrained to lie between ± 5 deg. Given a track width of 1.6 m, an active suspension actuator is required to lift or lower the vehicle body on its side by 7 cm. Furthermore, the vehicle is expected to drive along the lane center at the speed limit when entering and exiting the scenario, from and into road sectors with negligible bending.

Hence the lateral position of the first and the last waypoint is 0, velocity 80 km/h. This ensures acceptable behavior for the vehicles behind and on the adjacent lanes. No additional measure is taken to ensure the feasibility of the planned motion concerning vehicle dynamics. The aggressiveness of the motion has to be far below the friction limit to be considered comfortable by the passengers. This ensures that the performance is only directly influenced by the choice of weights in the cost function and not by the tightness of additional constraints. It is still possible to maintain a safety margin at low-friction conditions by only allowing a very small W_{time}.

5.2.4. OPTIMIZATION PROBLEM AND SOLVER

The motion plan consisting of $3N$ decision variables is determined by solving the optimization problem formulated as (5.10). For this purpose, we used the Sequential Quadratic Programming (SQP) algorithm in MATLAB R2020b. The step tolerance was reduced to 10^{-10} while the other parameters remain as default.

$$\begin{aligned} \text{min:} \quad & J(\mathbf{X}) \\ \text{where:} \quad & \mathbf{X} = \left[y_1 \dots y_N, v_1 \dots v_N, \phi_1 \dots \phi_N \right] \\ \text{s.t.:} \quad & y_{\min} \le y_1 \dots y_N \le y_{\max} \\ & v_{\min} \le v_1 \dots v_N \le v_{\max} \\ & \phi_{\min} \le \phi_1 \dots \phi_N \le \phi_{\max} \end{aligned} \tag{5.10}$$

5.3. RESULTS

5.3.1. AN EXAMPLE OF PLANNED MOTION

Fig. 5.1 presents the motion plan generated with the weighting factor $W_{\text{time}} = 12$. The optimal solution consists of 1557 decision variables, found after 1129 SQP iterations, and the cost function was evaluated approximately 1.8M times. The total computation time is 3066 s on a desktop computer with an Intel Core i5-9400F CPU. The optimization was terminated as the stopping criterion of step tolerance 10^{-10} had been met. The planner comprehensively utilizes the available lane space and the vehicle's roll capability to reduce lateral acceleration while coordinating the longitudinal velocity. The manner of space utilization highly resembles the racing line used in motorsport where the path curvature should be minimal. Velocity is adjusted in accordance with the curvature. The vehicle slows down prior to sharp turns and accelerates when the path bending is lower. The speed in the middle sector (20-30 s) ranges from 30-45 km/h, reflective of real-world values observed while actually driving on the site. The corner tilting capability is exploited in a restrained fashion thanks to the additional penalty term. The roll angle, visualized as a row of comb teeth perpendicular to the vehicle path in Fig. 5.1, does not necessarily follow the vehicle's turning direction. During the right-left-right turns between the two roundabouts, the vehicle only rolls to the right. Because the left turn is relatively short-lasting, changing the roll angle for it would harm comfort through the longer right turns. In the roundabouts, however, the three turns contribute almost equally to acceleration discomfort. The roll angle hence has to change its direction accordingly for minimizing the perceived lateral acceleration. The effect of curve tilting on minimizing passenger-perceived lateral acceleration is obvious from the sub-figure

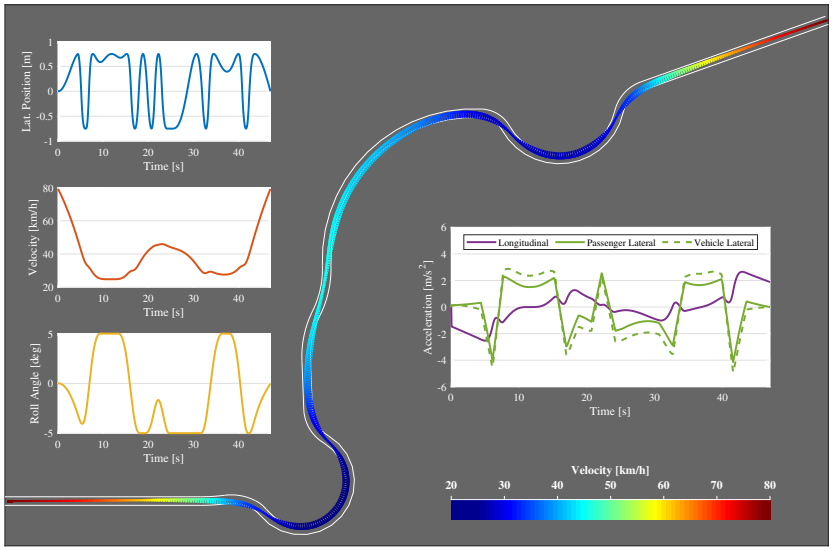

Figure 5.1: An optimal motion plan generated with $W_{\text{time}} = 12$. The main figure visualizes the vehicle's ideal motion to navigate through the scenario. The left subfigures show the plans for the lateral position, velocity, and roll angle. The resulting acceleration profile is shown in the subfigure on the right. The green solid line represents the lateral acceleration experienced by the passenger and the green dash line represents the lateral acceleration exerted on the vehicle body. This motion plan has a duration of 47.0 seconds and a discomfort rating of 205.9.

Table 5.1: Control quality of tracking the motion plan

Tracking Error	Position [10^{-1}m]	Velocity[km/h]	Roll [deg]
Max Absolute	1.331	0.895	0.394
Root-Mean-Square	0.535	0.258	0.122

on the right. A reduction of approximately 0.8 m/s^2 is observed when the roll angle is commanded to the full. Performing the planned motion in the simulation environment yields tracking errors as given in Table 5.1. The values highlight good feasibility of the motion planned by 3DOP.

5.3.2. PEAK ACCELERATIONS

The peak acceleration of each motion plan is collected in Fig. 5.2. As W_{time} increases, the maximum magnitude of lateral acceleration grows as expected. However, the longitudinal acceleration reaches a minimum at $W_{\text{time}} = 6$ before the monotonic upward trend that is observable in lateral acceleration. This is partly due to the length of the entry and exit straights. The smaller lateral acceleration comes at the cost of more change in longitudinal velocity, which has to happen within a limited distance. With W_{time} under 6, the benefit of reduced lateral acceleration outweighs the cost of increased longitudinal acceleration and the loss of time. The peaks of longitudinal and lateral accelerations are staggered so that the combined planar acceleration is below 5.81 m/s^2 or 0.59 g at

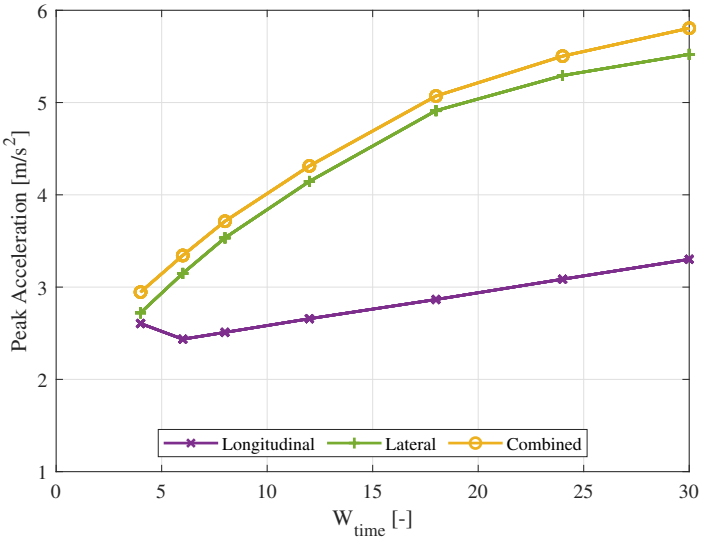

Figure 5.2: Variation of peak acceleration magnitude of the planned motions.

the largest W_{time}. This value implies that the motion plans can be performed by most passenger vehicles in high-friction conditions.

5.3.3. COMPARISON OF PERFORMANCE

We performed simulation runs using the ADM with various acceleration limits derived from Fig. 5.2. The performance indicators obtained from these runs are shown in Fig. 5.3. We calculate the weighted sum of time and discomfort of these points to locate the points lying the closest to the lower-left corner. These points represent the best performance of the ADM, effectively forming an approximate Pareto front. The road profile is processed separately by the speed-only and speed+path planning method using the same set of W_{time}. The comparison between 3DOP and these baseline methods is shown in Fig. 5.4. The string of two-fold scores is fitted as functions in the form of:

$$y = ax^b + c \tag{5.11}$$

which preserves the trend of increased emphasis on time efficiency accelerates the deterioration of comfort. The improvement of 3DOP over the baseline methods is illustrated in two different ways. Fig. 5.5 shows the potential gain in motion comfort without losing time efficiency and the potential savings in travel time with the same comfort level. Across the overlapping range of maneuver time, 3DOP achieves a maximum reduction of discomfort by 54.7% over optimal speed planning, 34.2% over the ADM, or 28.1% over optimal planar motion planning. Alternatively, it saves maneuver time by a maximum of 29.4%, 17.2%, and 14.3% over the three baselines. The time-saving advantage is more obvious when a high level of comfort is demanded because of the limited capability to roll the vehicle body. A higher amplitude of lateral acceleration means the reduction is

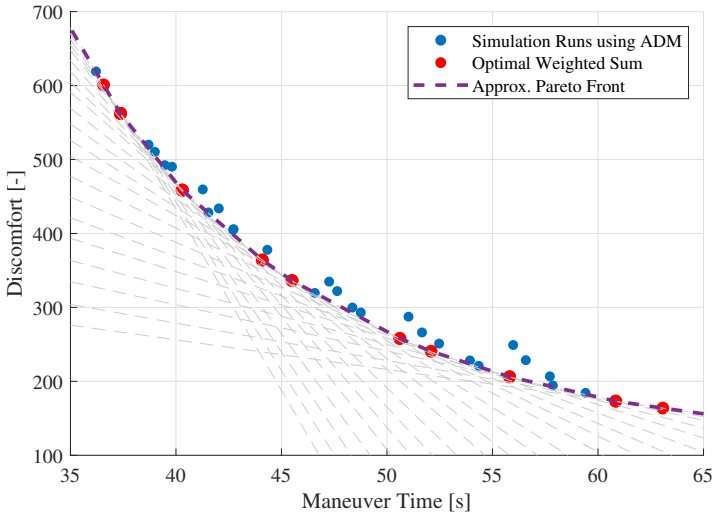

Figure 5.3: Performance of the artificial driver model. The settings with the minimal weighted sum of time and discomfort are marked in red. The dashed line segments connecting them form an approximate Pareto front representing the best performance achievable with the driver model.

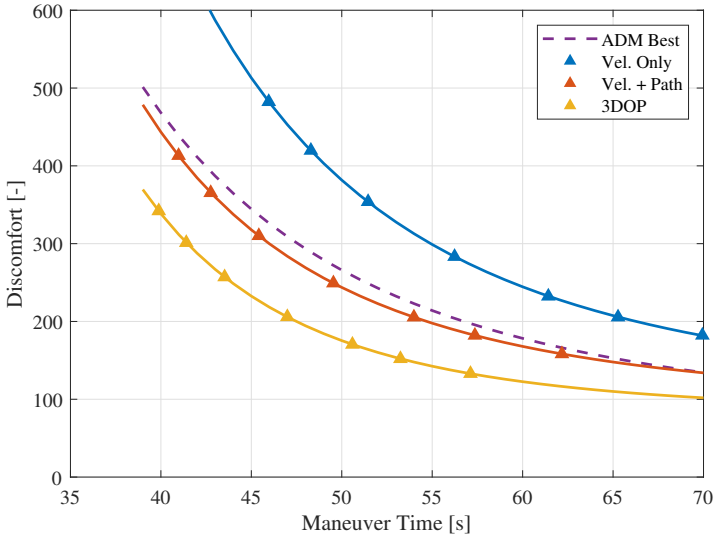

Figure 5.4: Comparison of the performance indicators between 3DOP and the baseline planners.

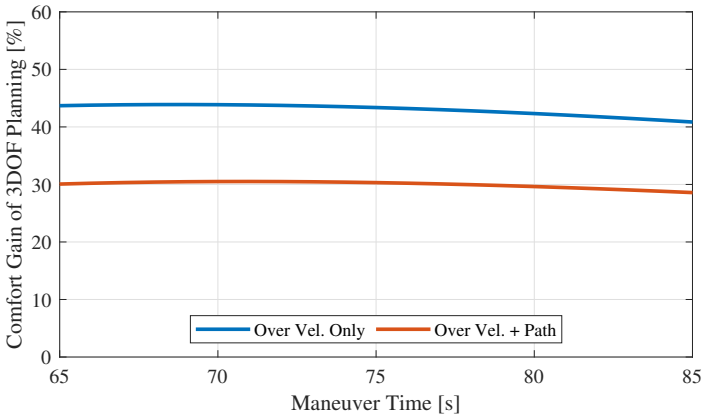

Figure 5.5: Advantages of 3DOP over baseline methods.

smaller in terms of proportion.

5.4. CONCLUDING REMARKS

We presented a motion planning method that jointly plans the path, speed, and roll motion of a vehicle equipped with active suspensions. The method exploits the possibility to actively roll the vehicle body, in order to further improve motion comfort as well as time efficiency. The planned motion is shown to be feasible as it can be tracked by a virtual passenger vehicle with limited error, even when using basic control structures. The results support the use of active suspensions on automated vehicles as the coordination between planar and roll motion can significantly enhance motion comfort. Compared with only optimizing within the horizontal plane, the proposed method improves comfort by up to 28.1% while consuming the same amount of time, or saves at most 14.4% of travel time while maintaining the same level of comfort. The advantage becomes more significant when compared with a driver model representative of highly experienced human drivers.

This work exhibits certain limitations while the understanding is to be deepened with follow-up studies. Firstly, solving the optimization problem for the entire scenario demands intensive computational effort. This approach cannot be implemented directly as a real-time motion planner. Receding-horizon and data-based approaches, similar to that presented in Chapter 3 could be explored to simplify online computation. Meanwhile, although the objective benefit of the proposed method is attractive, it remains uncertain whether the computed motion profiles are appreciated by users. This question could be answered by subjecting human participants to the planned motions and requesting subjective evaluations from them. This nonetheless demands for more expensive equipment in the form of a test vehicle with active suspensions and automated driving capabilities. Experimental studies can also be exploited to collect human driving data that replaces the parameterized driver model. One may refer to 2 for details of an attempt made within this dissertation.

BIBLIOGRAPHY

[1] Y. Zheng, B. Shyrokau, and T. Keviczky, "3DOP: Comfort-oriented motion planning for automated vehicles with active suspensions", in *Proc. IEEE Intell. Veh. Symp. (IV)*, IEEE, 2022, pp. 390–395.

[2] J. A. Joseph and M. J. Griffin, "Motion sickness from combined lateral and roll oscillation: Effect of varying phase relationships", *Aviation, space, and environmental medicine*, vol. 78, no. 10, pp. 944–950, 2007.

[3] B. E. Donohew and M. J. Griffin, "Motion sickness with fully roll-compensated lateral oscillation: Effect of oscillation frequency", *Aviation, Space, and Environmental Medicine*, vol. 80, no. 2, pp. 94–101, 2009.

[4] B. E. Donohew and M. J. Griffin, "Motion sickness with combined lateral and roll oscillation: Effect of percentage compensation", *Aviation, space, and environmental medicine*, vol. 81, no. 1, pp. 22–29, 2010.

[5] G. F. Beard and M. J. Griffin, "Discomfort caused by low-frequency lateral oscillation, roll oscillation and roll-compensated lateral oscillation", *Ergonomics*, vol. 56, no. 1, pp. 103–114, 2013.

[6] G. F. Beard and M. J. Griffin, "Motion sickness caused by roll-compensated lateral acceleration: Effects of centre-of-rotation and subject demographics", *Proceedings of the Institution of Mechanical Engineers, Part F: Journal of Rail and Rapid Transit*, vol. 228, no. 1, pp. 16–24, 2014.

[7] Z. Htike, G. Papaioannou, E. Siampis, E. Velenis, and S. Longo, "Minimisation of motion sickness in autonomous vehicles", in *Proc. IEEE Intell. Veh. Symp. (IV)*, IEEE, 2020, pp. 1135–1140.

[8] O. I. Kolev, "Thresholds for self-motion perception in roll without and with visual fixation target-the visual-vestibular interaction effect", *Functional neurology*, vol. 30, no. 2, p. 99, 2015.

[9] Y. Zheng, B. Shyrokau, T. Keviczky, M. Al Sakka, and M. Dhaens, "Curve tilting with nonlinear model predictive control for enhancing motion comfort", *IEEE Transactions on Control Systems Technology*, vol. 30, no. 4, pp. 1538–1549, 2021.

6

CONCLUSION

Civilization is an enormous device for economizing on knowledge.

Thomas Sowell

This chapter is a summary of the findings, limitations, remaining open questions, and future recommendations from Chapters 2-5.

6.1. FINDINGS

This dissertation has primarily led to a deeper understanding of how motion comfort could be improved using the solutions feasible on automated vehicles, as well as how the performance of the explored solutions compares to a passenger vehicle commonly seen on public roads at the moment with a human driver responsible for the planning and control.

The first step taken towards establishing such an understanding was to investigate the driving performance of human drivers regarding the comfort aspect. The initial attempt relied on existing naturalistic driving data collected in the ACFR dataset. The post-processed vehicle trajectories suggested the peak longitudinal acceleration falls between 0.54 and 1.25 m/s^2, whereas the lateral acceleration falls between 1.42 and 3.62 m/s^2. The number varies per type of maneuver performed at the recording location, namely turning right, driving straight-on, or turning left. The lower values were observed from the straight-moving traffic because the geometry of the roundabout has been designed for improving traffic flow in this direction. The fact that the peak longitudinal acceleration is lower than the peak lateral acceleration is partly attributed to the drivers' possible preference for maintaining a higher speed which reduces fuel consumption and saves time. Another factor leading to this difference is the limited coverage of the recording. Because of the choice of data acquisition method, which relied on the roof-mounted LiDAR on a vehicle parked near the intersection, the trajectories only extended for a short distance before the entry and after the exit of the roundabout. The major ac-/deceleration phases were missing. The vehicle's initial and terminal velocities were found to be much lower than the speed limit imposed on the corresponding segments. The incompleteness also hinders a comprehensive evaluation of the comfort-oriented driving performance because the factor of time is missing. It has been emphasized on multiple occasions the necessity of including time efficiency when evaluating comfort due to the inevitable conflict of interest. A fair comparison of comfort level could only be made among trajectories of similar durations. Alternatively, one could compare the durations among trajectories yielding similar comfort levels. Therefore, the analysis of the naturalistic dataset is insufficient for our evaluation purpose. Consequently, an experimental study was conducted in order to overcome these limitations. A comprehensive route was chosen and a group of 16 participants recruited from the public were requested to drive through it. The duration of each test run was timed using GPS-based triggering which minimizes the variation. In terms of peak accelerations, the experiment suggests an average of 3.57 and 1.90 m/s^2 for lateral and longitudinal directions, respectively. The mean peak lateral acceleration matches the findings from the naturalistic driving dataset despite the latter being collected in a different country, namely Australia. Meanwhile, the longitudinal acceleration is around 50% higher than in previous observations. This major difference could support the argument that the missing ac-/deceleration phases had led to a lower value in peak longitudinal accelerations. Through the 920-meter-long test route, the participants spent an average of 76.5 s driving time, with the fastest slightly above 70 s and the slowest around 85 s. When character-

ized by the energy of the acceleration signals, the discomfort accumulated through the maneuver has an average of 211.4 m^2/s^3, a maximum of 244.5 m^2/s^3, and a minimum of 169.4. The most comfortable ride was not the slowest one, however. This demonstrates the performance variances among the participants. It was unfortunately not possible to better characterize such variances in statistics due to the rather small sample group. Nevertheless, the relatively better-performing individuals could at least be representative of an averagely skillful human driver.

The second step taken was to study the possibility of improving acceleration-related motion comfort within the horizontal plane by means of motion planning algorithms. On top of minimizing all planar accelerations equally, the idea of targeting a specific frequency range that causes the most motion sickness was explored. The implementation was enabled by a novel method of calculating band-pass filtered acceleration signal in a variable-step fashion, which accompanies a spatiotemporal motion planning framework that defines vehicle motion with respect to its relative position in its driving lane. The effectiveness of this method is demonstrated by comparing it with the variant that regards all frequency components equally. The comparison reveals interesting differences as when the frequency-weighted accelerations are minimized, the acceleration profile appears to be more pointy, i.e. with more sharp and swift changes. This helps reduce the low-frequency acceleration components that are perceived as the most nauseogenic but also gives rise to jerks and total acceleration, resulting in deteriorated general motion comfort. When formulated in a receding-horizon fashion, the motion planners' performance is strongly influenced by the choices of preview time and nominal sampling time. A longer preview time yields better performance but comes at a cost of higher computational burdens. Contrary to expectation, a shorter step length is not necessarily beneficial when minimizing frequency-weighted accelerations. The cause of this is suspected to be the step-wise calculation of the frequency-weighting filter. The shorter step time gives the optimizer the option to command excessive initial acceleration without being heavily penalized. Meanwhile, the observation brings unexpected benefits in terms of computation time. The real-time threshold is relaxed with the increased sampling interval. The reduced dimension of the optimization problem partly offsets the increased complexity of performing the frequency-weighting calculations. The combination of 5s preview time and 0.5s sampling time required an average of 0.33s to find the optimal solution. The computational complexity was estimated to be at a factor of 5 to 6 over the alternative of minimizing general acceleration. Many differences between the motion planners and human drivers evaluated in Chapter 2 are noted. The average performance deficit is around 70.2% for frequency-weighted acceleration energy or 23.5% in overall acceleration energy, measured with equal driving time. Human drivers are reasonably capable of planning and performing a comfortable motion but not as much in avoiding motion sickness. This is related to the fact that drivers are significantly less susceptible to motion sickness than passengers. Hence they may not notice some features in vehicle motion they commanded that the passengers perceive as sickening. It should be emphasized that driving capability is not the sole contributor to the performance deficit. In other words, the exact upside potential in improving motion comfort or mitigating motion sickness with automated driving might be smaller than the numbers mentioned above. The simulated environment where the motion planner

is tested is simpler than the real world in many ways. For example, it assumes a perfectly flat road surface while some depressed pavement can be seen at the actual test location. The decision-making process of human drivers is also far more complicated than that of the motion planner. For example, they may prefer zero input when the situation allows in order to reduce physical workload. They also consider the possible scenario of having to yield to other road users and hence plan the speed more cautiously than when only time and comfort need to be minimized. Further plausible causes include the human drivers' consideration for reducing fuel consumption or the wear of brakes, both of which contribute to the cost of using a vehicle. Nonetheless, the findings from this comparison provide an approximate idea of how much potential do automated vehicles hold in mitigating the motion sickness paradox and hence argue for further development and mass deployment of automated vehicles.

In an independent branch of effort, the concept of reducing lateral acceleration with roll compensation has been explored. The concept relies on the capability of active suspensions to generate force and therefore manipulate vehicle body attitude. Using the nonlinear model predictive control method, 12.9%, 16.4%, and 38.0% smaller RMS tracking errors are achieved over the industrial state-of-the-art implementations with scenario-specific tunings for the motorway, rural, and urban driving scenarios, respectively. The issues of heavy computational burden that are commonly connected to the use of NMPC are overcome by the dedicated warm-start strategy, resulting in feasible real-time implementation in a hardware-in-the-loop setup, where the controller operated on a dSPACE MicroAutoBox while communicating via CAN with the IPG CarMaker environment running on a separate computer. Frequency-domain analysis revealed an attractive reduction in the frequency range around and below what is considered the most nauseogenic. However, the reduction is less significant in the more dynamic driving scenarios. It confirms the anticipations on the difficulty of implementing the tilting concept in road vehicles despite the use of an advanced control method. The bottleneck is believed to primarily lie within the reference generator for the desired roll motion. The parameters are chosen in a relatively conservative way in order not to surprise a human driver. The commanded roll angle is consequently somewhat reluctant in the more dynamic driving scenarios. This is further complicated by the unpredictable disturbances on the vehicle body attitude due to the strong influence of load transfer. A better performance could be expected if the roll angle planning is integrated into the motion planning framework proposed in Chapter 3. The novel idea was explored in Chapter 5 by extending the optimization problem to include the roll angle as a part of the decision variables and describing the effect of the roll angle on the lateral acceleration felt by the passengers. The need for a phase advance in roll angle with respect to the lateral acceleration was not explicitly formulated into the objective of the optimization problem. Instead, it was covered by the goal of minimizing planar accelerations, with the absolute change in roll angle being penalized additionally. It prompts the optimal motion plan to start increasing the roll angle before the rise of the lateral acceleration.

6.2. LIMITATIONS

Extra caution should be taken when using the conclusions in this dissertation. While some qualitative arguments could be transferable, the exact extent of the advantage of

the proposed methods explored here might vary given different conditions.

To begin with, the research effort described in Chapter 2 provides only an initial attempt to measure average human driving performance in balancing comfort and time efficiency. The relatively small number of test runs recorded limits the statistical significance of the baseline. This is especially complicated further by the fact that the performance is measured in a two-fold fashion by including both a comfort indicator and travel time. More samples are obviously helpful in increasing the chance of both determining the average performance and finding the upper limit of human drivers. Hence to avoid exaggerating the potential of automated vehicles, it is recommended to use the better-performing samples in the experimental data as a representation of the average human drivers until such data has been collected on a larger scale.

The motion planning algorithm proposed for mitigating motion sickness relies on the empirical model developed from the observed strong correlation between motion sickness and low-frequency oscillations. Optimizing for frequency-weighted accelerations resulted in an 11.3% reduction in this measure of motion sickness compared with optimizing for general acceleration comfort. The value is specific to the scenario being investigated, which involves highly dynamic maneuvering in a rather compact time span. A smaller advantage might be observed in milder scenarios such as motorway driving. The advantage also depends on the difference in width between the lane and the vehicle. Moreover, the reduction in frequency-weighted acceleration here should not be interpreted as a reduction of the same proportion in the severity of motion sickness in an individual, nor in the possibility of developing motion sickness in the general population in the ideal case of full-scale deployment of AVs. It remains unknown how such a reduction is reflected in human subjects. While the acceleration signal might be decomposed as a sum of various frequency components, one may not assume the resulting motion sickness level equal to the sum of the motion sickness levels caused by these frequency components. One may recommend the use of more complex models of motion sickness for more accurate prediction. However, Chapter 3 already shows that the relatively simple approach of frequency weighting is already on the verge of real-time computation threshold. It is not advised to further increase the online computational burden as the potential benefit of reduced incidence of motion sickness may not be worth the cost of amplified energy consumption. Alternative to the online optimization-based approach, learning-based methods could be explored for better computational efficiency. The reader may refer to [1] for an example of such attempts, which is a spin-off study of this dissertation under the supervision of the author.

When comparing human drivers with the proposed motion planning algorithms, the imperfections in the experimental setup for data collection should also be considered. The presence of elevation changes and road banking angle could have influenced the measured acceleration values in either direction. Such effects cannot be fully compensated for by cross-referencing with the GPS trajectory. In addition, human drivers are believed to have a more comprehensive decision-making process when planning and controlling vehicle motion. Albeit the experiment was conducted outside the busy hours to avoid traffic interaction as much as possible, the possibility of having to give way to other road users could not be excluded. The participants had to still account for a possible situation where another vehicle has priority when they approach one of the two

roundabouts. The extra caution is reflected by a lower speed adopted by the participants before entering the intersection, which costs more time without apparently benefiting comfort. There was an additional issue with one obvious piece of pavement damage across the test route. The location of the damage is before a straight section where a higher speed could have been adopted. Instead, the participants had to restrain from accelerating until they drove past this depressed patch. One could consider this as if the participants were solving an optimization problem with an additional dimension of vertical comfort. Furthermore, the human driver may tend to reduce input effort and keep a lower physical workload and avoid fatigue. For example, they tend to leave the vehicle coasting rather than control its speed precisely when the situation allows as no pedal input would be needed. While this partly explains the cause of performance difference, it does not make the potential improvement with AVs lessor because one should perceive being prone to fatigue as another disadvantage of human drivers.

The NMPC-based controller for active suspensions mainly causes challenges when refining the prediction model. An accurate description of system dynamics with the prediction model is fundamental for the application of MPC techniques. This involves the determination of both the types of dynamics (e.g., the dimension of the state space) and the exact parameters. In this specific case, the prediction model captures the roll, pitch, and heave motion of a rigid body subject to highly nonlinear suspension and damper forces. The dynamics of the wheel carrier, which exhibits a higher natural frequency, have been neglected for the sake of computational efficiency. It implies that the control quality is only ensured for high-quality pavement and is uncertain for situations with more vertical excitation. Besides, the control performance could be sensitive to the loading condition. The payload mass and its distribution across the vehicle would almost definitely be different from a fixed set of model parameters. Additional sensors and algorithms may be necessary to estimate and adapt the parameters accordingly. It is anticipated that the damper in a suspension assembly would have varying characteristics throughout its lifespan. Such variations could be more difficult to estimate. Hence the NMPC-based controller is considered still premature for production-level deployment. This is combined with the higher cost of manufacturing the actuator and equipping the vehicles with higher-performance computational hardware.

In Chapter 5, considerable potential in further coordinating the roll motion with a motion planner has been suggested. The advantage is characterized by planar accelerations due to the uncertainty in predicting motion sickness under combined motions, especially roll and yaw rotations. Hence the reduction in overall acceleration does not translate to the same amount of reduction in motion sickness. The realization of the suggested improvement is challenging, too. The optimization problem solved by the motion planner requires accurate knowledge of the road and does not consider interactions with other road users. In practice, motion planners would more likely operate in a receding-horizon fashion, using a limited preview distance and updating the motion plan for the constantly varying scenario. The performance deficit caused by this has been presented in Chapter 3. Nevertheless, the 2-dimensional baseline used in Chapter 5 is given the same amount of information as the proposed method. The comparison is still considered fair and could be useful in demonstrating the value of active suspension in automated vehicles. However, these results still do not justify whether the use of

active suspensions should indeed be equipped on automated vehicles on a large scale. The practical aspects including cost and energy consumption should be considered in addition.

6.3. OPEN QUESTIONS AND FUTURE RECOMMENDATIONS

The dissertation has left a few questions inconclusive while raising more to be answered. Recommendations are made based on the accumulated knowledge.

- How to characterize and evaluate the comfort-oriented driving performance of human drivers? This question can be divided into smaller sub-questions including but not limited to, what scenario can best expose the differences, what are the suitable performance indicators, how the necessary data should be collected, and what test facility and equipment should be used. Answering this question is necessary not only for understanding human drivers but also for concretely demonstrating the advantage of automated vehicles. It has been part of the goal of this dissertation to provide such a demonstration and several options have been explored. However, more work still needs to be done for the standardization of driving performance evaluations. Specifically, data on the subjective rating of motion comfort need to be collected for a wider range of scenarios and the typical pattern of car usage should be considered. A wider spectrum of motion data should be gathered and compared with the subjective rating in order to motivate the choice of a performance indicator.

- How to distinguish motion comfort and motion sickness in subjective evaluations? As shown in Chapter 3, optimizing for squared MSDV, an indicator of motion sickness, led to very different motion profiles from optimizing for squared accelerations, a motion comfort indicator. Presumably, acceleration- or jerk-based motion comfort indicators have an almost immediate effect on the subject. Motion sickness has slower temporal dynamics on the other hand. A rise in nauseous feeling could appear with a delay after certain motion inputs. For the participants of a relevant experiment, especially if continuous measurement is used, it could be difficult to identify if their current level of suffering is a result of direct discomfort or motion sickness from sustained exposure. In contrast, if sampled measurement is used, the participant may lose an accurate sense of discomfort that happened some time ago. A better understanding of this question is important for the validation of any motion planning algorithm that claims to either improve comfort or mitigate motion sickness.

- Is it worth attempting to minimize motion sickness and is it possible? There can be two interpretations of the goal. It could mean either minimizing the severity of motion sickness for an individual or minimizing the chance of anyone experiencing motion sickness in a group. This dissertation has chosen an indicator of motion sickness from the literature that is found to correlate with the severity of motion sickness and used it as the objective of an optimization problem. The reduction achieved in simulation is 11.3% compared with optimizing for accelerations. It could require a participant group of a considerable size to verify this

reduction in an experimental study, given the significant individual variance in motion sickness responses. It is probable that a more accurate motion sickness prediction model could be used but the computational demand is highly probable to be higher, too. It then poses more challenges when implementing such algorithms on a real vehicle. The cost incurred by using expensive computational hardware for running the more complex algorithm should be compared with the potential gain in reducing motion sickness. It might be a more viable option to use heuristic objectives instead that would result in a lower chance of motion sickness without requiring an accurate prediction of motion sickness.

- Will active suspensions eventually be applied to automated vehicles on a large scale? Chapter 5 has suggested an attractive improvement in acceleration comfort with the coordinated planning of the roll motion enabled by active suspensions. However, the concerns of excessive energy consumption remain less investigated. Especially in the context of electrified mobility, users are typically more sensitive to the consumption of auxiliary devices. Improving energy efficiency in active suspension actuators is therefore of high priority. Besides, there is a risk of worse handling quality of the vehicle which could compromise safety. For example, if the vehicle was at a tilted attitude when an emergency evasion needs to be performed, the imbalance in the wheel load distribution, excessive suspension extension, and skewed wheel alignment could limit the vehicle's friction potential and increase the chance of losing stability. It is recommended to investigate the vehicle dynamics quality at a larger roll angle in order to evaluate whether it is proper to perform roll compensation on lateral accelerations with active suspensions, as well as how the negative effects could be best overcome with corresponding control strategies.

BIBLIOGRAPHY

[1] N. Rajesh, Y. Zheng, and B. Shyrokau, “Comfort-oriented motion planning for automated vehicles using deep reinforcement learning”, *IEEE Open Journal of Intelligent Transportation Systems*, 2023.

ACKNOWLEDGEMENTS

The journey leading to the completion of this dissertation has been unforgettable. So many challenges were faced and so many obstacles were cleared. It would not be possible without the kind people who have been walking alongside me for almost 5 years. This chapter is dedicated to expressing my gratefulness to all of you, mentioned by name or not.

First of all, I would like to express my sincere gratitude to my supervisory team, Dr. Barys Shyrokau as my daily supervisor and Prof. Tamas Keviczky as my promotor. Barys and I collaborated before during my M.Sc thesis project. Actually, this entire Ph.D. story would not even start if it wasn't for the invitation from Barys to continue my research at TU Delft. He has always trusted me with a high degree of autonomy, to pace my work and explore my ideas. This trust is truly valuable as it both motivates and assures especially in the low times. Hopefully, the trust has proven worthwhile to him. Meanwhile, he would try his best to help me whenever asked, regardless of his own tight schedule. I hope we can work together again in the future, even after my career move to the industry. On the other hand, I have benefited greatly from the advice and critical comments from Tamas. He could easily see through my 'tricks' and ask the most important question. At the same time, he had gone through every single word and symbol in all my draft manuscripts to bring them to the level of an experienced professional scientific researcher. I could not do the same to the M.Sc. students I supervised even with apparently more time at my disposal.

Next, I would like to thank the members of the graduation committee. Your careful examination and approval of this dissertation are essential in leading to the final event of my graduation. I look forward to an interesting discussion with you in person.

Then it's time to turn to my close colleagues in the Intelligent Vehicles group. Prof. Dariu Gavrila, I will not forget the Einstein quote he mentioned after my first-year review: 'If we knew what it was we were doing, it would not be called research, would it?'. It inspired me to take on questions that no one yet has an answer to. The quote from Prof. Riender Happee is, 'PhD's are here to learn, anyway.'. It can easily be generalized beyond the course of doctoral education, as he himself serves as the perfect example of always learning. Then there are the always-positive Dr. Julian Kooij the Amsterdamer, Dr. Ksander de Winkel the motor knight (whose ideas on quantifying motion comfort were very inspiring although he only worked with us for a short period), Dr. Laura Ferranti who often brought Italian sweets to the meeting, Dr. Marko Cvetkovic the amazing photographer, Dr. Raj Desai the quiet but brilliant, Dr. Yancong Lin the look-too-strong-. and others who already possess a doctor's title when we met. Those who obtained the right to a doctorate title during my 5-year research career at TU Delft, Dr. Ewoud Pool the cider brewing master, Dr. Jork Stapel the science enthusiast and climber, Dr. Andras Palffy the 'Radar is better than LiDAR but I use a camera instead', Dr. Thomas Hehn the whatever-board rider and animal lover, Dr. Tugrul Irmak the true fighter with tremen-

dous strength both physically and mentally (extra note: the assurance I got from him on my English proficiency truly encouraged me to talk more and become a better speaker). These are the nice people who onboarded me into the IV group with a warm welcome and demonstrated to me what a qualified Ph.D. researcher looks like. Those who joined the group later and are still fighting their way through, I wish all of them great success in the end. These include my fellow Chinese colleagues Zimin Xia, whom I wish will become a Porsche owner and professor in the future; Xiaolin He, who cooks authentic Shandong fried chicken, and Shiming Wang who is a very knowledgeable person on historic and political matters. These lovely people made me feel less distant from home. There is also Team Asia including Vishrut Jain the entertainer and DJ with a bullet-proof Titanium leg, Varun Kotian the enthusiast in Chinese language and food, and Mubariz Zaffar the badminton professional. Then of course Team Europa with Alberto Bertipaglia, Hidde Boekema, with whom I went to the IV'22 in Aachen to represent our group, and Wilbert Tabone the president candidate, Ted de Vries the disciplined heavy lifter, and Chrysovalante Messiou with amazing diligence and dedication from day 1. I would like to mention here Jetze Schuurmans in addition, who was with us for merely 2 years. His approach of scheduling a 1-to-1 talk with every new colleague after joining us was really impressive during Corona time. Ronald Ensing, who was the first to approach me after my first attendance at the group's regular meeting, appraised the way I introduced myself and presented my previous works. This small action was very much needed for a new Ph.D. candidate facing a lot of uncertainty. Dr. Mario Garzon, he was the reliable technical support for setting up the hardware for my experiment. Additionally, special thanks go to our secretary Hanneke Hustinx. She always remembers what we need and tries her best to help.

Of course, life has another side next to the career. Many friends supported me along the way and made my life so lively and colorful (surely many colleagues fall into this category, too). To name a few, there were Team Old German Cars, Team Aviation Photographers, Team Snowsport Lovers, and a lot of other people whom I met because of a specific spare-time activity. Also important were my kind neighbors who live on Narcisstraat, in the beautiful city of Woerden. This place felt like a second home because of their warm hearts. Special thanks also go to the family of Marie-Luise & Hans de Groot. They were not only our good friends but were the first to volunteer for my experiment, and tried their best to spread the call for participants as wide as possible.

Last but not least, or in fact the most important, are my closest ones: my mother Yonghong Song, my father Canchao Zheng, and my dearest partner Yi Song (whose family name coincides with my mother's just by coincidence). I feel every day as if I am the luckiest on earth to have them around me. My parents had an open mind and empowered me to explore the outside world with a mindset to respect and understand differences and to befriend people from diverse backgrounds. This is more valuable than anything taught in any school. They supported my decision to take on new challenges and kept telling me they were proud of me. Yi, she has been with me all the time, we experienced everything together including the depression of Covid and then the joy of reopening. She assured me on a regular basis that I have a talent in the field of profession where I have a major interest. She gave up a relaxing and peaceful life and relocated with me across a thousand kilometers so that I could start a career that fits my passion. She

also joined me in many activities including karting, snowboarding, flying an airplane, and driving on the Nurburgring, where she had to overcome her own fear so that I was able to do them. I cannot imagine going through these years without her.

I regret not being able to mention the names of all the people to whom I want to say thank you. But every single bit of their kindness will be reminded of whenever I reopen this dissertation.

CURRICULUM VITÆ

Yanggu ZHENG

01-07-1993 Born in Beijing, China.

EDUCATION

2011–2015 B. SC., Automotive Engineering
Tsinghua University, Beijing, China

2016–2018 M. Sc. (cum laude), Vehicle Engineering
Delft University of Technology, Delft, the Netherlands

2018–2023 Ph. D., Intelligent Vehicles
Delft University of Technology, Delft, the Netherlands
Thesis: Improving motion comfort with motion planning and suspension control
Promotor: Prof. T. Keviczky
Supervisor: Dr. B. Shyrokau

AWARDS

2021 SAE Vincent Bendix Award

List of Publications

Doctoral Research

1. **Y. Zheng**, B. Shyrokau, T. Keviczky, M. A. Sakka and M. Dhaens, "Curve Tilting With Nonlinear Model Predictive Control for Enhancing Motion Comfort", in *IEEE Transactions on Control Systems Technology*, vol. 30, no. 4, pp. 1538-1549, 2022.

2. **Y. Zheng**, B. Shyrokau, and T. Keviczky, "Comfort and Time Efficiency: A Roundabout Case Study", *2021 IEEE International Intelligent Transportation Systems Conference (ITSC)*, Indianapolis, IN, USA, pp. 3877-3883.

3. **Y. Zheng**, B. Shyrokau, and T. Keviczky, "3DOP: Comfort-oriented Motion Planning for Automated Vehicles with Active Suspensions", *2022 IEEE Intelligent Vehicles Symposium (IV)*, Aachen, Germany, pp. 390-395.

4. **Y. Zheng**, B. Shyrokau, and T. Keviczky, "Mitigating Motion Sickness with Optimization-based Motion Planning", In review at *IEEE Transactions on Intelligent Vehicles*.

5. **Y. Zheng**, B. Shyrokau, and T. Keviczky, "Comfort-oriented driving: performance comparison between human drivers and motion planners", In review at *IEEE Transactions on Intelligent Transportation Systems*.

Master Thesis

1. **Y. Zheng**, and B. Shyrokau, "A Real-Time Nonlinear MPC for Extreme Lateral Stabilization of Passenger Vehicles", *2019 IEEE International Conference on Mechatronics (ICM)*, Ilmenau, Germany, pp. 519-524.

Supervised and Participated Works

1. L. Ferranti, B. Brito, E. Pool, **Y. Zheng**, R. M. Ensing, R. Happee, B. Shyrokau, J. F. P. Kooij, J. Alonso-Mora, and D. M. Gavrila, "SafeVRU: A Research Platform for the Interaction of Self-Driving Vehicles with Vulnerable Road Users", *2019 IEEE Intelligent Vehicles Symposium (IV)*, Paris, France, pp. 1660-1666.

2. K. Chatrath, **Y. Zheng**, and B. Shyrokau, "Vehicle Dynamics Control Using Model Predictive Control Allocation Combined with an Adaptive Parameter Estimator", in *SAE International Journal of Connected and Automated Vehicles(2020)*, vol. 3, no. 2, pp. 103-117, 2020.

3. Y. R. Khusro, **Y. Zheng**, M. Grottoli, and B. Shyrokau, "MPC-Based Motion-Cueing Algorithm for a 6-DOF Driving Simulator with Actuator Constraints", in *Vehicles*, vol. 2, no. 4, pp. 625-647, 2020.

4. C. Yu, **Y. Zheng**, B. Shyrokau, and V. Ivanov, "MPC-based Path Following Design for Automated Vehicles with Rear Wheel Steering", *2021 IEEE International Conference on Mechatronics (ICM)*, Kashiwa, Japan, pp. 1-6.

5. N. Rajesh, **Y. Zheng**, and B. Shyrokau, "Comfort-Oriented Motion Planning for Automated Vehicles Using Deep Reinforcement Learning", in *IEEE Open Journal of Intelligent Transportation Systems*, vol. 4, pp. 348-359, 2023.

PROPOSITIONS ACCOMPANYING THE DISSERTATION

1. It is wrong to presume that male drivers are more aggressive or female drivers are more sluggish.
   This proposition pertains to Chapter 2

2. Acceleration magnitude is the most recommendable motion comfort-related criterion when designing and evaluating motion planning algorithms.
   This proposition pertains to Chapter 3

3. Model predictive control with a complex prediction model cannot be widely implemented in the automotive industry.
   This proposition pertains to Chapter 4

4. Scientific disciplines are equally valuable but never equally valued.

5. Paper disposables such as straws and bags, only reduce people's guilty feelings, not their environmental impact.

6. Human beings are selfish as individuals and self-destructive as a group.

7. Personal achievements are largely attributed to luck rather than perseverance.

8. In the future, customers should always be given the option to buy a new car that is categorized as SAE Level 0, i.e. with automation limited to warning and momentary assistance [1].

9. This proposition will be forgotten.

[1] https://www.sae.org/standards/content/j3016_202104/